UNIVERSITÀ DELLA CALABRIA

Dipartimento di Farmacia e

Scienze della Salute e della Nutrizione

Dottorato di Ricerca in

"Medicina Traslazionale"
(XXX Ciclo)

MED 04/Patologia Generale

Estrogen Receptor alpha interferes with LKB1/AMPK/mTOR signaling activation in adiponectin-treated breast cancer cells

Coordinatore: Ch.mo Prof. Sebastiano Andò

Tutors: Prof.ssa Maria Luisa Panno

Dott.ssa Loredana Mauro

Dottorando

Dott.ssa Giuseppina Daniela Naimo

Anno Accademico 2016/2017

INDEX

Abstract

Breast cancer is the most common type of tumor and the leading cause of cancer-related deaths in women, worldwide. The cause of breast cancer is multifactorial and includes hormonal, genetic and environmental cues. Obesity is now an accepted risk factor for breast cancer in postmenopausal women, particularly for the hormone-dependent subtype of mammary tumor.

Obesity has regarded as a multifactorial disorder characterized by an increased number and size of adipocytes. Adipose tissue is an active metabolic and endocrine organ that secretes many adipocytokines, which act as key mediators in several obesity-associated diseases. Among these, adiponectin represents the most abundant adipose tissue-excreted protein, which exhibits insulin sensitizing, anti-inflammatory, and antiatherogenic properties Adiponectin has been proposed as having a key role in the pathogenesis of cardiovascular disease and type 2 diabetes along with obesity-associated malignancies, such as breast cancer. An inverse correlation is reported between obesity and adiponectin, for which low levels of adiponectin represent a risk factor for breast cancer. The role of adiponectin on breast tumorigenesis seems to be dependent on cell phenotypes. Indeed, several *in vitro* and *in vivo* studies demonstrated that low adiponectin levels repressed growth in ERα-negative breast cancer cells whereas increased proliferation in ERα-positive cells. Adiponectin interacts with specific receptors and exerts its effects, including regulation of cell survival, apoptosis and metastasis, via a plethora of

signaling pathways. The key molecule of adiponectin action is AMP-activated protein kinase (AMPK), which is mainly activated by liver kinase B1 (LKB1).

On the basis of this observations, the aim of the present study was to investigate the effect of adiponectin on LKB1/AMPK signaling in ERα-negative (MDA-MB-231) and positive (MCF-7) breast cancer cells.

In MCF-7 cells, upon low adiponectin levels, ERα impaired LKB1/AMPK interaction by recruiting LKB1 as coactivator at nuclear level, sustaining breast tumor growth. In this condition, AMPK signaling was not working, letting fatty acid synthesis still active. In contrast, in MDA-MB-231 cells the phosphorylated status of AMPK and ACC appeared enhanced, with consequent inhibition of both lipogenesis and cell growth. Thus, in the presence of adiponectin, ERα signaling switched energy balance of breast cancer cells towards a lipogenic phenotype. The same results on tumor growth were reproduced in a xenograft model.

These results emphasize how adiponectin action in obese patients is tightly dependent on ERα, addressing that adiponectin may work as growth factor in ERα-positive breast cancer cells.

Introduction

1.1 Obesity and breast cancer

Breast cancer is one of the most common forms of female malignancy worldwide, with more than 1.6 million new cases detected each year *[Torre LA et al., 2015]*. This represents about 25% of all diagnosed cancers in women, suggesting that of every four women across the globe who are diagnosed with any type of cancer, one is a case of breast cancer *[Torre LA et al., 2015]*. Although better therapeutic strategies have allowed important improvements in prognosis over the past 20 years, breast cancer remains the second most fatal cancer type among women *[De Santis C et al., 2011; Siegel R et al., 2012]*.

Clinical and epidemiological studies have identified many important breast cancer risk factors. Some of these are intangible or beyond our control, such as age or family history. The incidence of breast cancer is extremely low before age 30, after which it increases linearly until the age of 80 *[Singletary SE, 2003]*.

Genetic predisposition is one of the most intriguing factors associated with increased risk for breast cancer and represents the approximately 20% of breast tumor patients who have a positive family history of this cancer type *[Singletary SE, 2003]*.

Aside from the genetic predisposition, a myriad of other factors can contribute to the pathogenesis of breast cancer, such as lifestyle and environmental factors, hormone replacement therapy with estrogen and progesterone, radiation exposure, early menarche, late menopause, age at first childbirth *[Singletary SE, 2003]*.

Among the modifiable factors, obesity has been designated as a serious health problem among women. Obesity is a chronic and multifactorial disorder, characterized by an enlarged mass of adipose tissue caused by a combination of size increase of preexisting adipocytes (hypertrophy) and *de novo* adipocyte differentiation (hyperplasia) that is reaching epidemic proportions. It is at the origin of chronic inflammation of white adipose tissue and is associated with dramatic changes in the biology of adipocytes leading to their dysfunction.

Accumulated evidences related the excess of body weight to many metabolic disorders like hypertension, type 2 diabetes, metabolic syndrome, and cardiovascular disease, and to an increased risk of cancer development in different tissues, such as cervix, ovaries, uterus, colon, and breast.

The association between obesity and breast cancer risk is complex and can be different depending on menopausal status *[Rose DP and Vona-Davis L, 2010]*, the use of postmenopausal therapy *[Munsell MF et al., 2014]*, breast cancer subtype *[Suzuki R et al., 2009]* and racial/ethnic group *[Bandera EV et al., 2015]*. However, there are abundant and consistent epidemiological evidences suggesting that obesity is a serious risk for breast carcinogenesis and it is positively correlated with a poor outcome in postmenopausal women, particularly with the hormone-dependent subtype of breast cancer *[Pischon T et al., 2008]*. Traditionally, the adverse effect of obesity on breast cancer prognosis has been linked to the higher estrogen levels produced, consequent to a greater aromatase activity due to the excess of adipose tissue *[McTiernan A et al., 2003]*. Metabolism of steroid hormone causes different effects on obesity and breast cancer in pre- and post-menopausal women *[Davoodi SH et al., 2013]*. Before

menopause, ovaries are the main source of estrogens production, while after menopause, secretion of estrogens has reduced. Instead of that, estrogens have produced in adipose tissue, increasing the incidence of breast cancer in obese women.

Despite the well-documented relationship between obesity and estrogenic activity, it is evident that this cannot fully explain the association between body weight and breast cancer risk and prognosis.

Many experimental and epidemiological supports highlight several estrogen-independent mechanisms that may contribute to the development of obesity-related breast cancer (Fig. 1).

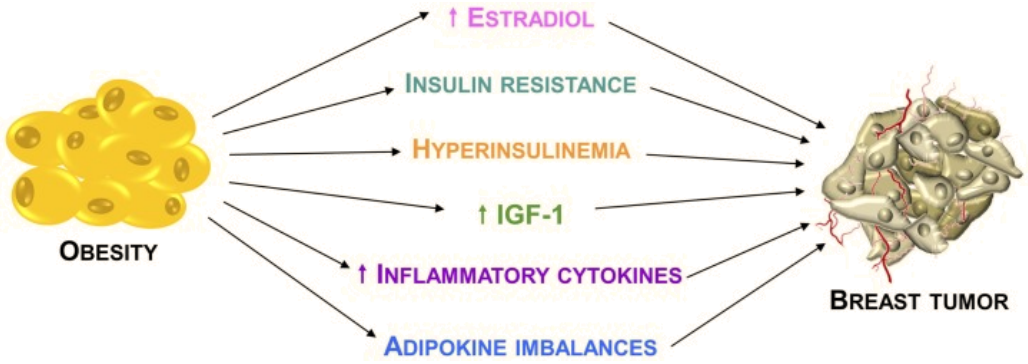

Figure 1. Relationship between obesity and breast cancer.

Obesity, in addition to an increase in circulating levels of estrogen, is characterized by elevated levels of insulin and insulin-like growth factors (IGFs), and insulin-resistance *[Calle EE and Thun MJ, 2004; Maccio` A et al., 2009; Roberts DL et al., 2010]*. This rise in insulin level is found to be associated with the greater bioavailability of insulin-like growth factor-I (IGF-I) and the activation of IGF system. Insulin, IGF-1 and insulin like growth factor-1 receptor (IGF-1R)

are overexpressed in several subtypes of breast cancer *[Law JH et al., 2008]*. The binding of this ligand to IGF-1R leads to activation of its tyrosine kinase activity *[Pollak MN et al., 2004]*, promoting cell migration and breast tumorigenesis *[Chan BT et al., 2008]*. In addition, IGF-1R induces the activation of PI3K/Akt and Ras-raf-MAPK signaling which alter the expression of genes involved in cellular proliferation and survival *[LeRoith D et al., 2003]*. Overall, this altered hormonal and growth factor profile is associated with increased breast cancer risk.

Apart from these mechanisms, another important element in obesity-mediated breast carcinogenesis is represented by the interaction between tumor cells and the surrounding microenvironment, which comprises stromal cells, soluble factors, signaling molecules, and extracellular matrix that can promote tumorigenesis, and make the tumor resistant from host immunity and therapeutic response.

Although the physiological role of adipose tissue is to store fat when it is in excess and to supply it when needed *[Hajer GR et al., 2008]*, the identification of leptin in 1994 has led to the general awareness that adipose tissue cannot be considered simply as a storage reservoir for excess energy. Indeed, adipose tissue is now widely considerate as an active endocrine and metabolic organ involved in the regulation of different physiological functions and related pathological processes of the body like energy homeostasis, metabolism of carbohydrates and lipids, coagulation of blood, feeding behavior, inflammation, immunity, endocrine balance, and bone remodeling *[Barb D et al., 2007; Kelesidis I et al., 2006]*. The communication between adipose tissue and other biological systems is possible through the expression and secretion of a large number of bioactive molecules known as adipocytokines or adipokines. Currently, adipose tissue is responsible

for the biosynthesis and secretion of more than 50 hormones and cytokines *[MacDougald OA et al., 2007]* (Fig. 2).

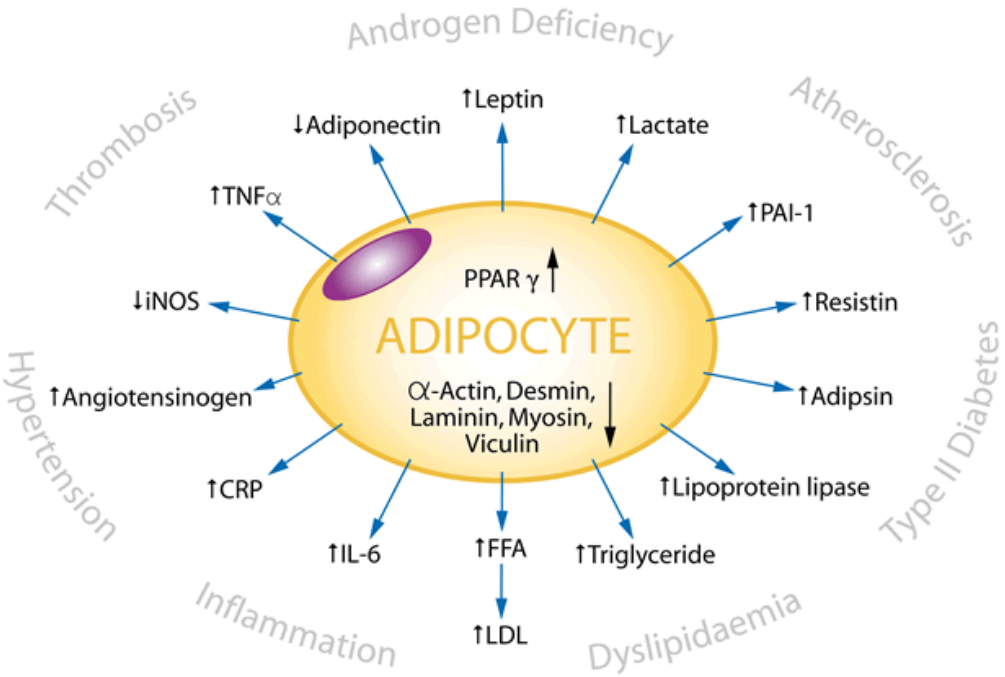

Figure 2. Adipokines secreted by adipose tissue

Some of these exert local autocrine actions and paracrine, which mainly concern remodeling, the adipogenesis and the angiogenesis of the adipose tissue itself and they are not found in circles. Other factors allow the adipocytes to play important roles in the mechanisms of systemic feedback.

Obesity leads to altered expression profiles of various adipokines and cytokines including leptin, adiponectin, IL-6, TNFα and IL-1β.

Particularly, white adipose tissue in obese individuals exhibits chronic mild inflammatory status, mostly defined by infiltration of leukocytes, including

macrophages *[Osborn O et al., 2012]*. For instance, stromal adipocytes directly influence breast cancer cells growth and progression through the secretion of several adipokines *[Andò S et al., 2011; Vona-Davis L and Rose DP et al., 2007]*, which have a chemo-attractant action, causing the recruitment of macrophages. The activated macrophages release pro-inflammatory molecules, including TNFα, IL-1β, and IL-6. These cytokines play both local and systemic actions, contributing to insulin resistance and breast cancer tumorigenesis *[Howe LR et al., 2013; Wolin KY et al., 2010]*.

The two most important adipokines, which are associated with breast cancer development, are leptin and adiponectin. The increased levels of leptin and decreased adiponectin secretion are directly associated with breast cancer development *[Khan S et al., 2013]*.

Furthermore, obesity reduces the oxygen level in the tumor microenvironment leading to hypoxic condition *[Ye J et al., 2007]*. Hypoxia in the peri-tumoral fat is reported to promote tumor site hypoxia. The up regulation of hypoxia-inducible factor-a (HIF-1a) takes place in the hypoxic state, which leads to altered expression of several genes involved in angiogenesis, cell proliferation and apoptosis that ultimately results in cellular adaptation to low oxygen concentration *[Vaupel P, 2004]*.

2.1 Structure and secretion of adiponectin

Adiponectin, also known as ACRP30 (adipocyte complement-related protein of 30 kDa), GBP28 (gelatin-binding protein-28), ADIPOQ, and apM1 gene product (gene product of the adipose most abundant gene transcript-1), is an adipokine hormone that was first discovered in 1995 *[Scherer PE et al., 1995]*. This adipokine is the main protein synthesized and secreted by white adipose tissue. Several studies have reported that also other tissues likely express vastly lower quantities of adiponectin such as brown adipose tissue, skeletal muscle *[Delaigle AM et al., 2004]*, liver *[Kaser S et al., 2005]*, colon *[Fayad R et al., 2007]*, cardiac tissue *[Pineiro R et al., 2005]*, salivary glands *[Katsiougiannis S et al., 2006]*, bone marrow *[Brochu-Gaudreau K et al., 2010]*, fetal tissue *[Brochu-Gaudreau K et al., 2010]*, placenta *[Chen J et al., 2006]*, and cerebrospinal fluid *[Kusminski CM et al., 2007]*. The human adiponectin gene, coding for 244-amino acid polypeptide, is located on chromosome 3q27, a region associated with susceptibility for developing metabolic syndrome and type 2 diabetes in Caucasians *[Comuzzie AG et al., 2001]*. Adiponectin gene spans 16 kb and contains three exons and two introns *[Saito K et al., 1999]* (Fig. 3).

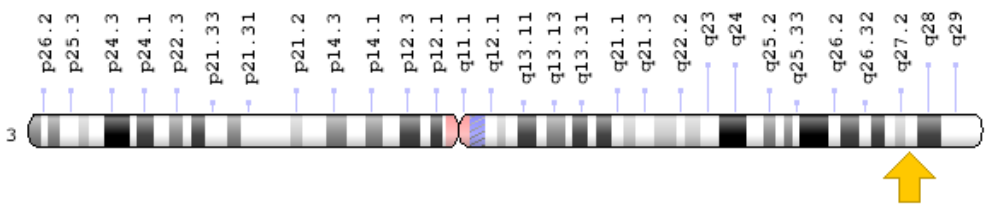

Figure 3. Adiponectin gene locus

Several single nucleotide polymorphisms (SNPs), in the coding region and surrounding sequence, were identified from different populations, which are associated with alterations of adiponectin function and important clinical conditions. In particular, SNPs are associated with the strengthening of adiponectin effects on insulin resistance, type 2 diabetes, obesity, dyslipidemia, and many obesity-related malignancies *[Takahashi M et al., 2000]*. The full-length (fAd) adiponectin (30kDa) consists of four distinct domains (Fig. 4): an amino-terminal signal peptide made up of 18 amino acids, followed by a species-specific variable domain of 28 amino acids, a collagen-like region of 22 Gly-X-Y repeats, and a 137-amino acid carboxy-terminal globular domain *[Nishida M et al., 2007]*.

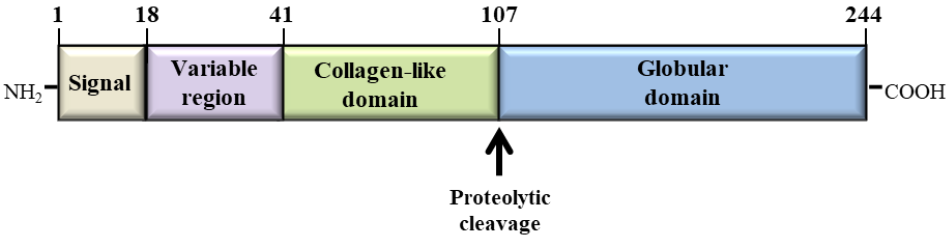

Figure 4. Adiponectin domains

The latter globular domain shows homology with C1q molecule of complement cascade and TNF-trimeric cytokines family *[Shapiro L and Scherer PE, 1998; Yokota T et al., 2000]*. Once synthesized, adiponectin undergoes post-translational modifications, as sialylation and glycosylation that are critical determinants of its activity and binding to its receptors *[Tsao TS et al., 2002; Tsao TS et al., 2003]* (Fig. 5).

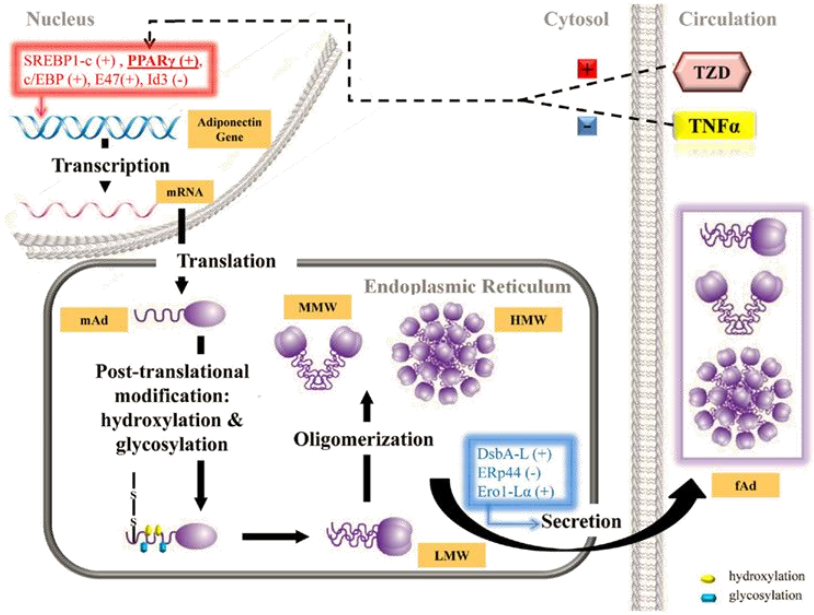

Figure 5. Adiponectin expression and secretion

Even though adiponectin is expressed as a single subunit, full-length adiponectin is assembled in four different isoforms. Before secretion, in analogy to other collagen-domain proteins, adiponectin forms homotrimers (low-molecular weight, LMW), that are generate by non-covalent interactions between the globular head domains. This adiponectin isoform can oligomerize to produce hexamer-rich middle molecular weight (MMW) and high-molecular weight (HMW) forms *[Wang Y et al., 2006]*. The monomeric form of adiponectin is thought to be present only in the adipocyte because it has not yet been detected in the circulation *[Chandran M et al., 2003]*. Particularly, in plasma adiponectin is found in its full-length (fAg) or as a smaller fragment produced by proteolytic cleavage of fAg at amino acid 110, that gives rise to a globular domain of the

protein, gAd *[Pajvani UB et al., 2003; Waki H et al., 2003]*. Globular adiponectin is probably generated by elastase digestion *[Fruebis J et al., 2001; Waki H et al., 2005]* (Fig. 6).

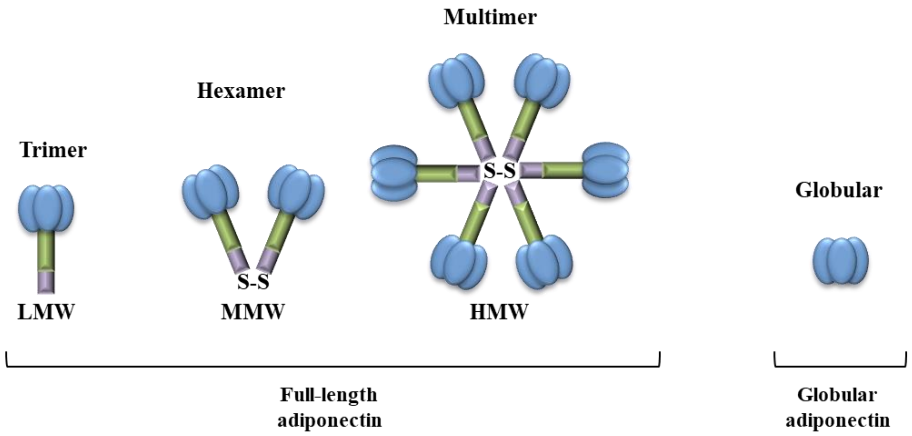

Figure 6. Adiponectin isoforms

Experimental evidences suggest that the structural heterogeneity of adiponectin serum forms induces different biological response dependent on target tissue. The HMW isoform constitutes nearly 70% of circulating adiponectin biologically active form and acts as pro-inflammatory cytokines. Many reports show that this adiponectin isoform mediates the majority of adiponectin's effects in the liver *[Trujillo ME et al., 2005]*, endothelial cells *[Ouchi N et al., 2004]*, and probably in skeletal muscle *[Hada Y et al., 2007]*, and is strongly associated with insulin resistance, cardiovascular diseases and metabolic syndrome *[Nakano Y et al., 2006; Tishinsky JM et al., 2012]*. On the other hand, LMW isoform is present in low plasma concentration, probably due to its shorter half-life, and exerts anti-inflammatory actions *[Fruebis J et al., 2001; Pajvani UB et al., 2003]*. The

globular adiponectin appears to be as efficient as fAd, decreasing serum glucose and free fatty acid levels *[Berg AH et al., 2001]*.

Circulating adiponectin levels are regulated by different genetic, hormonal, inflammatory, dietary, and pharmacological factors. The levels of this adipokine are abundant in plasma, with concentrations ranging from 3 to 30 μg/ml *[Chandran M et al., 2003]*, and they are about two to three times lower in male compared to female, which may due to the difference in concentration of estrogen and androgen. This suggest a presumably stimulating role of estrogen on adiponectin synthesis and secretion. The concentration of adiponectin in the circulation displays a diurnal variation, reaching nadir at night and peak in the morning *[Cnop M et al., 2003; Gavrila A et al., 2003]*, and is several times higher than other cytokines, such as IL-6, TNF-α and leptin *[Petridou ET et al., 2009; Petridou E et al., 2006]*. Unlike most of the other adipocyte derived proteins, serum adiponectin levels are reduced in obesity, especially in central obesity, and correlate negatively with body mass index (BMI) *[Galic S et al., 2010]*. Thus, circulating adiponectin levels are lower in obese than normal-weight individuals *[Surmacz E, 2013]* (Fig. 7).

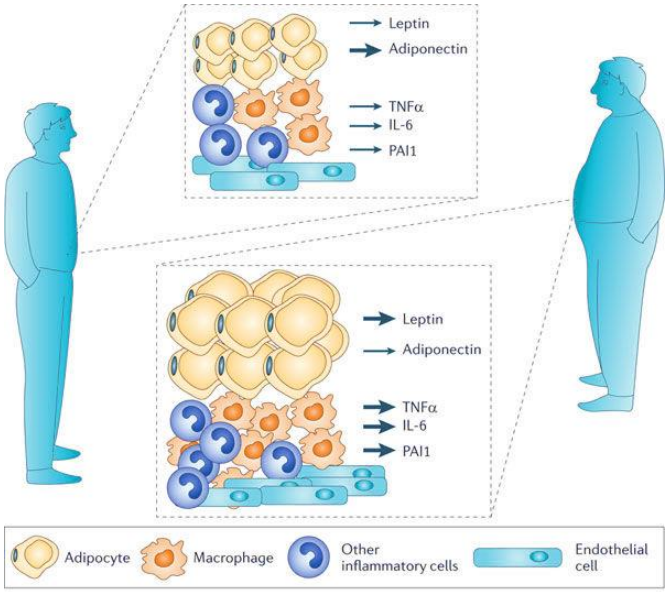

Figure 7. Changes in adipokines production in obesity.

Moreover, low-circulating levels of adiponectin are found in type 2 diabetes *[Okamoto Y et al., 2006]*, and mice lacking adiponectin develop metabolic syndrome, with insulin resistance, glucose intolerance, hyperglycemia, and hypertension *[Kubota N et al., 2002; Maeda N et al., 2002]* (Fig. 8).

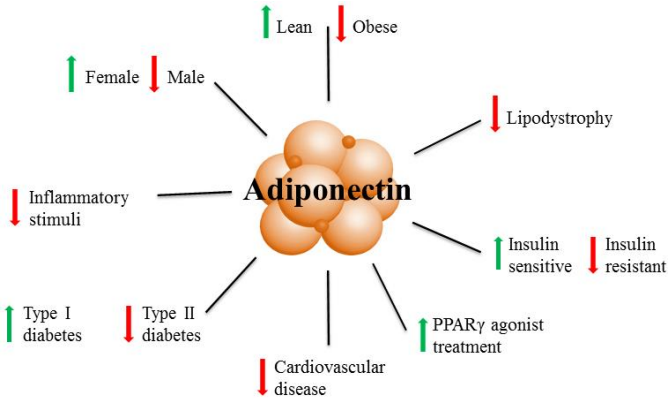

Figure 8. Physiological effects of adiponectin

The mechanisms responsible for the adiponectin down regulation is not known. It has been speculated that its reduced levels in obesity may be caused by the enhanced production of pro-inflammatory cytokines, in particular, by the tumor necrosis factor α (TNFα) *[Tilg H et al., 2006]* and IL-6 that are considered inhibitors of adiponectin synthesis. However, other potential explanations of adiponectin down-regulation could be: the generation of a hypoxic micro-environment in augmented fat mass adipocytes, increased production of insulin like growth factor binding protein-3, which inhibits adiponectin transcription via hypoxia inducible factor-1a dependent pathway, and the expression of its receptors during the development of obesity *[Dalamaga M et al., 2012]*. Indeed, adiponectin may control its own and probably the expression of its receptor via a regulatory feedback loop. Regarding other hormonal factors, adiponectin production may be negatively regulated by prolactin, GH, and glucocorticoids *[Swarbrick MM and Havel PJ, 2008]*. Many studies also have found that plasma adiponectin expression and secretion is up regulated by some anti-diabetic drugs, such as PPAR-γ agonists (thiazolidinedione-TZD), which increase insulin sensitivity *[Combs TP et al., 2002; Maeda N et al., 2001; Yu JG et al., 2002]*, while anti-HIV drugs, such as protease inhibitors, decrease it.

Control of total and HMW adiponectin expression, secretion, and circulating serum levels plays a substantial role in obesity and associated cancer risks; yet, the mechanisms governing these processes remain unclear.

2.2 Adiponectin receptors

Functions of adiponectin have been found to be mediated by three receptor subtypes: the adiponectin receptor 1 (Adipo R1), the adiponectin receptor 2 (Adipo R2) *[Brochu-Gaudreau K et al., 2010]*, and T-cadherin. The first two are integral membrane proteins, and consist of seven transmembrane domains with an internal N-terminal collagenous domain and an external globular C-terminus; thus, they are both structurally and functionally distinct from G-protein-coupled receptors (GPCR) *[Yamauchi T et al., 2003]*. Adipo R1 and Adipo R2 share 67% identity of protein sequence but exhibit different binding affinities for diverse forms of adiponectin. Adipo R1 presents high affinity for gAd and low affinity for the full-size ligand *[Wang H et al., 2004]*, while Adipo R2 has intermediate affinity for both forms of adiponectin. Although both receptors are expressed ubiquitously, one or the other receptor usually prevails. Adipo R1 being found abundantly in skeletal, while Adipo R2 is mainly present in hepatocytes *[Chen X and Wang Y, 2011]*. This different expression of adiponectin receptors is related with the fact that gAd exerts its insulin mimetic and insulin-sensitizing effect more efficiently compared to fAd in skeletal muscle *[Yamauchi T et al., 2003]*.

The non-classical third adiponectin receptor is a glycosyl-phosphatidylinositol receptor that lacks a transmembrane domain, belonging to the cadherin family. T-cadherin is expressed in endothelial, smooth muscle cells and in the myocardium, and shows affinity for MMW and HMW adiponectin isoforms but not for the trimeric or globular forms of adiponectin *[Asada K et al., 2007; Chan DW et al., 2008; Hug C et al., 2004]*. Numerous studies have suggested the involvement of this receptor, which plays an important role in cell adhesion and in calcium-

mediated cell to cell interactions and signaling *[Hug C et al., 2004]*, in mediating pro-angiogenic and cardio-protective functions.

Since T-cadherin lacks an intracellular domain needed for signal transduction, it has been suggested that it may function as a co-receptor by competing with Adipo R1 and Adipo R2 for adiponectin binding or interfering with adiponectin signal transduction *[Lee MH et al., 2008]*.

The expression of Adipo R1/R2 seems to be decreased in obesity, thereby diminishing adiponectin sensitivity, which in turn leads to a vicious cycle of insulin resistance *[Ouchi N et al., 2000]*. Adiponectin receptors are expressed in a plethora of malignant tissues including breast *[Takahata C et al., 2007]*, prostate *[Mistry T et al., 2006]*, hepatocellular, gastric, colon *[Kim AY et al., 2010]*, lung cancer *[Barb D et al., 2007; Petridou ET et al., 2007]* and pancreatic adenocarcinoma *[Dalamaga M et al., 2009]*. Although the functional relevance of adiponectin receptors in cancerous cells has not yet been clarified, there is evidence that activation of adiponectin receptors limits the proliferation of cancer cell lines *in vitro [Barb D et al., 2007]*.

2.3 Adiponectin physiology

Adiponectin exerts pleiotropic effects on different tissues and organs, playing pivotal role against various diseases, including type 2 diabetes, central obesity, insulin resistance, cardiovascular disease, and several malignancies *[Chandran M et al., 2003]*. Adiponectin exhibits insulin-sensitizing, anti-inflammatory, anti-atherogenic, and anti-tumoral effects as well as distinct effects on lipid

metabolism *[Barb D et al., 2007; Kelesidis I et al., 2006; Ziemke F et al., 2010]*. It is well known that this adipokine aids to insulin sensitivity through several mechanisms, such as the regulation of glucose and lipid metabolism by stimulating fatty acid oxidation and decreasing hepatic glucose output, the increased mitochondria number and function and the improvement to insulin signaling pathway. Particularly, adiponectin enhanced insulin-induced phosphorylation of the insulin receptor and the ability of insulin to activate the phosphorylation of the adaptor protein insulin receptor substrate 1 (IRS-1) *[Stefan N et al., 2002; Wang C et al., 2007]*. In addition, adiponectin exerts a direct effect on insulin secretion regulating pancreatic β-cell proliferation *[Kharroubi I et al., 2003]*.

Several studies have been reported that adiponectin explains its anti-atherogenic propriety acting in the injured vascular wall by reducing the ability of macrophages to transform into foamy cells, inhibiting subendothelial lipid accumulation, and stimulating vasodilatation and increased blood flow *[Ouchi N et al., 1999]*.

Adiponectin also reduces secretion of pro-inflammatory cytokines, such as IL-6 and TNFα, and acts a mediator of the anti-inflammatory cytokine IL-10 *[Kubota N et al., 2007]*. Thus, low adiponectin levels cause the increased expression of pro-inflammatory cytokine resulting in chronic inflammation and inflammation-associated cancers.

2.4 Adiponectin signaling pathways

The interaction between adiponectin and its membrane receptor Adipo R1 and Adipo R2 induces the activation of a plethora of intracellular signaling pathways, exerting a variety of complex metabolic and immunological effects. Recently, it has been identified many different adiponectin receptor binding proteins *[Buechler C et al., 2010]*. Among these, the first and best characterized is the adaptor protein APPL1 which containing a pleckstrin homology domain, a phosphotyrosine binding (PTB) domain, and a leucine zipper motif *[Buechler C et al., 2010; Mao X et al., 2006]*. APPL-1 interacts with the N-terminal intracellular region of Adipo R1 and Adipo R2 through its PTB domain, thereby inducing adiponectin actions through the sequential activation of downstream signaling. Emerged data suggests that APPL1 plays an important role in mediating many of adiponectin's effects, including metabolic, anti-inflammation, anti-atherogenic, and cytoprotection responses *[Deepa SS et al., 2009; Obeid S and Hebbard L, 2012]*. APPL-1 also plays a crucial role in the cross talk between adiponectin and insulin-signaling pathways *[Deepa SS et al., 2009]*.

Adiponectin exerts its effects mostly through the activation of AMP-activated protein kinase (AMPK) but also mitogen-activated protein kinase (MAPK), phosphatidylinositol 3-kinase (PI3K)-v-akt murine thymoma viral oncogene homolog (Akt), peroxisome proliferator-activated receptor alpha (PPAR-α), mammalian target of rapamycin (mTOR), nuclear factor-B (NF-B), c-Jun N-terminal kinase (JNK), and signal transducer and activator of transcription (STAT3) *[Dalamaga M et al., 2012; Obeid S and Hebbard L, 2012]* (Fig. 9).

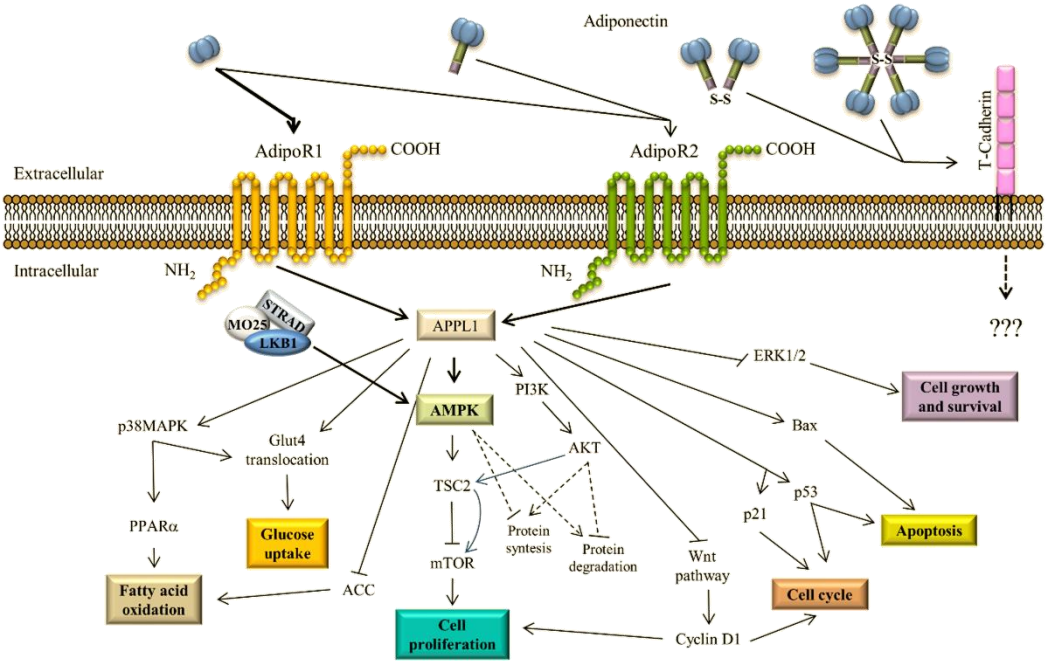

Figure 9. Adiponectin signaling pathways

AMPK is a sensor of cellular energy charge, which regulates physiological processes that consume or regenerate ATP to restore the energy homeostasis in the cell *[Hardie DG et al, 2003]*. AMPK is switched on during situation in which ATP cellular level is depleted and both ADP and AMP level are increased. Activation of AMPK restores cellular energy homeostasis promoting glucose uptake and utilization, which results in an increased fatty-acid oxidation, and reducing energy-consuming anabolic processes, such as protein synthesis and gluconeogenesis in the liver. AMPK is a heterotrimeric serine/threonine protein kinase, consisting of a catalytic subunit α, and two regulatory subunits, β and γ. Particularly, AMP triggers AMPK activation by binding to a pair of cystathionine-beta-synthase (CBS) domains *[Hardie DG et al., 2004]*, located on the AMPKγ subunit, thereby stimulating phosphorylation of Thr172 in T-loop of AMPKα-

catalytic subunit *[Carling D et al., 2004; Hardie DG et al., 2004; Kahn et al, 2005]*. So far, it has been identified two kinases that phosphorylate AMPK in Thr172, when ATP levels fall: the upstream liver kinase B1 (LKB1) and calcium-calmodulin-dependent protein kinase kinase *β* (CaMKK*β*) *[Anderson KA et al., 1998; Hawley SA et al., 2003; Woods A et al., 2003]*.

LKB1 (also known as serine/threonine kinase 11, STK11) has been identified as a critical cancer suppressor in many tumor cells, even though recent studies have been reported some paradoxical results, and imply that under specific conditions, LKB1 can be a cancer promoter. Physiologically, LKB1 possesses multiple cellular functions in the regulation of cell bioenergetics metabolism, cell cycle arrest, embryo development, cell polarity, and apoptosis.

Studies carried out recently have evidenced that the cytoplasmic localization of LKB1 is crucial for its role in mediating biological processes. Under normal condition, LKB1 is mostly localized in the nucleus, with a small portion in the cytoplasm. The nuclear accumulation of LKB1 may be attributed to its nuclear signal domain presents in the N-terminal region. The ability of LKB1 to activate AMPK depends on the interaction with two proteins, the STe20-Related Adaptor (STRAD) and the scaffolding MOuse protein 25 (MO25), in the cytosol *[Alessi DR et al., 2006; Baas AF et al., 2003]*. The interaction between LKB1 and STRAD induces the translocation of LKB1 from the nucleus to the cytoplasm, and the acquisition of kinase function through a conformational change with a consequent AMPK phosphorylation. Instead MO25, directly binding to the conserved Trp-Glu-Phe sequence at the STRAD carboxyl-terminus, plays an important role in stabilizing this complex in the cell cytoplasm as well as

enhancing LKB1 catalytic activity *[Baas AF et al., 2003; Milburn CC et al., 2004; Zeqiraj E et al., 2009]*.

Once activated, AMPK regulates, directly or indirectly, a numbers of metabolic enzymes involved in a variety of biological processes, including cellular growth and proliferation, fatty acid synthesis, and mRNA translation. Among the main AMPK downstream proteins can be detected acetyl-CoA carboxylase (ACC), fatty acid synthetase (FAS), and mTOR.

An intermediate in the mTOR regulation is the tuberous sclerosis complex, consists of two proteins TSC1 and TSC2 that is considered a critical integrator of growth factor, nutrient and stress signals to control protein synthesis, cell growth and other cellular processes. The TSC1/TSC2 complex acts as a GTP-activating protein (GAP) on the mTOR activator, Rheb, which is low relative to that of other small G-proteins, thereby expending the conversion of Rheb-GTP into Rheb-GDP *[Alessi DR et al., 2006]*.

Interestingly, active AMPK suppresses mTOR signaling through a molecular mechanism that involves the phosphorylation of TSC2 at Thr1387. This phosphorylation enhances the activity of TSC1/TSC2 complex to inhibit mTOR signaling and its downstream effectors ribosomal p70 S6 kinase (S6K) and 4EB1, via TSC2 GAP activity *[Huang J and Manning BD, 2008; Pan D et al., 2004]* (Fig. 10).

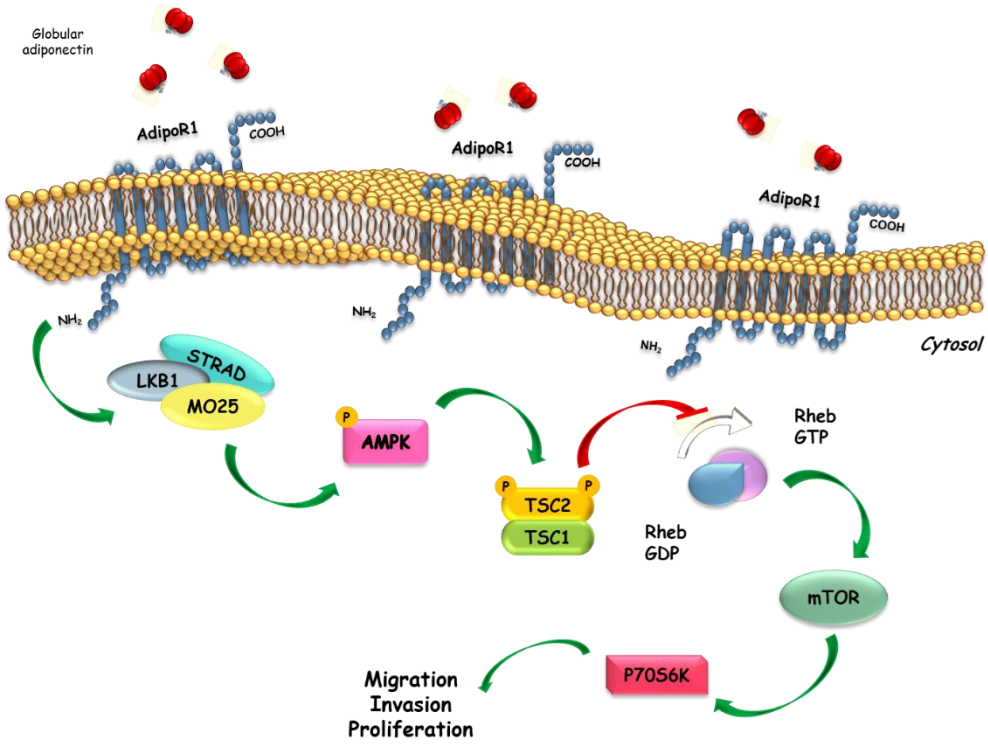

Figure 10. AMPK transductional pathway

LKB1/AMPK signaling also can inhibit fatty acid synthesis enhancing the phosphorylated status of ACC, leading to its inactivation and inhibit sterol synthesis through suppression of 3-hydroxy-3-methylglutaryl-CoA reductase (HMGR).

Adiponectin exerts its cytoprotective and anti-inflammatory effects via the PI3K/Akt signaling pathway. Activation of PI3K leads to a cascade of events resulting in cellular survival, growth and proliferation, and an increase in glycolysis and fatty acid synthesis. Additionally, Akt is another key regulator of the TSC2 pathway. Indeed, PI3K/Akt removes the inhibitory effect of AMPK/TSC2 axis on Rheb, through the directly phosphorylation of TCS2 at Ser939 and Thr1462. This determines the activation of both mTOR and its

downstream protein p70S6k, with the consequent maintenance of cell growth and survival *[Gan B et al., 2010; Jia S et al., 2008; Shaw RJ and Cantley LC, 2006]* (Fig. 11).

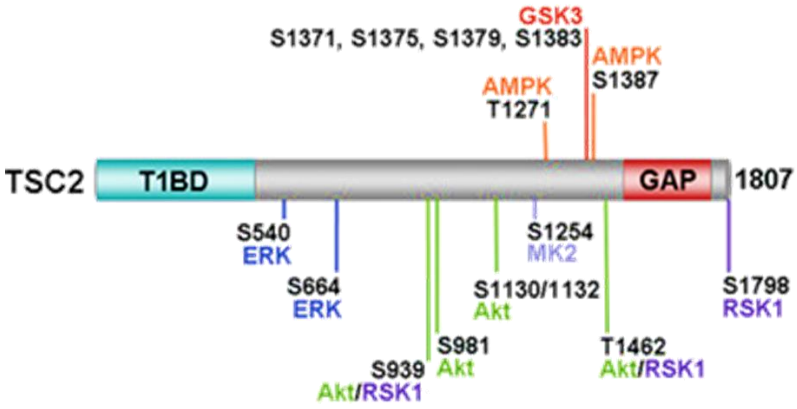

Figure 11. Direct phosphorylation sites on TSC2

Furthermore, adiponectin regulates the activity of MAPKs superfamily members, including c-Jun N-terminal Kinases (JNK), MAPKp38 and extracellular signal-regulated kinases (ERK) 1/2. The proliferative effects of adiponectin could be mediated by the activation, *via* APPL-1, of the ERK1/2-MAPK pathway, which is crucial for cell cycle initiation, cell growth, and survival *[Pearson G et al., 2001]*, while cJNK and MAPKp38 seems to have variable effects on cell proliferation and apoptosis.

In addition, adiponectin exerts its insulin-sensitizing effects through the activation of PPAR-α, thereby enhancing fatty-acid combustion and energy consumption, leading to a tissue decrease content of triglycerides in the liver and skeletal muscle, and improving insulin sensitivity *in vivo [Yamauchi T et al., 2001]*.

Particularly, the stimulation of PPAR-α could be attributed to adiponectin binding to AdipoR2 *[Yamauchi T et al., 2007]*.

The inhibition of nuclear factor kappa-light-chain-enhancer of activated B cells (NF-kB) pathway, induced by adiponectin through the suppression of inhibitor of NF-kB phosphorylation, could represent an important molecular mechanism for monocyte adhesion inhibition to endothelial cells, conferring to this adipokine anti-inflammatory and anti-atherosclerotic property *[Ouchi N et al., 2000]*.

Adiponectin also exerts its anti-proliferative effects through the inhibition of Wnt signaling pathway. The activation of the cell surface receptor, frizzled, by Wnt, induces the inactivation of glycogen synthase kinase-3β (GSK3β) and enhanced nuclear accumulation of β-catenin *[Karim RZ et al., 2004]*, leading positive effects on cellular growth and proliferation. Many reports have been shown that adiponectin stimulate Wnt-inhibitory factor 1, which antagonizes Wnt signaling and cell progression, causing reduction of cyclin D1 expression and block of cell cycle *[Liu J et al., 2008]*.

Moreover, adiponectin induces cell cycle arrest though the down-regulation of c-myc, cyclin D, and Bcl-2 levels, and apoptosis by increasing p53, p21 and Bax expression *[Dieudonne MN et al., 2006; Luo Z et al., 2005; Obeid S et al., 2012]*.

2.5 Adiponectin and breast cancer

Emerged data addresses adiponectin as a crucial adipokine involved in breast carcinogenesis in women with obesity. Indeed, it has been well documented that the pathogenesis of mammary cancer is not only dependent on genetic alterations but also largely on the interactions between malignant cells and components of the

breast microenvironment, which exerts an important influence on the phenotype of the neoplastic cells and on tumor progression. Particularly, several recent studies have shown a close association between low-serum adiponectin concentrations and a high incidence of obesity-related cancer diseases, including endometrial, prostate, gastric and breast cancer *[Barb D et al., 2006; Chen DC et al., 2006; Kelesidis I et al, 2006; Mantzoros C et al, 2004]*. Moreover, it has been suggested that breast tumors in women with hypoadiponectinemia are more likely to show a biologically aggressive phenotype such as large size, high histological grade, estrogen receptor negativity, and increased metastatic potential *[Mantzoros C et al, 2004; Miyoshi Y et al, 2003]*. Thus, obesity has been correlated with poor breast cancer prognosis *[Miyoshi Y et al., 2003]*. However, the role of this adipokine on breast development and progression is still unclear, and it seems to be dependent on cell types. Many reports have identified adiponectin as a critical regulator of tumor cell proliferation. Generally, adiponectin has been shown to inhibit, with a varying degree of efficiency, the growth of the ERα-normal MCF-10A human mammary epithelial cells. Several *in vitro* and *in vivo* studies have revealed that low-adiponectin doses mediate an anti-proliferative response in ERα-negative MDA-MB-231 breast cancer cells through the regulation of genes involved in cell cycle, such as p53, Bax, Bcl-2, c-myc, and Cyclin D1 *[Dieudonne MN et al., 2006; Luo Z et al., 2005; Obeid S and Hebbard L, 2012]*. Furthermore, it has been reported that low doses of adiponectin inhibited ERK1/2 signaling *[Dieudonne MN et al., 2006]* and limited the anchorage-independent growth *[Dieudonne MN et al., 2006; Mauro et al., 2015]* of MDA-MB-231 breast cancer cells. In ERα-negative breast cancer cells, most of the effects of this adipokine are

mediated by the AMPK activation, which in turn inhibits mTOR/S6 axis, through tuberous sclerosis complex2 (TSC2), thus counteracting carcinogenesis *[Inoki K et al., 2003; Luo Z et al., 2005]*. In addition, activated AMPK plays a crucial role in the regulation of growth arrest and apoptosis by stimulating p21 and p53 *[Igata M et al., 2005]*. Activation of protein phosphatase 2A (PP2A), a tumor suppressor involved in the inhibition of Akt and small GTP hydrolase Ras-like A *[Sablina AA and Hahn WC et al., 2007]*, was also shown to depend on adiponectin/AMPK signaling in MDA-MB-231 breast cancer cells *[Kim KY et al., 2009]*. On the other hand, in ERα-positive MCF-7 and T47D cells, adiponectin, at low concentrations, appears to stimulate *[Landskroner-Eiger S et al., 2009; Pfeiler GH et al., 2008]* or to inhibit cell growth *[Dieudonne MN et al., 2006; Grossmann ME et al., 2008; Korner A et al., 2007]*, or to play no noticeable effect *[Treeck O et al., 2008]*. Possible explanations of the different cellular responses may be different content of ERα, differences in culture conditions, specific adiponectin isoform used, incubation time, or dosage.

Recent studies have elucidated the complex mechanisms involved in the adiponectin response in breast cancer growth in dependency on ERα status. Particularly, it has demonstrated that, in ERα-positive breast cancer cells, globular adiponectin binds to Adipo R1 and provokes physical interaction between its receptor, the adaptor protein APPL1, membrane ERα, IGF-IR, and c-Src, leading to MAPK phosphorylation. This contributes to ERα activation at genomic level through the phosphorylation at Ser118. For instance, MAPK activation, induced by adiponectin/ERα-mediated effect, produces MCF-7 cell proliferation, and it represents the discriminator factor determining the opposite effect induced by

adiponectin in ERα-positive and ERα-negative breast cancer cells *[Mauro L et al., 2014]*. Furthermore, in MCF-7 cells adiponectin influences cell proliferation by upregulating the expression of Cyclin D1 and increasing their anchorage-independent growth, cell-cell adhesion and 3D growth. It is extremely intriguing to note how the breast cancer growth in ERα-positive cells depends on an increased MAPK activation and reduced AMPK phosphorylation. On the contrary, phosphorylation of AMPK resulted stably upregulated in ERα-negative cells concomitantly with an inhibition of cell growth *[Mauro et al., 2015]*. This data provides further evidences on cell-type dependency of adiponectin action in breast cancer.

Many studies point toward a direct negative effect of adiponectin on the PI3K/Akt pathway, involved in the positive regulation of a plethora of effector molecules that influence cell survival, growth, and proliferation. Treatment of breast cancer cells with adiponectin was shown to significantly reduce the phosphorylation and activation of PI3K and Akt *[Li G et al., 2011]*.

Adiponectin plays also inhibitory effects on Wnt signaling, an important pathway implicated in carcinogenesis. Several studies have been shown that adiponectin antagonizes Wnt signaling and cancer progression through a direct stimulation of Wnt-inhibitory factor-1 *[Liu J et al., 2008]* or a decrease Akt phosphorylation *[Wang Y et al., 2006]*. In MDA-MB-231 breast cancer cells, prolonged adiponectin treatment inhibits the phosphorylation of GSK3β, induces degradation of β-catenin, causing reduction of Cyclin D1 expression and block of cell cycle *[Wang Y et al., 2006]*.

2.6 Potential therapeutic of adiponectin

Obesity-related cancer development rates in women are elevated globally in economically developed countries, making it one of the primary health problems in the worldwide. Due to its importance in carcinogenesis, adiponectin may represents a promising potential therapeutic tool for treating breast cancer.

Because it is extremely difficult to synthesize adiponectin and to convert its full-size protein into a viable drug to be use in human, research efforts should be aimed at identifying ways to increase endogenous circulating adiponectin levels, to increase adiponectin receptors and to modulate their sensitivity.

In recent years, several adiponectin receptor agonists have been developed and tested to treat hypoadiponectinemia, typically present in obese subjects and correlated with tumorigenesis *[Dalamaga M et al., 2012]*.

Interestingly, a new adiponectin-based short peptide, ADP 355, mimicking globular adiponectin action through the bind to Adipo R1, reduced proliferation in many cancer cell lines, modulating several adiponectin-signaling pathways, such as AMPK, Akt, STAT3, and ERK1/2. Furthermore, ADP 355 suppressed the growth of orthotopic human breast cancer xenografts *in vivo [Otvos L Jr et al., 2011; Surmacz E, 2013; Surmacz E and Otvos L, 2015]*.

Lately, it has been optimized the monomeric structure of this peptide, generating a dimer with 5-10 fold increased agonistic activity *[Otvos L Jr et al., 2015]*.

Another pharmacological agent that present a tangible benefit in breast cancer treatment is the anti-diabetic drug Metformin. It can prevent breast cancer cell growth through the stimulation of AMPK, inhibition of mTOR signaling and reduction of HER2 protein. Thus, metformin appears to partially mimic

adiponectin signal in the treatment of obesity-related breast cancer *[Khan S et al., 2013; Surmacz E, 2013]*.

Adiponectin gene and protein expression is enhanced in a dose-dependent manner by the synthetic PPARγ agonists, such as Rosiglitazone and Troglitazone, sustaining anti-cancer activity *[Wei S et al., 2009]*.

Although understanding the link of adiponectin with cancer might provide potential therapeutic targets, lifestyle amelioration remains the most important component in preventing obesity-related malignancies. Indeed, reduction of calories in diet, physical exercise, moderate amounts of alcohol, increase adiponectin production, preventing cancer development *[Katira A and Tan PH, 2016]*.

Thus, therapeutic strategies to increase adiponectin concentration, such as up regulation of its plasma concentration, increased expression of adiponectin receptors, or the development of adiponectin receptor agonists, as well as the administration of human recombinant adiponectin, should be considered with the goal of enhancing pharmacological armamentarium for treating malignancies in women in the near future.

AIM

A significant increased relationship has been found between adiponectin levels and breast cancer risk *[Katira A and Tan PH, 2016]*.

Recent studies demonstrated that in MCF-7 breast cancer cells adiponectin/AdipoR1 signaling, in response to low concentration of adiponectin, was able to sustain a stimulatory effect on cell growth *[Mauro L, et al., 2014; Mauro L, et al., 2015; Panno ML et al., 2016]*. In contrast, the classically described inhibitory effects of adiponectin on cell growth and proliferation were observed in MDA-MB-231 cells *[Mauro L, et al., 2014; Mauro L, et al., 2015; Panno ML et al., 2016;]*.

ERα-positive MCF-7 and ERα-negative MDA-MB-231 cells have been reported to exhibit higher expression of Adipo R1 *[Takahata C et al., 2007]*, providing the most suitable model to study how adiponectin/Adipo R1 signaling may work in the presence or absence of ERα expression.

Thus, the aim of the present study, was to investigate the molecular mechanisms sustaining such a dichotomic effects induced by adiponectin concentrations comparable to those found in obese women, focusing on the uncoupling role of ERα on LKB1/AMPK/mTOR signaling in breast cancer cell lines.

Materials and Methods

1.1 Cell culture

Human MCF-7 and MDA-MB-231 breast cancer epithelial cells were obtained from American Type Culture Collection where they were authenticated, stored according to supplier's instructions, and used within 4 months after frozen aliquots resuscitations (Manassas, VA). Every 4 months, cells were authenticated by single tandem repeat analysis at our Sequencing Core; morphology, doubling times, estrogen sensitivity, and mycoplasma negativity were tested (MycoAlert, Lonza). The cells were maintained in DMEM/F-12 containing 5% fetal bovine serum and supplemented with 1% L-glutamine and 1% penicillin/streptomycin (Life Technologies, Milan, Italy). Cells were cultured in 1% dextran charcoal-stripped fetal bovine serum to reduce steroid concentration, at least 24h before each experiment.

1.2 Plasmids

The DNA construct encoding human wild-type GST-LKB1 was purchased from University Dundee, Scotland. Wild-type YFP-ERα plasmid was generously provided by Dr S.A.W. Fuqua (Baylor College of Medicine, Houston, TX, USA). XETL plasmid containing an estrogen-responsive element, was a gift from Dr D. Picard (University of Geneva, Geneva, Switzerland).

1.3 Western Blotting

Whole cell extracts were prepared in ice-cold lysis buffer containing 50 mM HEPES (pH 7.5), 150 mM NaCl, 1.5 mM $MgCl_2$, 1 mM EGTA, 10% glycerol, 1% Triton X-100, supplemented with protease and phosphatase inhibitors (aprotinin, phenylmethylsulfonyl fluoride, and sodium orthovanadate). The protein content was determined using Bradford dye reagent (Bio-Rad). Equal amounts of total protein were resolved, under denaturing conditions, on SDS-polyacrilamide gels and transferred onto a nitrocellulose membrane by electro-blotting. The membranes were blocked in 5% non-fat dry milk and probed overnight at 4°C with an appropriate dilution of specific primary antibodies. The antigen-antibody complex was detected by incubation of the membranes for 1 h at room temperature with a peroxidase-coupled anti-IgG antibody and revealed using an enhanced chemiluminescence system (ECL, Santa Cruz, Biotechnology, Milan, Italy).

1.4 Antibodies

The following antibodies were used: anti-phosphoAkt^{Ser473}, LKB1, anti-phosphoMAPK (ERK1/2$^{Thr44/Tyr42}$), MAPK (ERK1/2), STRAD, MO25, ERα, and βActin from Santa Cruz Biotechnology; Akt, anti-phosphoAMPK^{Thr172}, AMPK, anti-phosphoLKB1^{Ser428}, anti-phosphoACC^{Ser79}, anti-phosphoTSC2$^{Thr1462/Ser939/Ser1387}$, TSC2, anti-phosphomTOR^{Ser2448} , mTOR, and anti-phospho p70S6K^{Thr389}, and p70S6K from Cell Signaling technology; anti-GST from Novus Biologicals.

1.5 Transfections

Cells were grown into 10 cm dishes. The medium was replaced with DMEM lacking phenol red as well as serum on the day of transfection, which was done using the FuGENE 6 Reagent as recommended by the manufacturer.

A set of experiments was performed co-transfecting MCF-7 with 8 µg of LKB1-GST and 8 µg ERα-YFP plasmids.

In another set of experiments cells were co-transfected with a constant dose of LKB1-GST (8 µg) and increasing doses of ERα-YFP (5, 10, 20 µg) plasmids. After transfection the cells were treated and lysed as described above.

Cellular lysate was used to perform the immunoprecipitation.

1.6 Immunoprecipitation analysis

Cells were grown into 10 cm dishes and then switched to medium lacking serum for 24 h, before to add 1 and 5 µg/ml of adiponectin for the times indicated in figure legend. For LKB1-GST immunoprecipitation, 500 µg of cytosolic and/or nuclear extracts were pre-cleared for 1h with protein A/G-Agarose beads (Santa Cruz, Biotechnology) at 4°C and centrifuged at 12,000 x g for 5 minutes, to avoid nonspecific binding. The supernatants were incubated overnight at 4°C with 10µl of anti-GST in HNTG buffer (20 mM HEPES, pH 7,5, 150 mM NaCl, 0.1% Triton X-100, 10% glycerol, 0.1 mM Na_3VO_4, 1 mM phenylmethylsulfonyl fluoride, 10 µg/ml aprotinin). The antigen-ab complex were recovered by incubation with protein A/G-agarose for 2 h in HNTG buffer rotating. For ERα-YFP immunoprecipitation 500 µg of

cytosolic extracts were incubated overnight at 4°C, shaking with 700 µl of lysis buffer and 25 µl of GFP-nAb Agarose (Allele GFP-nAb), previously equilibrate in 1X Binding Buffer (200 mM Tris-HCl pH 7.5, 3 M NaCl). The beads containing bound proteins were washed three times by centrifugation in HNTG or 1X Wash Buffer (100 mM Tris-HCl p H 7.5, 5 M NaCl), then denatured by boiling in Laemmli sample buffer, and analyzed by Western Blotting to identify the co-precipitating effector proteins. Immunoprecipitation with protein A/G or GFP-nAb Agarose alone was used as the negative control.

1.7 Phopho-ACC measurement by ELISA

Phospho-Acetyl-CoA Carboxylase (Ser79) was measured by PathScan Phospho-Acetyl-CoA Carboxylase (Ser 79) Sandwich ELISA Kit (Cell Signaling). MCF-7 and MDA-MB-231 were grown in PRF-SFM and stimulated with 1 or 5 µg/ml adiponectin for 30 minutes or 24 h. Cells were then lysed in 500 µl of ice-cold cell lysis buffer (1 mM β-glycerophosphate, 1mM EDTA disodium salt, 1 mM EGTA, 1 µg/ml leupeptin, 150 mM sodium chloride, 20 mM sodium Pyrophosphate, 25 mM Sodium Fluoride, sodium orthovanadate, 20 mM Tris-CI, Triton X- 100 in water) plus 1 mM PMSF, scraped and sonicated. Cell lysates were diluted in 100 µl of Sample Diluent (0.1% Tween-20, < 0.1% sodium azide in 20X PBS) and added into the appropriate microwell for 2 h at 37°C. Next the wells were washed four times with 200 µl of 1X Wash Buffer (1% tween-20, 0.5% Kathon® in 20X

PBS) and incubated with 100 µl of Detection Antibody at 37°C for 1 h. The washing procedure was repeated for another four times and then 100 µl of HRP-linked secondary antibody was incubate for 30 minutes at 37°C. TMB substrate (0.05% 3,3',5,5' tetramethylbenzidine, 0.1% hydrogen peroxide complex polypeptides in midly acidic buffer) was used to detect endogenous levels of Acetyl-CoA carboxylase when phosphorylated at Ser79. The absorbance readings at 450 nm are shown as % *vs* C. Results are presented as mean of three separate experiments.

1.8 RNA silencing

MCF-7 were transfected with RNA duplex of stealth siRNA (Qiagen, Milan, Italy) targeted for the human ERα or LKB1 mRNA sequence, or with a control siRNA that does not match with any human mRNA, used as a control for non-sequence-specific effects. Cells were transfected using RNAiFect Transfection Reagent (Qiagen, Milan, Italy) as recommended by the manufacturer with minor modifications. After 5 h transfection medium was changed with serum-free medium and cells were treated as indicated.

1.9 Fluorescence microscopy

MCF-7 and MDA-MB-231 cells were fixed with 4% paraformaldehyde, permeabilized with PBS 0.2% Triton X-100 followed by blocking with 5% bovine serum albumin and incubated with anti-human-LKB1 antibody. 4',6-

Diamidino-2-phenylindole (DAPI, Sigma-Aldrich, Milan, Italy) staining was used for nuclei detection. Fluorescence was photographed with a Leica TCS SP8 confocal laser scanning microscope (Leica Microsystems, Buffalo Grove, IL) at ×400 magnification.

1.10 Proximity ligation assay

Proximity ligation assay was performed using Duolink detection kits (Sigma-Aldrich, Milan, Italy) to identify the interaction between two different proteins. Cells were seeded on glass slides, fixed with 4% paraformaldehyde, permeabilized with 0.2% Triton X-100, 0.2% bovine serum albumin-PBS followed by blocking with 1% BSA-PBS and incubated with the primary antibodies that bind the proteins to be detected for 1 h (Fig. 12A). After three wash with PBS, it is added the secondary antibodies conjugated with oligonucleotides (PLA probe MINUS and PLA probe PLUS) for 1 h (Fig. 12B). The Ligation solution, consisting of two oligonucleotides and Ligase, is added and the oligonucleotides will hybridize to the two PLA probes and join to a closed circle if they are in close proximity (Fig. 12C). The amplification solution, consisting of nucleotides and fluorescently labeled oligonucleotides, is added together with Polymerase. The oligonucleotide arm of one of the PLA probes acts as a primer for a rolling-circle amplification (RCA) reaction using the ligated circle as a template, generating a concatemeric (repeated sequence) product. The fluorescently labeled oligonucleotides will hybridize to the RCA product (Fig. 12D). The signal is easily visible as a distinct fluorescent spot. Fluorescence was

detected using a Leica TCS SP8 (Leica Microsystems, Buffalo Grove, IL) at ×400 magnification.

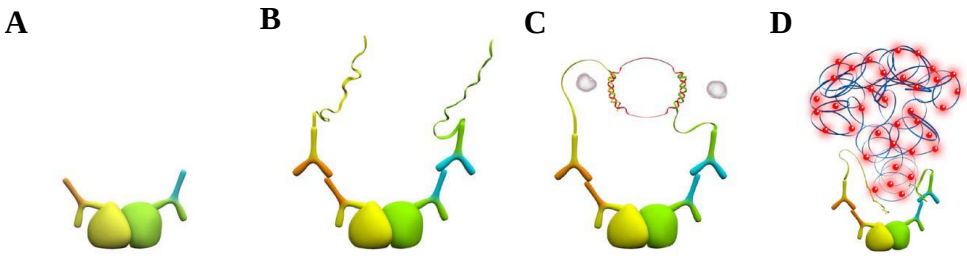

Figure 12. Schematic representation of Duolink *in situ* fluorescence.

1.11 Luciferase assay

MCF-7 were seeded at the density of 5 x 10^4/well in 24 well plates. After 24 h cells were transfected using FuGENE 6 reagent (Roche Diagnostics, Milan, Italy) with a mixture containing 0.5 µg/well XETL plasmid. In addition, to assess transfection efficiency, each DNA mixture contained 5 ng of pRL-TK-Luc, a plasmid encoding *Renilla* luciferase.

Upon transfection, the cells were shifted to serum-free medium for 6 h and then treated with adiponectin as previously indicated for 24 h.

Firefly and *Renilla* luciferase activities were measured with the Dual Luciferase kit (Promega, Milan, Italy). Firefly luciferase values were normalized to the internal transfection control provided by the *Renilla* luciferase activity.

Empty vector was used to ensure that DNA concentration were constant in each transfection.

1.12 MTT cell proliferation assay

Cell viability was assessed by the 3-[4,5-Dimethylthiazol-2-yl]-2,5-diphenyltetrazolium bromide reagent (MTT; Sigma-Aldrich, Milan, Italy) assay. MCF-7 cells (1×10^4 cells/ml) were grown in 96-well plates and exposed to treatments as indicated, in 1% DCC for 72 h. 100 µl of MTT (2 mg/ml, Sigma, Milan, Italy) were added to each well, and the plates were incubated for 4 h at 37°C followed by medium removal and solubilization in 100 µl Dimethyl sulfoxide (DMSO). The absorbance was measured at a test wavelength of 570 nm in Thermo Scientific Coulter.

1.13 RNA-Seq

The sequencing of total RNA, extracted from MCF-7 and MDA-MB-231 cells untreated or treated with adiponectin (5 and 30µg/ml) for 24 h, was carried out at the laboratory of Molecular Medicine and Genomics, Department of Medicine, Surgery and Dentistry "Scuola Medica Salernitana", Baronissi (SA), Italy. RNA concentration was determined with NanoDrop-1000 spectrophotometer and quality assessed with Agilent-2100-Bioanalyzer and Agilent-RNA-6000 nanocartridges (Agilent Technologies).

High quality RNA from three independent experiments was used for library

preparation. Indexed libraries were prepared from 1μg/ea. of purified RNA with TruSeq-RNA-Sample-Prep-Kit (Illumina). Libraries quality controls were performed using Agilent-2100-Bioanalyzer and Agilent DNA-1000 cartridges and concentrations were determined in each case with Qubit-2.0 Fluorometer (Life Technologies). Libraries were sequenced (paired-end, 2×100 cycles) at a concentration of 8 pmol/L per lane on HiSeq2500 platform (Illumina).

The raw sequence files generated (.fastq files) underwent quality control analysis using FASTQC (http://www.bioinformatics.babraham.ac.uk/projects/fastqc/) and the quality checked reads were then aligned to the human genome (assembly hg38) using STAR version 2.5.0a *[Dobin A et al., 2013]*. Quantification of gene signal was performed with HTSeq-Count *[Anders S et al., 2015]*. Differentially expressed RNAs were identified using DESeq2 *[Love MI et al., 2014]*. The differential expression was reported as Fold-Change≥|1.5| along with associated adjusted pvalues (FDR≤0.05) computed according to Benjamini-Hochberg. Heatmaps were generated with MeV TM4 v.4.9 *[Howe EA et al., 2011]*. Functional enrichment analysis was performed with the Ingenuity Pathway Analysis tool (IPA; Qiagen).

1.14 *In Vivo* experiments

Female 45-day-old athymic nude mice (*nu/nu Swiss*; Envigo, Milan, Italy) were maintained in a sterile environment. MCF-7 and MDA-MB-231 cells were pretreated with or without 30 μg/ml recombinant human gAdiponectin/gAcrp30 (Prospec) for 72 h. At day 0, estradiol pellets (1.7

mg/pellet, 60-day release; Innovative Research of America, Sarasota, FL) were subcutaneously implanted into the intrascapular region of the mice receiving inoculation of ERα-positive MCF-7 cells. The next day, $5x10^6$ cells were inoculated subcutaneously in 0.1 ml of Matrigel (BD Biosciences, Bedford, MA). Xenograft tumor growth was monitored twice a week by caliper measurements, and tumor volumes (cm^3) were estimated by the following formula: $TV=ax(b^2)/2$, where *a* and *b* are tumor length and width, respectively, in centimeters. At day 35, the animals were sacrificed following standard protocols; the tumors were dissected from the neighboring connective tissue, frozen in nitrogen, and stored at -80°C for further analyses. All the procedures involving animals and their care were conducted in accordance with the institutional guidelines and regulations at the University of Calabria, Italy. The project was approved by the local ethical committee.

1.15 Histologic and Immunohistochemical analysis

Formalin-fixed, paraffin-embedded sections of tumor xenografts were sectioned at 5 µm, and stained with Hematoxylin and Eosin Y (Bio-Optica, Milan, Italy). Immunohistochemical experiments were performed with mouse polyclonal Ki67 primary antibody at 4°C overnight (Dako Italia Spa, Milan, Italy). Then, a biotinylated goat-anti-rabbit IgG was applied for 1 h at room temperature, followed by the avidin biotin-horseradish peroxidase complex (Vector Laboratories, CA). The epithelial nature of the tumors was verified by immunostaining using human cytokeratin 18 antibody (Santa Cruz

Biotechnology, Milan, Italy). Immunoreactivity was visualized by diaminobenzidine chromogen (Sigma-Aldrich, Milan, Italy). Nuclei were counterstained with hematoxylin. The primary antibody was replaced by normal serum in negative control sections.

1.16 Statistical analysis

Each datum point represents the mean ± S.D. of at least three independent experiments. Data were analyzed by Student's t test using the GraphPad Prism 4 software program. Statistical comparisons for *in vivo* studies were made using the Wilcoxon-Mann-Whitney test. $p<0.05$ was considered as statistically significant.

Results

1.1 Activation of adiponectin/Adipo R1 signaling in breast cancer cells

Adiponectin actions are mediated by specific receptors, Adipo R1 and Adipo R2 that once stimulated, induce activation of numerous signaling pathways *[Panno ML et al., 2016]*. Among these, adiponectin is able to modulate, through c-Src, MAPK and PI3K-Akt, both involved in the proliferative response and survival in ERα-positive breast cancer cell *[Lam JB et al., 2009; Mauro L et al., 2014; Mauro L et al., 2015]*.

We previously demonstrated that ERα expression may influence adiponectin-induced activation of MAPK at relatively low concentration *[Mauro L et al., 2014]*, while it remains to be explored how this may work on LKB1/AMPK/mTOR cascade.

In the present study, we confirmed previous data obtained in MCF-7 cells, showing that short treatment with adiponectin led to MAPK activation *[Mauro L et al., 2014]*, this is consistent with an enhanced phosphorylation of LKB1 at Ser428, concomitant with AMPK signaling inhibition (Fig. 13A). In contrast, in MDA-MB-231 cells, as also recently demonstrated, MAPK was not active *[Mauro L et al., 2014]*, while AMPK phosphorylation was significantly enhanced upon adiponectin exposure (Fig. 13A).

The proteins downstream of AMPK include the mammalian homologue of the target of rapamycin (mTOR) *[Dalamaga M et al., 2012; Luo Z et al., 2005; Smith DP et al., 1999]*, which is constitutively regulated by TSC2 *[Huang J and*

Manning BD, 2008]. In MCF-7 cells, Akt activation (Fig. 13A) induced phosphorylation of TSC2 in Ser939 and Thr1462, enabling mTOR to activate its downstream effector p70S6K (Fig. 13B). In contrast, in MDA-MB-231 cells, active AMPK phosphorylated TSC2 at Ser1387, resulting in the inhibition of downstream mTOR/p70S6K signaling upon adiponectin exposure (Fig. 13B).

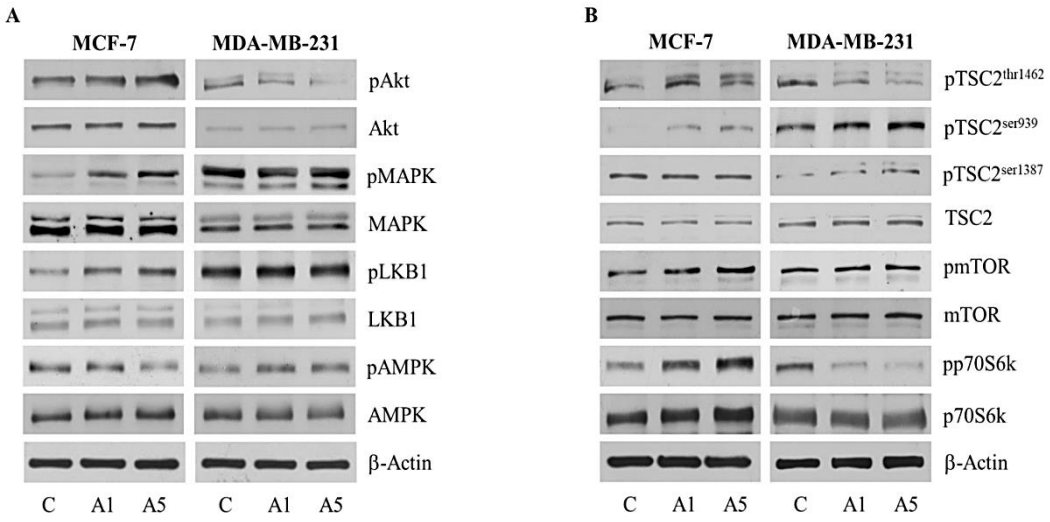

Figure 13. Adiponectin effect on signaling activation in ERα-positive and negative breast cancer cells.

MCF-7 and MDA-MB-231 cells were treated for 30 minutes with adiponectin 1 and 5 µg/ml (A1 and A5 respectively). Levels of phosphorylated (p) Akt^{Ser473}, MAPK ($ERK1/2^{Thr44/Tyr42}$), $LKB1^{Ser428}$, $AMPK^{Thr172}$, $TSC2^{Thr1462/Ser939/Ser1387}$, $mTOR^{Ser2448}$ and $p70S6K^{Thr389}$, and total non-phosphorylated proteins were evaluated in cellular extracts by Western Blotting analysis.

To confirm the direct involvement of MAPK in LKB1 phosphorylation in Ser428 we used the specific MAPK inhibitor PD98059. Under these conditions

the phosphorylation of LKB1 was completely abrogated (Fig. 14). These results are in line with literature data *[Esteve-Puig et al., 2009]*.

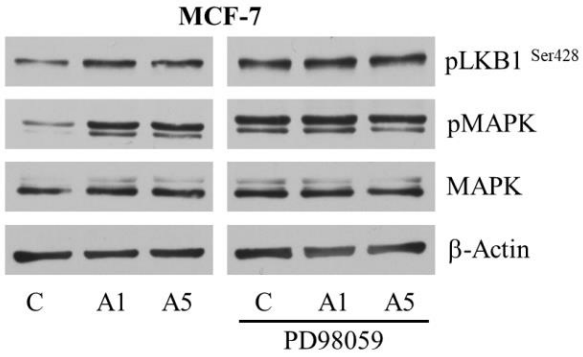

Figure 14. MAPK phosphorylation of LKB1 at Ser428.
MCF-7 were pretreated with 10 μM of PD98059 and untreated or treated with 1 or 5 μg/ml of adiponectin (A1 and A5 respectively) for 30 minutes. Levels of phosphorylated (p) LKB1^{Ser428}, MAPK (ERK1/2$^{Thr44/Tyr42}$) and total non-phosphorylated proteins were evaluated by Western Blotting. β-actin was used as a loading control.

The functional correlates of these events are revealed from measurement of the AMPK-induced phosphorylation of the downstream protein Acetyl-CoA Carboxylase (ACC) at Ser79, which resulted in inhibition of endogenous lipogenesis. The phosphorylated status of ACC at Ser79, evaluated through ELISA, remained unchanged in MCF-7 cells (Fig. 15A), while it was enhanced in a dose-related manner in MDA-MB-231 cells (Fig. 15B), as also confirmed by Western Blotting analysis (Fig. 15 A and B).

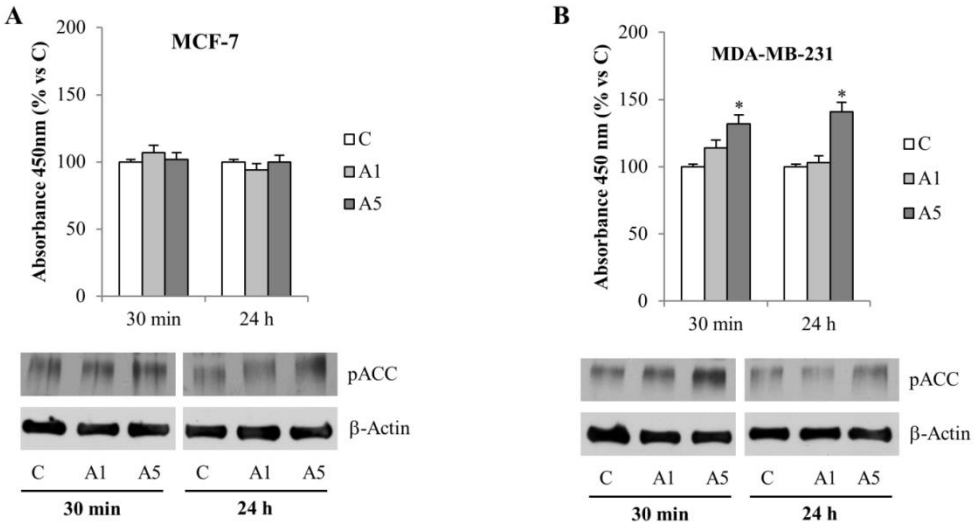

Figure 15. Effect of adiponectin on phosphorylated status of ACC in ERα-positive and negative breast cancer cells.

Phosphorylation of Acetyl-CoA Carboxylase (ACC^{Ser79}) detected by ELISA in MCF-7 (A) and MDA-MB-231 (B) cells treated with adiponectin 1 and 5 μg/ml per 30 minutes or 24 h and then lysed. The absorbance readings at 450 nm are shown in the top panels, while the corresponding Western blotting using phospho-ACC^{Ser79} antibody are shown in the bottom panels. β-Actin was used as loading control. *$p<0.05$ vs control (C).

1.2 Influence of ERα on adiponectin signaling pathways.

The crucial role played by ERα in modulating the above mentioned signaling cascade emerged from the evidence that, upon ERα knock-down with a specific siRNA, MAPK activation was abrogated, concomitantly with a reduction of LKB1 phosphorylation at Ser428, fueling AMPK which in turn phosphorylate TSC2 at Ser1387, thereby inhibiting mTOR/p70S6K signaling (Fig. 16).

Thus, lack of ERα in MCF-7 cells is able to reproduce the responses to adiponectin observed in ERα -negative MDA-MB-231 cells.

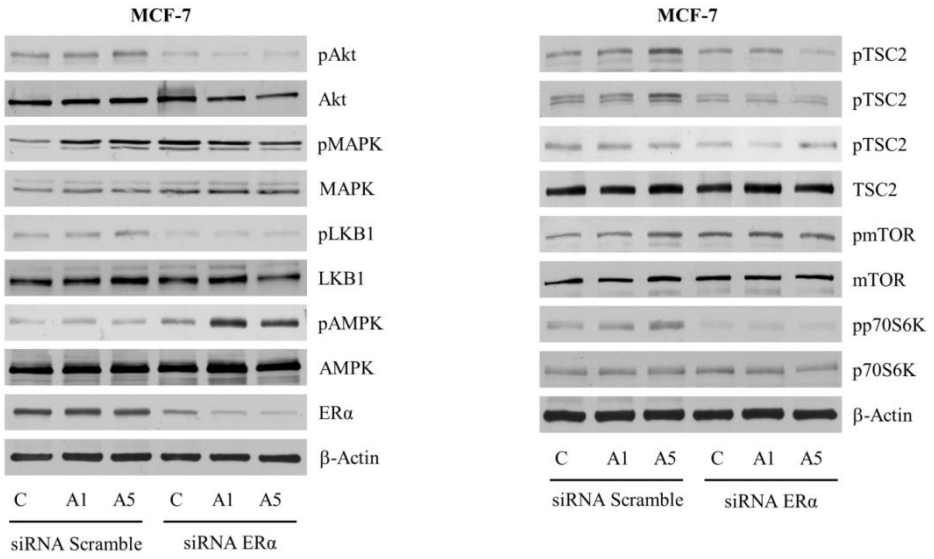

Figure 16. ERα interferes with adiponectin signaling in MCF-7 breast cancer cells. Levels of phosphorylated (p) Akt^{Ser473}, MAPK (ERK1/2$^{Thr44/Tyr42}$), LKB1^{Ser428}, AMPK^{Thr172}, TSC2$^{Thr1462/Ser939/Ser1387}$, mTOR^{Ser2448} and p70S6K^{Thr389} and total non-phosphorylated proteins were evaluated by Western Blotting in protein extracts from MCF-7 cells transfected and treated as indicated. β-Actin was used as loading control.

1.3 Adiponectin allows the interplay between ERα and LKB1

LKB1 contains a nuclear localization signal domain, making this protein able to localize in the nucleus *[Smith DP et al., 1999]*.

Indeed, immunofluorescence analysis in 24 h adiponectin-treated cells evidenced how in MCF-7 cells LKB1 was mostly located in the nucleus, whereas in MDA-MB-231 cells this protein was found mainly in the cytoplasm (Fig. 17 A and B).

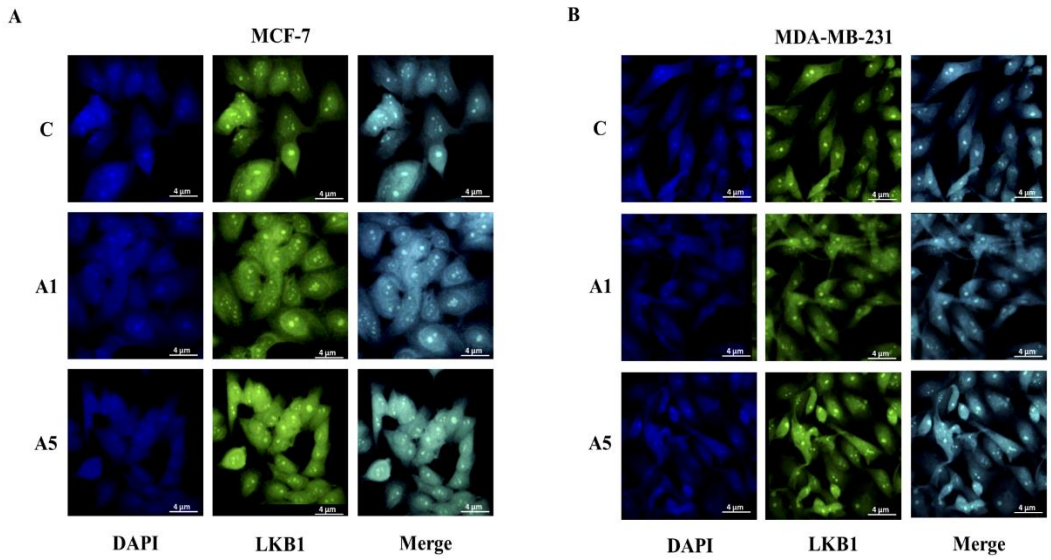

Figure 17. Localization of LKB1 in breast cancer cells.

MCF-7 (A) and MDA-MB-231 (B) cells were treated with adiponectin 1 and 5 μg/ml for 24 h. Then the cells were fixed in 4% (v/v) paraformaldehyde and immunostained with anti-LKB1 antibody. The cells were imaged using cofocal microscope. The images shown are representative of three separate experiments.

Stemming from the evidences that LKB1 may act as ERα coactivator *[Nath-Sain S et al., 2009],* we hypothesize that the different localization of LKB1 could be related to its capability to co-localize in the nucleus with ERα. This was confirmed by Proximity Ligation Assay (PLA) displaying how LKB1/ERα protein interaction may occur in the nucleus of MCF-7 cells, and appeared enhanced upon adiponectin (Fig. 18A).

Immunoprecipitation assay, in MCF-7 cells expressing GST-tagged LKB1, revealed that upon long exposure to adiponectin the ERα/LKB1 interaction persisted in both cytoplasmic and nucleus compartments (Fig. 18B).

Moreover, in MCF-7 cells transfected with increasing doses of ERα-YFP tag

(5, 10, 20µg/plate), immunoprecipitation assay evidenced that the cytosolic association between ERα and LKB1 increased in a dose-related manner and it was enhanced in adiponectin-treated cells (Fig. 18C).

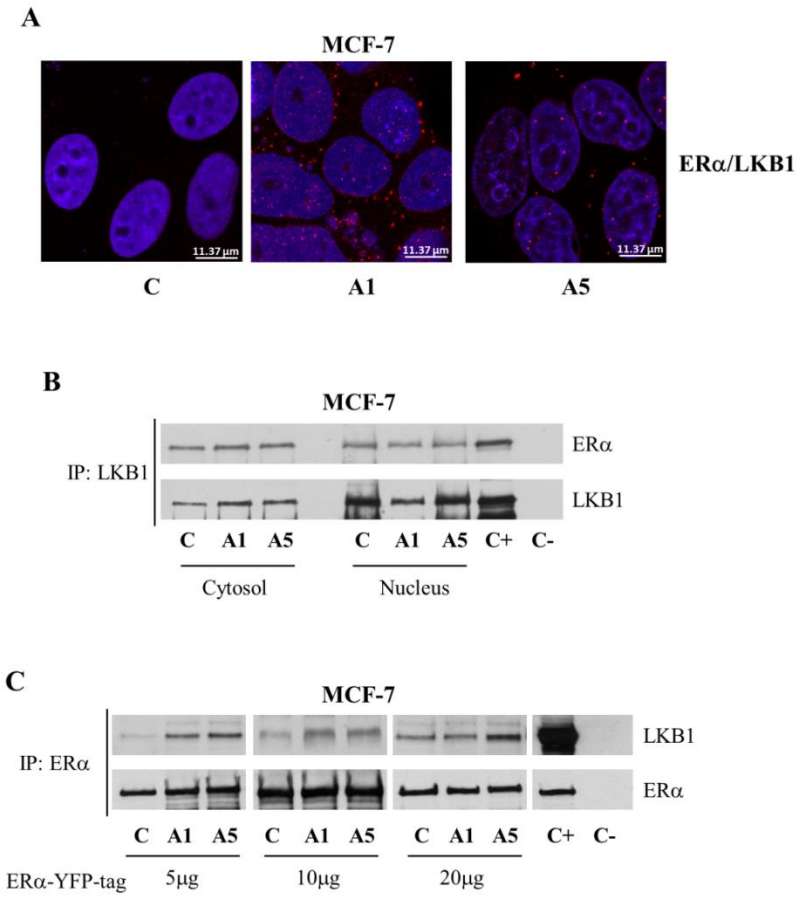

Figure 18. LKB1 interacts with ERα in MCF-7 breast cancer cells.

(A) Duolink staining (red) to detect LKB1 and ERα interaction in MCF-7 cells. The cells were treated as indicated for 24 h and the assay was performed as reported in Materials and Methods. MCF-7 cells were transfected with GST-LKB1 (B) or increasing doses of ERα-YFP (C). Five hundred micrograms of cytosolic or nuclear protein lysates from MCF-7 cells, untreated (C) or treated with adiponectin 1 and 5 µg/ml (A1 and A5) for 24 h, were immunoprecipitated with GST to detect LKB1 or GFP-nAb-Agarose to recognize ERα and then blotted with the indicated antibodies. C+, positive control; C-, negative control.

To further demonstrate how upon adiponectin exposure LKB1 may be recruited by ERα as coactivator, we transfected MCF-7 cells with XETL plasmid in the presence of a specific siRNA for LKB1. In these conditions, we observed that ERα trans-activation in response to adiponectin was abrogated (Fig. 19).

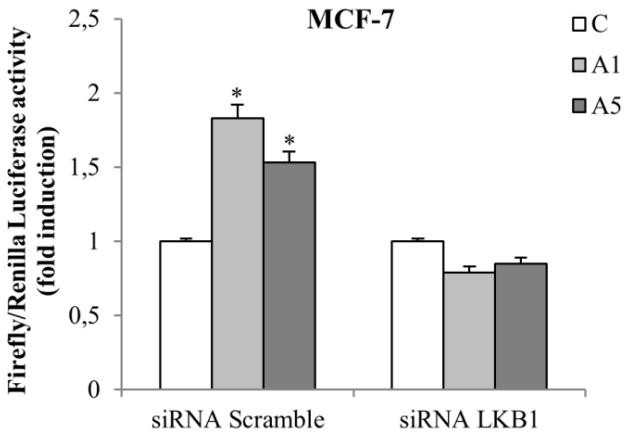

Figure 19. LKB1 interacts with ERα in MCF-7 breast cancer cells.

MCF-7 cells were transiently transfected with the luciferase reported plasmid XETL in the absence or presence of LKB1 siRNA. The cells were untreated or treated for 48 h with adiponectin 1 and 5 μg/ml. The values represent the means ±SD of three different experiments. In each experiment, the activities of the transfected plasmid were assayed in triplicate transfections. *$p < 0.05$ compared with control (C).

These results led us to reasonably investigate whether nuclear recruitment of LKB1 by ERα may interfere with its interaction with AMPK. Indeed, PLA in MCF-7 cells revealed that the interaction between LKB1/AMPK in the cytoplasm is scantly detectable (Fig. 20A) compared to what observed in MDA-MB-231 cells (Fig. 20B).

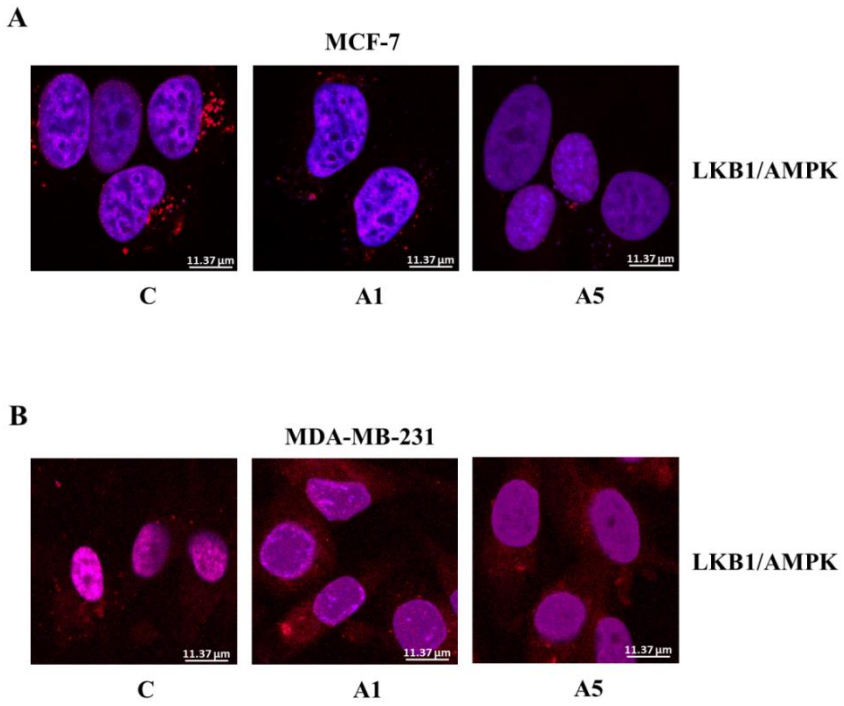

Figure 20. Influence of adiponectin on LKB1/AMPK interaction.
Duolink staining (red) to detect LKB1 and AMPK interaction in MCF-7 (A) and MDA-MB-231 (B) cells. The cells were treated as indicated for 24 h and the assay was performed as reported in Materials and Methods. Images are representative of three different experiments.

As previously described, LKB1 kinase activity depends on the interaction with two other proteins: STRAD and MO25 *[Alessi DR et al., 2006]*.

Thus, we evaluated the expression levels of these proteins and the formation of the tripartite complex. In MCF-7 cells, MO25 decreased upon long term adiponectin exposure (Fig. 21A) suggesting that, in such way, it may interfere with STRAD/LKB1 binding. In contrast, in MDA-MB-231 cells, adiponectin long exposure increased the expression of STRAD and MO25 (Fig. 21B),

addressing how the trimeric complex LKB1/STRAD/MO25 may be much more stable in MDA-MB-231 than in MCF-7 cells. This may well correlate with the above described effect on ACC as downstream protein of AMPK signaling, which appeared blocked through it phosphorylation at Ser79 only in MDA-MB-231 cells.

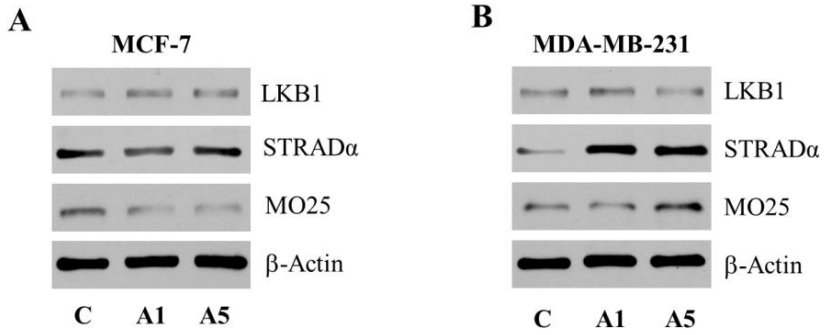

Figure 21. Effects of adiponectin on the heterotrimeric complex LKB1/STRAD/MO25.

Western blotting of LKB1, STRAD and MO25 expression in MCF-7 (A) and MDA-MB-231 (B) cells, untreated (C) or treated with adiponectin 1 and 5 μg/ml (A1 and A5) for 48 h. Images are representative of three different experiments. β-Actin was used as loading control.

1.4 Low versus high adiponectin levels effects in breast cancer cells.

Adiponectin levels are abundant in human plasma, with concentrations ranging from 3 to 30 μg/ml, and they are reduced in obesity *[Dalamaga M et al., 2012]*. It has been previously tested the effects of low adiponectin concentrations *in vitro* in MCF-7 and MDA-MB-231 cells, revealing a

dichotomic effect on signaling involved in cell survival and proliferation. Here, it has been compared, in our cellular models, the effects on cell proliferation and tumor growth of 5 μg/ml, which corresponds to the plasma level in obese women, and 30 μg/ml adiponectin, presents in normal weight subjects.

Results confirmed that 5 μg/ml of adiponectin increased cell proliferation in MCF-7 cells *[Mauro L et al., 2014],* while a slight reduction was observed at the concentration of 30 μg/ml. In MDA-MB-231 cells, instead, a significant inhibition of cell growth was evidenced at either doses of adiponectin used (Fig. 22).

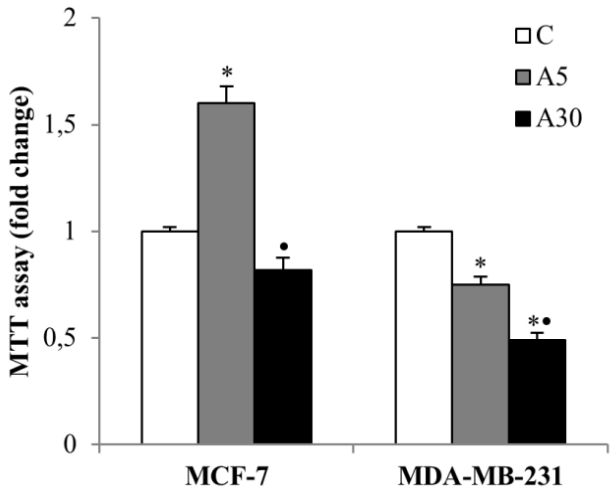

Figure 22. Effect of high adiponectin levels on breast cancer cell growth.
MTT growth assays in MCF-7 and MDA-MB-231 cells untreated (C) or treated with adiponectin 5 (A5) or 30 μg/ml (A30) for 72 h. Cell proliferation is expressed as fold change ± S.D. relative to C, and is representative of three different experiments each performed in triplicate. *p<0.05 *vs* C.

RNA-seq analysis confirmed the above described different effect induced by adiponectin in MCF-7 respect to MDA-MB-231 cells (Fig. 23; Table 1 see appendix A). Table 1 lists the transcripts differentially expressed in MCF-7 and MDA-MB-231 cells, in relationship to adiponectin treatment.

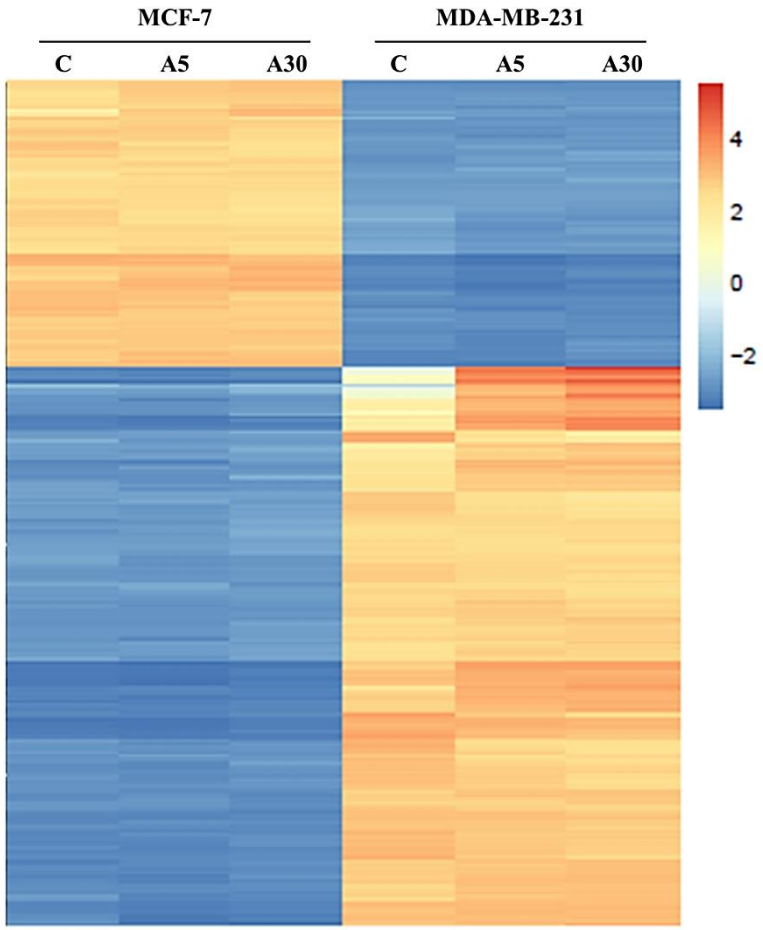

Figure 23. Adiponectin effect on global changes of gene expression in MCF-7 and MDA-MB-231 cells.

The cells were treated with 5 and 30 µg/ml adiponectin (A5 and A30, respectively) for 24 h, before RNA extraction. Global gene expression analysis was done by RNA sequencing. Heat map shows differential regulation of genes in untreated or adiponectin-treated cells. Three repeats per condition were performed.

These results were subjected to Ingenuity Pathway Analysis (IPA) to identify over-represented biological processes. This revealed that adiponectin treatment was able to specifically modulate the expression of genes involved in cell proliferation, cell cycle progression, apoptosis, necrosis and differentiation (Fig. 24).

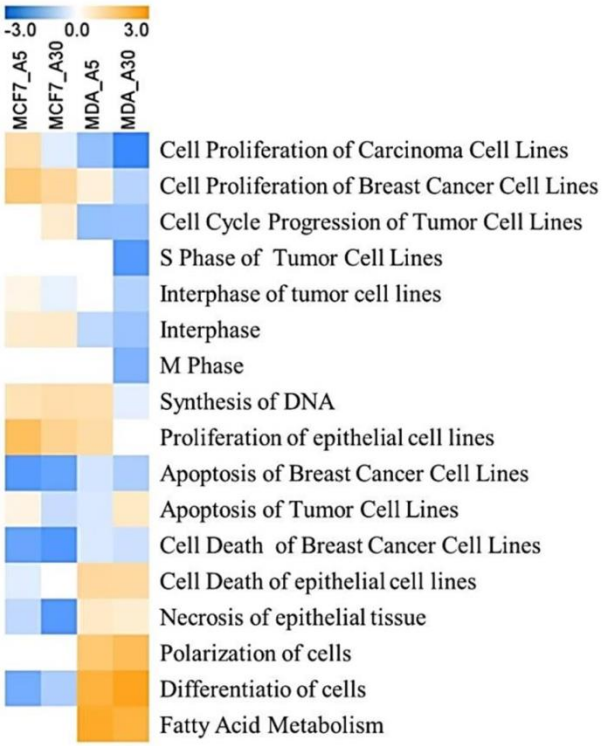

Figure 24. Role of adiponectin on biological processes in breast cancer cells. Functional analysis (performed with IPA software) showing biological processes affected by differentially expressed genes in adiponectin-treated cells.

Figure 25 showed the regulation of genes involved in cell cycle progression, cell proliferation, cell death and apoptosis, in MCF-7 and MDA-MB-231 adiponectin-treated cells.

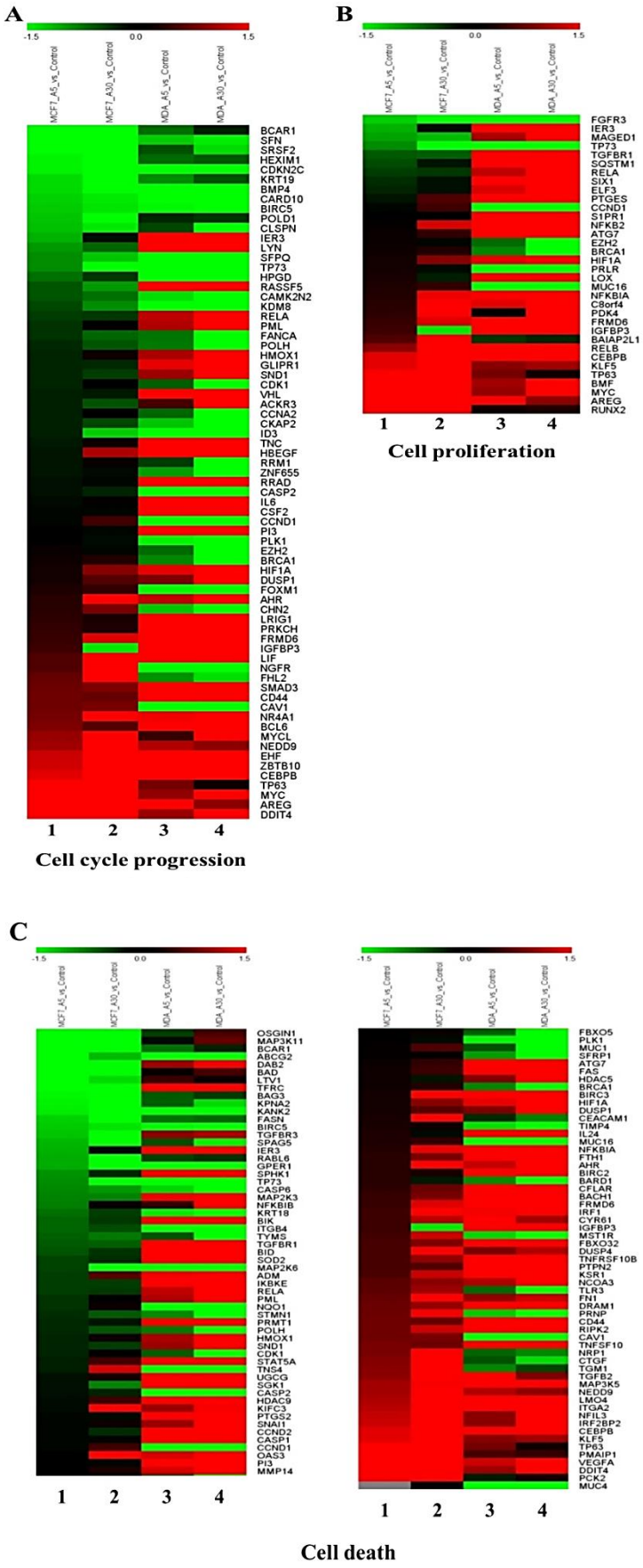
A
-1.5
0.0
1.5
MCF7_A5_vs_Control
MCF7_A30_vs_Control
MDA_A5_vs_Control
MDA_A30_vs_Control
BCAR1
SFN
SRSF2
HEXIM1
CDKN2C
KRT19
BMP4
CARD10
BIRC5
POLD1
CLSPN
IER3
LYN
SFPQ
TP73
HPGD
RASSF5
CAMK2N2
KDM8
RELA
PML
FANCA
POLH
HMOX1
GLIPR1
SND1
CDK1
VHL
ACKR3
CCNA2
CKAP2
ID3
TNC
HBEGF
RRM1
ZNF655
RRAD
CASP2
IL6
CSF2
CCND1
PI3
PLK1
EZH2
BRCA1
HIF1A
DUSP1
FOXM1
AHR
CHN2
LRIG1
PRKCH
FRMD6
IGFBP3
LIF
NGFR
FHL2
SMAD3
CD44
CAV1
NR4A1
BCL6
MYCL
NEDD9
EHF
ZBTB10
CEBPB
TP63
MYC
AREG
DDIT4
1
2
3
4
Cell cycle progression
B
-1.5
0.0
1.5
MCF7_A5_vs_Control
MCF7_A30_vs_Control
MDA_A5_vs_Control
MDA_A30_vs_Control
FGFR3
IER3
MAGED1
TP73
TGFBR1
SQSTM1
RELA
SIX1
ELF3
PTGES
CCND1
S1PR1
NFKB2
ATG7
EZH2
BRCA1
HIF1A
PRLR
LOX
MUC16
NFKBIA
C8orf4
PDK4
FRMD6
IGFBP3
BAIAP2L1
RELB
CEBPB
KLF5
TP63
BMF
MYC
AREG
RUNX2
1
2
3
4
Cell proliferation
C
-1.5
0.0
1.5
MCF7_A5_vs_Control
MCF7_A30_vs_Control
MDA_A5_vs_Control
MDA_A30_vs_Control
OSGIN1
MAP3K11
BCAR1
ABCG2
DAB2
BAD
LTV1
TFRC
BAG3
KPNA2
KANK2
FASN
BIRC5
TGFBR3
SPAG5
IER3
RABL6
GPER1
SPHK1
TP73
CASP6
MAP2K3
NFKBIB
KRT18
BIK
ITGB4
TYMS
TGFBR1
BID
SOD2
MAP2K6
ADM
IKBKE
RELA
PML
NQO1
STMN1
PRMT1
POLH
HMOX1
SND1
CDK1
STAT5A
TNS4
UGCG
SGK1
CASP2
HDAC9
KIFC3
PTGS2
SNAI1
CCND2
CASP1
CCND1
OAS3
PI3
MMP14
1
2
3
4
-1.5
0.0
1.5
MCF7_A5_vs_Control
MCF7_A30_vs_Control
MDA_A5_vs_Control
MDA_A30_vs_Control
FBXO5
PLK1
MUC1
SFRP1
ATG7
FAS
HDAC5
BRCA1
BIRC3
HIF1A
DUSP1
CEACAM1
TIMP4
IL24
MUC16
NFKBIA
FTH1
AHR
BIRC2
BARD1
CFLAR
BACH1
FRMD6
IRF1
CYR61
IGFBP3
MST1R
FBXO32
DUSP4
TNFRSF10B
PTPN2
KSR1
NCOA3
TLR3
FN1
DRAM1
PRNP
CD44
RIPK2
CAV1
TNFSF10
NRP1
CTGF
TGM1
TGFB2
MAP3K5
NEDD9
LMO4
ITGA2
NFIL3
IRF2BP2
CEBPB
KLF5
TP63
PMAIP1
VEGFA
DDIT4
PCK2
MUC4
1
2
3
4
Cell death

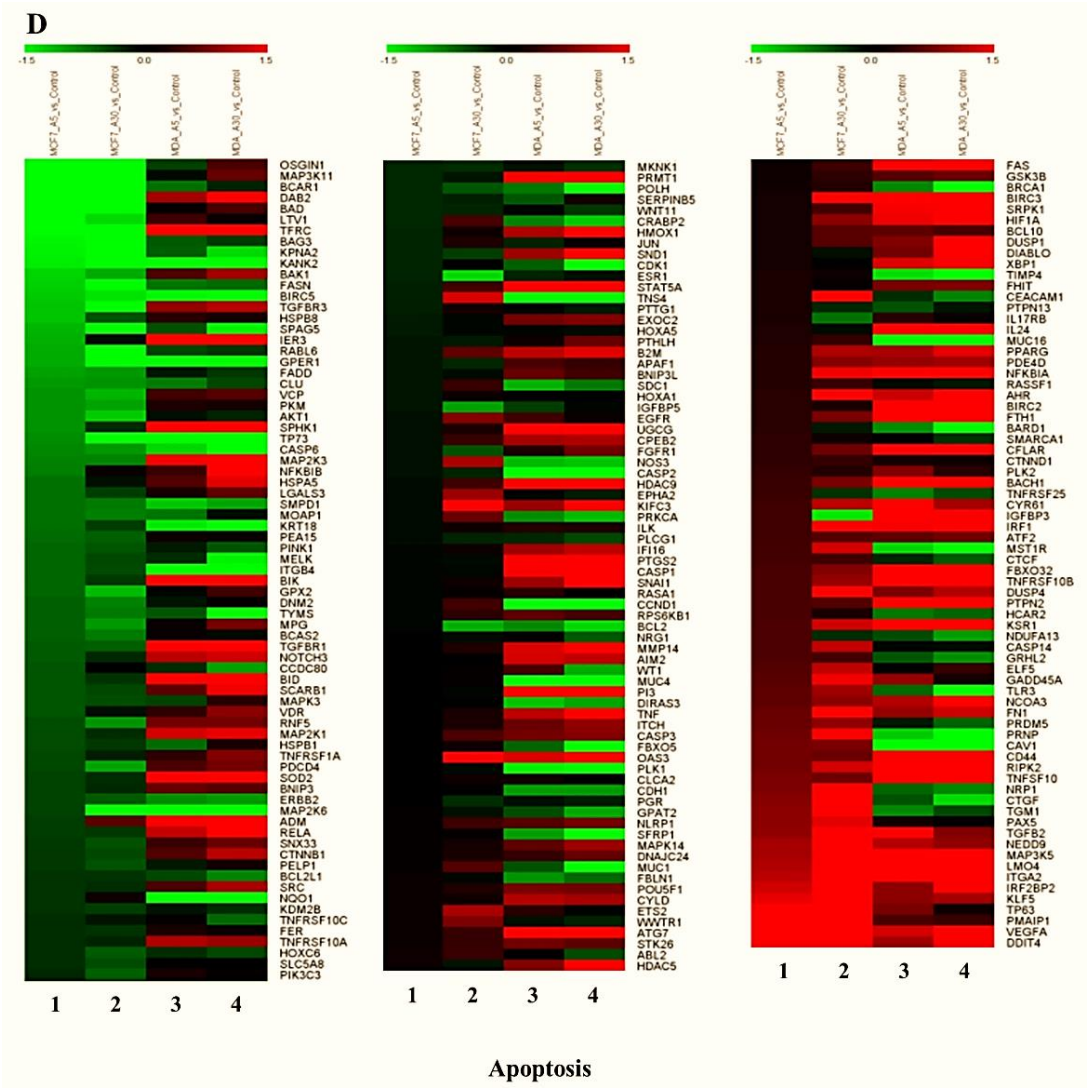

Figure 25. Modulation of gene expression involved in specific biological processes by adiponectin.

Heat maps showing differential expression of genes involved in cell cycle progression (A), cell proliferation (B), cell death (C) and apoptosis (D) in MCF-7 (A5 vs C, column 1; A30 vs C, column 2) and MDA-MB-231 (A5 vs C, columns 3; A30 vs C, column 4) cells.

In particular, we observed that the expression of genes involved in the control of cell proliferation and cell cycle progression was significantly increased in MCF-7 cells, under adiponectin treatment, concomitantly with the inhibition of those involved in apoptosis and cell death. In contrast, in MDA-MB-231 cells, genes regulating cell proliferation were inhibited at both 5 and 30 µg/ml of adiponectin (activation z-score-1.24 and-2.30, respectively), while apoptosis and cell death were less inhibited compared to MCF-7 cells (Fig. 26). Concerning genes involved in fatty acid metabolism, these appeared strongly up-regulated in MDA-MB-231 cells (activation z-score 2.50 and 2.25 at the doses of 5 and 30 µg/ml, respectively) (Fig. 26), indicating how adiponectin tents to antagonize the lipogenic phenotype present in this cell line.

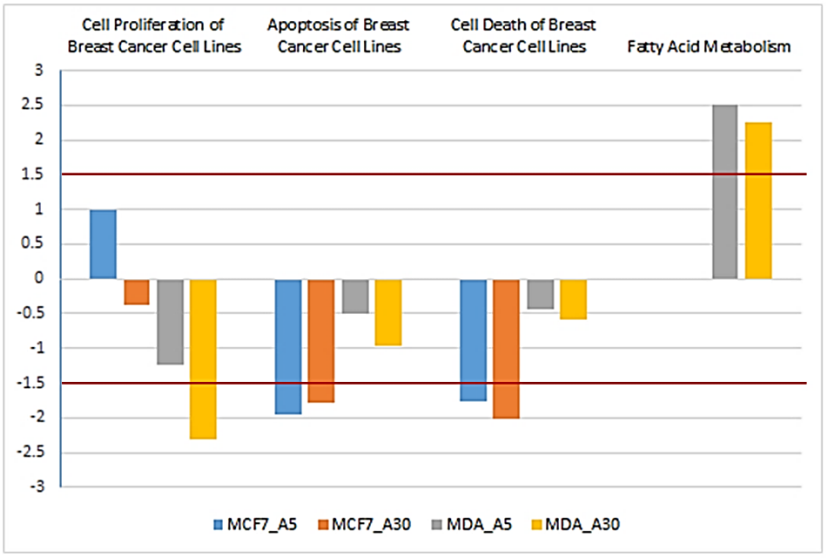

Figure 26. Activation z-score values of biologic functions in cells exposed to adiponectin.

Overrepresented processes are referred to as activation z-score values of the indicated biologic functions performed with IPA software, comparing MCF-7 and MDA-MB-231 adiponectin-treated cells.

Figure 27 showed the predicted regulation of cell cycle progression, confirming a marked inhibition of this pathway in MDA-MB-231 compared to MCF-7 cells.

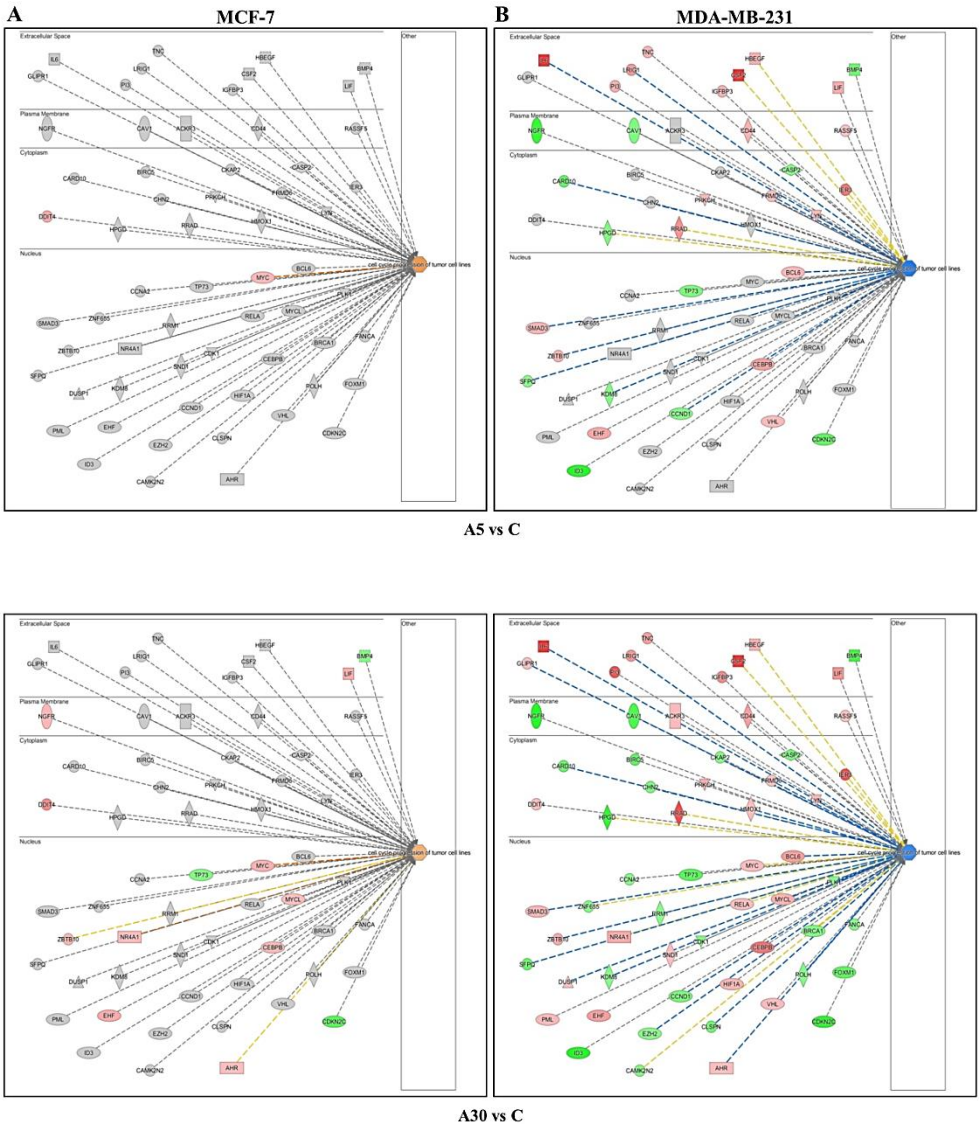

Figure 27. Predicted regulation of cell cycle progression in adiponectin- treated cells.

Functional networks showing upregulated and downregulated genes and predicted regulation of cell cycle progression in MCF-7 (A) and MDA-MB-231 (B) cells upon treatment with adiponectin 5 μg/ml (upper panel) and 30 μg/ml (lower panel).

Previous *in vivo* investigation demonstrated that low adiponectin doses (1 and 5 μg/ml) induced a significant increase of the volume of MCF-7 cell tumors but a reduction of that of MDA-MB-231 cell tumors *[Mauro et al., 2015].* Here, we used the mouse xenograft model to test the effect of a higher adiponectin concentration (30 μg/ml) on breast cancer growth, to verify the persistence of such dichotomic effect. MCF-7 and MDA-MB-231 cells were pre-treated with or without adiponectin for 72 h and then injected into the intrascapular region of female nude mice, as previously reported *[Mauro et al., 2015].* The procedures were well tolerated because no change in body weight or in food and water consumption was observed, along with no evidence of reduced motor function. Histological analysis revealed that all tumors were predominantly composed of tumor epithelial cells (Fig. 28).

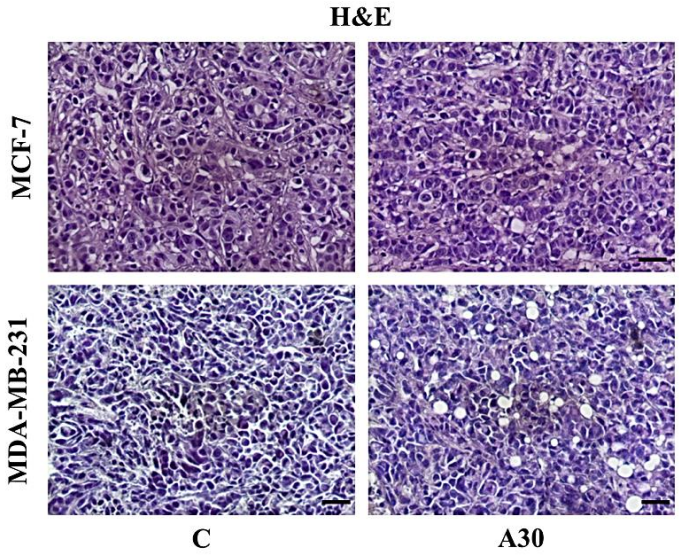

Figure 28. Staining of MCF-7 and MDA-MB-231 xenograft tumors. Representative pictures of Hematoxylin and Eosin (H&E) stained histologic images. Scale bars=25 μm

As also previously reported *[Mauro et al., 2015],* immunostaining with anti-human-Cytokeratin 18 antibody confirmed the human epithelial nature of the tumors (Fig. 29A).

In addition, in tumors from mice injected with MCF-7 cells after adiponectin 30 μg/ml treatment, we observed a slight reduction in Ki67 expression, a well-known marker for cell proliferation (Fig. 29B). On the other hand, under the same conditions a markedly reduced expression of Ki-67 was observed in MDA-MB-231 cell tumors (Fig. 29B)

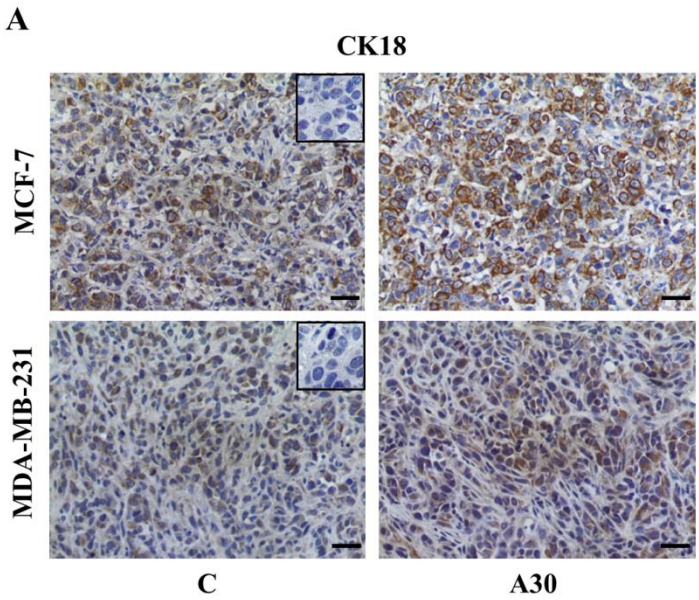

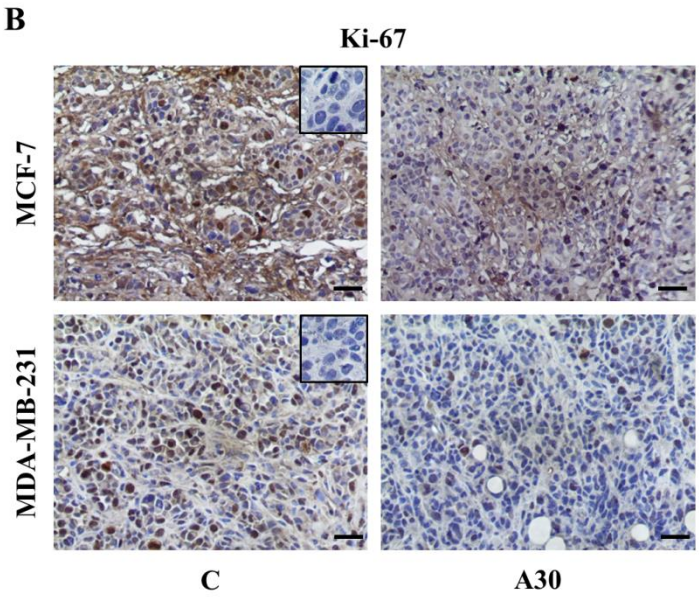

Figure 29. Immunohistochemical staining of xenograft tumors.
Representative pictures of human Cytokeratin 18 (A) and human Ki-67 (B) immunohistochemical staining of MCF-7 or MDA-MB-231 xenograft tumor sections. Scale bars=25 μm.

As shown in Figure 30A, the injection of MCF-7 cells pretreated with 30 μg/ml exhibited a slight reduction of tumor volume. In contrast, a significant decrease was observed in mice injected with adiponectin-pretreated MDA-MB-231 cells (Fig. 30B). It is worth to note that, in MCF-7 xenograft tumors, no phosphorylation of MAPK and AMPK was observed (Fig. 30C), whereas in MDA-MB-231 xenografts adiponectin 30 μg/ml induced a remarkable activation of AMPK (Fig. 30D).

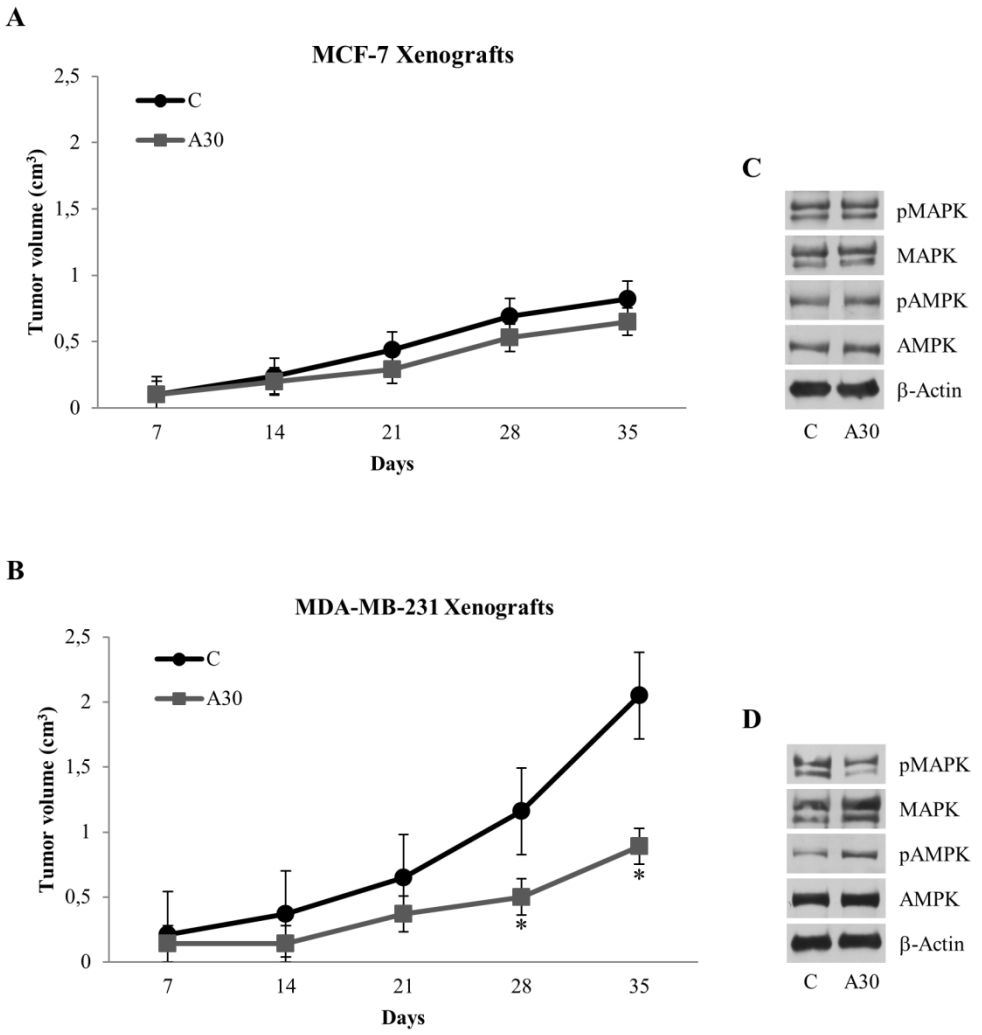

Figure 30. Impact of adiponectin on tumor growth in MCF-7 and MDA-MB-231 xenografts.

MCF-7 (A) and MDA-MB-231 (B) cells were untreated or pretreated with adiponectin 30 μg/ml (A30) for 72 h and implanted subcutaneously into nude mice (6 mice/each group). Tumor growth was monitored by measuring the visible tumor sizes at indicated time points. *$p<0.05$ *vs* control group. Representative immunoblot analysis on protein extracts from MCF-7 (C) or MDA-MB-231(D) xenograft tumors excised from mice, showing MAPK and AMPK activation. The immunoblots were stripped and reprobed with total MAPK and AMPK. β-Actin was used as loading control

Discussion

Adipose tissue plays a crucial role in signaling pathways that influence breast cancer development and progression. This depends not only from the adipose tissue mass but also from breast adipocytes that surround breast tumor epithelial cells, which are the most abundant cell types in stroma of mammary gland *[Körner A et al., 2007]*.

Adipose tissue is a bioactive endocrine organ *[Park J et al., 2011]* that secretes a wide array of soluble factors, called adipocytokines, and contributes significantly to the development of the normal mammary gland *[Landskroner-Eiger S et al., 2010]* as well as to breast carcinogenesis *[Macciò A et al., 2011]*. Amongst these adipocytokines, adiponectin has been shown to have a critical role in the pathogenesis of obesity-associated malignancies, including breast cancer *[Panno ML et al., 2016]*.

Many studies demonstrated the relationship between hypo-adiponectinemia and increased breast cancer risk, highlighting how breast cancer patients with lower adiponectin levels show a more aggressive phenotype *[Dalamaga M et al., 2012]*. Direct evidence has been reported supporting the role of adiponectin as an inhibitory factor for breast cancer development *[Wang Y et al., 2006]*, and how it does attenuate the growth of MDA-MB-231 cells by inhibiting cell proliferation and inducing apoptosis *[Kang JH et al., 2005; Dieudonne MN et al., 2006]*. On the other hand, adiponectin does not increase DNA fragmentation and apoptosis in T47D cells suggesting that its pro-apoptotic effect results from

a cell type-specific response *[Wang Y et al., 2006]*.

In the recent years, a crucial role of the ERα in adiponectin response of breast cancer cells is emerging. For instance, we recently demonstrated that low concentrations of adiponectin increase proliferation of ERα-positive breast cancer cells, through the activation of ERα at both genomic and non-genomic levels *[Mauro L et al., 2014]*. At genomic level adiponectin regulates the expression of a critical modulator of cell cycle progression, such us cyclin D1 through recruitment of ERα to its promoter *[Mauro L et al., 2015]*. At non-genomic level, in MCF-7 cells adiponectin, via c-Src, induced a rapid activation of MAPK, which in turn is responsible for ERα phosphorylation at Ser118 and its nuclear transactivation. Thus, ERα underwent ligand-independent activation by adiponectin, leading to transcription of receptor-responsive genes driving cell growth *[Mauro L et al., 2014]*. ERK1/2 plays a crucial role in the modulation of G0/G1 transition and cell cycle progression to mitosis, thus our findings taken together reveal how adiponectin, at the low concentrations tested in the present study, can work as a growth factor in ERα-positive breast cancer cells, as also previously reported in other cell types *[Lee MH et al., 2008]*.

This was confirmed by gene expression profiling, whereby analysis of the genes responsive under the different experimental conditions investigated here, provided further evidence that specific effects of adiponectin dependent on the presence of ERα. In MCF-7 cells, for instance, functional analysis, performed to investigate the most significant adiponectin-responsive biological processes, revealed how this adipocytokine stimulated genes involved in cell proliferation and cell cycle progression, and inhibited those involved in cell apoptosis and cell

death. On the contrary, the same genetic pathways displayed an opposite pattern of response in MDA-MB-231 cells. For instance, Ingenuity Pathways Analysis confirmed, at the doses tested, the dichotomic effect of adiponectin on the genes involved in the proliferative pathways in MCF-7 and MDA-MB-231 breast cancer cells. In addition, it is worth to note how the genes involved in fatty acid metabolism resulted drastically upregulated in MDA-MB-231 cells. All these results confute, in our view, the misleading paradigm that adiponectin univocally reduces the proliferation of breast cancer cells independently of ERα status. Thus, we may reasonably speculate that low levels of adiponectin may have a different effect on the tumor burden and clinical progression in ERα-positive and ERα-negative breast cancer obese patients.

Tumor progression requires the coexistence of three conditions in obese patients with ERα-positive breast cancer: 1) enhanced local estrogen production due to increase of aromatase activity related to the abundance of breast adipose tissue *[McTiernan A et al., 2003]*; 2) dysregulated circulating factors stimulating ERα-positive breast cancer cell viability and growth by facilitating non-genomic ERα cross-talk with the PI3K/Akt and MAPK signaling pathways *[Mauro L et al., 2015; Panno ML et al., 2016]*; 3) low adiponectin levels which are able per se to activate ERα at genomic level thereby affecting its target genes, as well as to potentiate rapid non-genomic ERα actions *[Mauro L et al., 2014]*.

Additionally, we demonstrated here that MAPK activation, induced in MCF-7 cells by adiponectin, is crucial in enhancing LKB1 phosphorylation at Ser428. LKB1 is a constitutively active serine/treonine kinase which is generally phosphorylated by several upstream kinases at different serine residues

sequestering it in the nucleus *[Korsse SE et al., 2013]*. It has been demonstrated, in other cell types, that such kinases may be inactivated by the adiponectin-induced phosphatases *[Deepa SS et al., 2011]*. As shown here, ERα activation by adiponectin induces recruitment of LKB1 as receptor coactivator and contributes to tether it in the nucleus. Interestingly, adiponectin is no longer able to transactivate ERα when LKB1 expression is reduced by a specific siRNA. It is not surprisingly that a tumor suppressor protein may paradoxically function as nuclear receptor coactivator. The retinoblastoma protein, for example, has been shown to act as a coactivator of estrogen (ERα), androgen (AR), progesterone (PR) and Glucocorticoid (GR) receptors, despite being the archetypical tumor suppressor *[Nath-Sain S et al., 2009]*.

Thus, we demonstrate, that low adiponectin levels, through ERα may block the growth-inhibitory action of LKB1. It occurs through the interaction with ERα, that sequesters LKB1 in the nucleus, preventing its association in the cytosolic tripartite complex with the two scaffold protein STRAD and MO25, that enables it to activate AMPK signaling. This is confirmed in MCF-7 cells upon ERα downregulation with siRNA, that results in LKB1 free to activate AMPK, mimicking what observed in MDA-MB-231 cells, where LKB1 is prevalently located in the cytoplasm.

Based on the above results, we propose that exposure of MCF-7 cells to adiponectin doses tested, produces an uncoupling effect on LKB1/AMPK signaling through a double mechanism: i) rapid effect converging on ERα signaling able to activate MAPK and resulting in the inhibition of LKB1 through the phosphorylation on Ser428; ii) long-term effects related to ERα ability to

recruit LKB1 in the nucleus, impairing its interaction with AMPK.

The functional correlation of both rapid and long-term events is represented by the fact that in both circumstances AMPK signaling is not working and is thus unable to phosphorylate and inhibit its main downstream protein ACC, leaving fatty acid synthesis unchallenged.

In MCF-7 cells under these conditions, fatty acid synthesis may be considered a secondary effect of adipocytokine, sustained by ERα-induced activation of PI3K/Akt/mTOR and MAPK pathways, able to antagonize AMPK signaling. In other words, unexpectedly, in the presence of low adiponectin concentrations, ERα signaling switches energy balance of breast cancer cells towards a lipogenic phenotype. In ERα-negative MDA-MB-231 cells, instead, the phosphorylated status of ACC resulted enhanced upon adiponectin exposure, negatively influencing lipogenesis.

When combined, these results suggest a possible mechanisms to explain how this adipocytokine regulates lipid metabolism also in non-classically insulin-sensitive tissues.

A schematic representation of LKB1/AMPK/mTOR signaling in adiponectin-treated ERα-positive and ERα-negative breast cancer cells is shown in Figure 31.

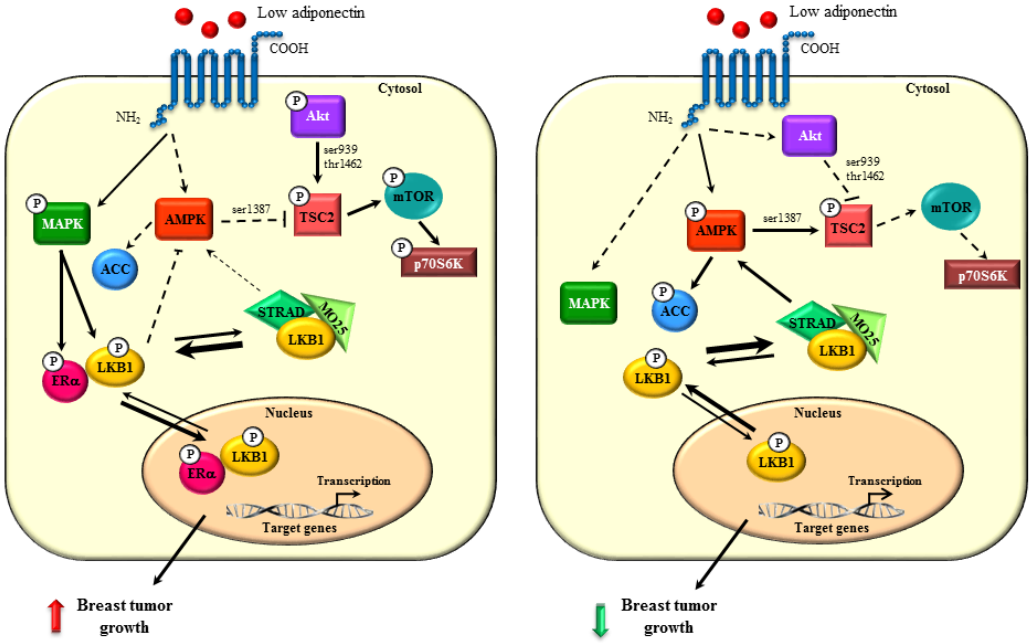

Figure 31. Proposed model for activation of adiponectin/AdipoR1 signaling in ERα-positive (A) and ERα-negative (B) breast cancer cells

Conclusions

In conclusion, adiponectin, at all the concentrations tested, plays an inhibitory role on ERα-negative breast cancer cell growth and progression either *in vitro* or *in vivo*, as previously largely documented *[Dos Santos E et al., 2008; Grossmann ME et al., 2008; Kang JH et al., 2005; Mauro L et al., 2014; Mauro L et al., 2015]*. In contrast, low adiponectin levels, similar to those circulating in obese patients, act on ERα-positive breast cancer cells as growth factor stimulating their growth and progression. An effect no longer noticeable *in vivo* in the presence of a higher adiponectin concentration, comparable to that found in normal weight patients.

On the basis of these data we may reasonably conclude that ERα signaling, interfering on adiponectin/AdipoR1/LKB1/AMPK functional axis controlling cellular energy expenditure, could set higher the potential inhibitory threshold of adiponectin. The results described may have translational relevance when considering that adiponectin and its receptors are potential pharmacological targets of novel therapeutic strategies for breast cancer by: i) conversion of adiponectin into a viable drug, ii) artificially increase of endogenous circulating adiponectin levels, iii) using Adipo R1/R2 agonists and/or iv) implementing other strategies designed to increase expression of these receptors and to modulate their sensitivity to adiponectin. Based on the present results, any of these approaches should need separate therapeutic assessment in ERα-negative and ERα-positive obese breast cancer patients, in the latter case a combined therapy with antiestrogens should be considered.

References

Alessi DR, Sakamoto K, Bayascas JR. LKB1-dependent signaling pathways. *Annu Rev Biochem* **2006**; 75:137-63.

Anders S, Pyl PT, Huber W. HTSeq--a Python framework to work with high-throughput sequencing data. *Bioinformatics* **2015**; 31(2):166-9.

Anderson KA, Means RL, Huang QH, Kemp BE, Goldstein EG, Selbert MA, Edelman AM, Fremeau RT and Means AR. Components of a calmodulin-dependent protein kinase cascade. Molecular cloning, functional characterization and cellular localization of Ca2+ /calmodulin-dependent protein kinase kinase beta. *J. Biol. Chem* **1998**; 273, 31880–31889.

Andò S, Catalano S. The multifactorial role of leptin in driving the breast cancer microenvironment. *Nat Rev Endocrinol* **2011**; 8:263–75.

Asada K, Yoshiji H, Noguchi R, Ikenaka Y, Kitade M, Kaji K, Yoshii J, Yanase K, Namisaki T, Yamazaki M, Tsujimoto T, Akahane T, Uemura M, Fukui H. Cross talk between high-molecular-weight adiponectin and T-cadherin during liver fibrosis development in rats. *Int J Mol Med* **2007**; 20:725–9.

Baas AF, Boudeau J, Sapkota GP, Smit L, Medema R, Morrice NA, Alessi DR, Clevers HC. Activation of the tumor suppressor kinase LKB1 by the STE20-like pseudokinase STRAD. *EMBO J* **2003**; *22* 3062–3072.

Bandera EV Maskarinec G, Romieu I, John EM. Racial and ethnic disparities in the impact of obesity on breast cancer risk and survival: a global perspective. *Adv Nutr* **2015**; 6(6) 803-819.

Barb D, Pazaitou-Panayiotou K, Mantzoros CS. Adiponectin: a link between obesity and cancer. *Expert Opin Investig Drugs* **2006**; 15:917-31.

Barb D, Williams CJ, Neuwirth AK, Mantzoros CS. Adiponectin in relation to malignancies: a review of existing basic research and clinical evidence. *Am J Clin Nutr* **2007**; 86:s858–s866.

Berg AH, Combs TP, Du X, Brownlee M, Scherer PE. The adipocyte-secreted protein Acrp30 enhances hepatic insulin action. *Nat Med* **2001**; 7:947–953.

Brochu-Gaudreau K, Rehfeldt C, Blouin R, Bordignon V, Murphy BD, Palin MF. Adiponectin action from head to toe. *Endocrine* **2010**; 37:11–32.

Buechler C, Wanninger J, Neumeier M. Adiponectin receptor binding proteins–recent advances in elucidating adiponectin signaling pathways. *FEBS Lett* **2010**; 584:4280–6.

Calle EE, Thun MJ. Obesity and cancer. *Oncogene* **2004**; 23:6365–78.

Carling D. The AMP-activated protein kinase cascade--a unifying system for energy control. *Trends Biochem Sci* **2004**; 29(1):18-24.

Chan BT, Lee AV. Insulin receptor substrates (IRSs) and breast tumorigenesis. *J Mammary Gland Biol Neoplasia* **2008**; 13:415–22.

Chan DW, Lee JM, Chan PC, Ng IO. Genetic and epigenetic inactivation of T-cadherin in human hepatocellular carcinoma cells. *Int J Cancer* **2008**; 123:1043–52.

Chandran M, Phillips SA, Ciaraldi T, Henry RR. Adiponectin: more than just another fat cell hormone? *Diabetes Care* **2003**; 26:2442-2450.

Chen DC, Chung YF, Yeh YT, Chaung HC, Kuo FC, Fu OY, Chen HY, Hou MF, Yuan SS. Serum adiponectin and leptin levels in Taiwanese breast cancer patients. *Cancer Lett* **2006**; 237:109-14.

Chen J, Tan B, Karteris E, Zervou S, Digby J, Hillhouse EW, Vatish M, Randeva HS. Secretion of adiponectin by human placenta: differential modulation of adiponectin and its receptors by cytokines. *Diabetologia* **2006**; 49:1292– 1302.

Chen X, Wang Y. Adiponectin and breast cancer. *Med Oncol* **2011**; 28:1288–95.

Cnop M, Havel PJ, Utzschneider K M, Carr DB, Sinha MK, Boyko EJ, Retzlaff BM, Knopp RH, Brunzell JD, Kahn SE. Relationship of adiponectin to body fat distribution, insulin sensitivity and plasma lipoproteins: evidence for independent roles of age and sex. *Diabetologia* **2003**; 46:459–469.

Combs TP, Wagner JA, Berger J, Doebber T, Wang WJ, Zhang BB, Tanen M, Berg AH, O'Rahilly S, Savage DB, Chatterjee K, Weiss S, Larson PJ, Gottesdiener KM, Gertz BJ, Charron MJ, Scherer PE, Moller DE. Induction of adipocyte complement-related protein of 30 kilodaltons by PPAR_ agonists: a potential mechanism of insulin sensitization. *Endocrinology* **2002**; 143:998–1007.

Comuzzie AG, Funahashi T, Sonnenberg G, Martin LJ, Jacob HJ, Black AE, Maas D, Takahashi M, Kihara S, Tanaka S, Matsuzawa Y, Blangero J, Cohen D, Kissebah A. The genetic basis of plasma variation in adiponectin, a global endophenotype for obesity and the metabolic syndrome. *J Clin Endocrinol Metab* **2001**; 86:4321–5.10.1210/jcem.86.9.7878.

Dalamaga M, Diakopoulos KN, Mantzoros CS. The role of adiponectin in cancer: a review of current evidence. *Endocr Rev* **2012**; 33:547–94.

Dalamaga M, Migdalis I, Fargnoli JL, Papadavid E, Bloom E, Mitsiades N, Karmaniolas K, Pelecanos N, TseleniBalafouta S, Dionyssiou-Asteriou A, Mantzoros CS. Pancreatic cancer expresses adiponectin receptors and is associated with hypoleptinemia and hyperadiponectinemia: a case-control study. *Cancer Causes Control* **2009**; 20:625– 633.

Davoodi SH, Malek-Shahabi T, Malekshahi-Moghadam A, Shahbazi R, Esmaeili S. Obesity as an Important Risk Factor for Certain Types of Cancer. *Iran J Cancer Prev* **2013**; 6(4):186-94.

Deepa SS, Dong LQ. APPL1: role in adiponectin signaling and beyond. *Am J Physiol Endocrinol Metab* **2009**; 296: E22–E36.

Deepa SS, Zhou L, Ryu J, Wang C, Mao X, Li C, Zhang N, Musi N, DeFronzo RA, Liu F, Dong LQ. APPL1 mediates adiponectin-induced LKB1 cytosolic localization through the PP2A-PKCzeta signaling pathway. *Mol Endocrinol* **2011**; 25(10):1773-85.

Delaigle AM, Jonas JC, Bauche IB, Cornu O, Brichard SM. Induction of adiponectin in skeletal muscle by inflammatory cytokines: in vivo and in vitro studies. *Endocrinology* **2004**; 145:5589 –5597.

DeSantis C, Siegel R, Bandi P, Jemal A. Breast cancer statistics, 2011. *CA Cancer J Clin* **2011**; 61:409–18.

Dieudonne MN, Bussiere M, Dos Santos E, Leneveu MC, Giudicelli Y, Pecquery R. Adiponectin mediates antiproliferative and apoptotic responses in human MCF7 breast cancer cells. *Biochem Biophys Res Commun* **2006**; 345:271-9.

Dobin A, Davis CA, Schlesinger F, Drenkow J, Zaleski C, Jha S, Batut P, Chaisson M, Gingeras TR. STAR: ultrafast universal RNA-seq aligner. *Bioinformatics* **2013**; 29(1):15-21.

Dos Santos E, Benaitreau D, Dieudonne MN, Leneveu MC, Serazin V, Giudicelli Y, et al. Adiponectin mediates an antiproliferative response in human MDA-MB-231 breast cancer cells. *Oncol Rep* **2008**; 20:971-7.

Esteve-Puig R, Canals F, Colomé N, Merlino G, Recio JA. Uncoupling of the LKB1-AMPKalpha energy sensor pathway by growth factors and oncogenic BRAF. *PLoS One;* **2009**; 4(3):e4771.

Fayad R, Pini M, Sennello JA, Cabay RJ, Chan L, Xu A, Fantuzzi G. Adiponectin deficiency protects mice from chemically induced colonic inflammation. *Gastroenterology Endocrine Reviews* **2007**; 33(4):547–594.

Fruebis J, Tsao TS, Javorschi S, Ebbets-Reed D, Erickson MR, Yen FT, Bihain BE, Lodish HF. Proteolytic cleavage product of 30-kDa adipocyte complement-related protein increases fatty acid oxidation in muscle and causes weight loss in mice. *Proc Natl Acad Sci USA* **2001**; 98:2005–2010.

Galic S, Oakhill JS, Steinberg GR. Adipose tissue as an endocrine organ. Mol Cell *Endocrinol* **2010**; 316:129–39.10.1016/j.mce.2009.08.018.

Gan B, Hu J, Jiang S, Liu Y, Sahin E, Zhuang L, Fletcher-Sananikone E, Colla S, Wang YA, Chin L, Depinho RA. Lkb1 regulates quiescence and metabolic homeostasis of haematopoietic stem cells. *Nature* **2010**; 468: 701-4.

Gavrila A, Peng CK, Chan JL, Mietus JE, Goldberger AL, Mantzoros CS. Diurnal and ultradian dynamics of serum adiponectin in healthy men: comparison with leptin, circulating soluble leptin receptor, and cortisol patterns. *J Clin Endocrinol Metab* **2003**; 88:2838–2843.

Grossmann ME, Nkhata KJ, Mizuno NK, Ray A, Cleary MP. Effects of adiponectin on breast cancer cell growth and signaling. *Br J Cancer* **2008**; 98(2):370-9.

Hada Y, Yamauchi T, Waki H, Tsuchida A, Hara K, Yago H, Miyazaki O, Ebinuma H, Kadowaki T. Selective purification and characterization of adiponectin multimer species from human plasma. *Biochem Biophys Res Commun* **2007**; 356:487– 493.

Hajer GR, van Haeften TW, Visseren FL. Adipose tissue dysfunction in obesity, diabetes, and vascular diseases. *Eur Heart J* **2008**; 29: 2959-2971.

Hardie DG, Scott JW, Pan DA, Hudson ER. Management of cellular energy by the AMP-activated protein kinase system. *FEBS Lett* **2003**; 546: 113–120.

Hardie DG. The AMP-activated protein kinase pathway-new players upstream and downstream. *J Cell Sci* **2004**; 117(Pt 23):5479-87.

Hawley SA, Boudeau J, Reid JL, Mustard KJ, Udd L, Makela TP, Alessi DR, Hardie DG. Complexes between the LKB1 tumor suppressor, STRAD alpha/beta and MO25 alpha/beta are upstream kinases in the AMP-activated protein kinase cascade. *J Biol* **2003**; 2, 28.

Howe EA, Sinha R, Schlauch D, Quackenbush J. RNA-Seq analysis in MeV. *Bioinformatics* **2011**; 27(22):3209-10.

Howe LR, Subbaramaiah K, Hudis CA, Dannenberg AJ. Molecular pathways: adipose inflammation as a mediator of obesity-associated cancer. *Clin Cancer Res* **2013**; 19:6074–83.

Huang J, Manning BD. The TSC1-TSC2 complex: a molecular switchboard controlling cell growth. *Biochem J* **2008**; 412(2):179-90.

Hug C, Wang J, Ahmad NS, Bogan JS, Tsao TS, Lodish HF. T-cadherin is a receptor for hexameric and high-molecular-weight forms of Acrp30/adiponectin. *Proc Natl Acad Sci USA* **2004**; 101:10308–13.

Igata M, Motoshima H, Tsuruzoe K, Kojima K, Matsumura T, Kondo T, Taguchi T, Nakamaru K, Yano M, Kukidome D, Matsumoto K, Toyonaga T, Asano T, Nishikawa T, Araki E. Adenosine monophosphate activated protein kinase suppresses vascular smooth muscle cell proliferation through the inhibition of cell cycle progression. *Circ Res* **2005**; 97:837–44.

Inoki K, Zhu T, Guan KL. TSC2 mediates cellular energy response to control cell growth and survival. *Cell* **2003**; 115:577–90.

Jia S, Liu Z, Zhang S, Liu P, Zhang L, Lee SH, Zhang J, Signoretti S, Loda M, Roberts TM, Zhao JJ. Essential roles of PI(3)K-p110beta in cell growth, metabolism and tumorigenesis. *Nature* **2008**; 454: 776-9.48.

Kahn BB, Alquier T, Carling D, Hardie DG. AMPK-activated protein kinase: ancient energy gauge provides clues to modern understanding of metabolism. *Cell Metab* **2005**; 1:15-25.

Kang JH, Lee YY, Yu BY, Yang BS, Cho KH, Yoon DK, Roh YK. Adiponectin induces growth arrest and apoptosis of MDAMB-231 breast cancer cell. *Arch Pharm Res* **2005**; 28:1263-9.

Karim RZ, Tse GM, Putti TC, Scolyer RA, Lee CS. The significance of the Wnt pathway in the pathology of human cancers. *Pathology* **2004**; 36: 120-8.

Kaser S, Moschen A, Cayon A, Kaser A, Crespo J, PonsRomero F, Ebenbichler CF, Patsch JR, Tilg H. Adiponectin and its receptors in non-alcoholic steatohepatitis. *Gut* **2005**; 54:117–121.

Katira A, Tan PH. Evolving role of adiponectin in cancer-controversies and update. *Cancer Biol Med* **2016**, 13:101-119.

Katsiougiannis S, Kapsogeorgou EK, Manoussakis MN, Skopouli FN. Salivary gland epithelial cells: a new source of the immunoregulatory hormone adiponectin. *Arthritis Rheum* **2006**; 54:2295–2299.

Kelesidis I, Kelesidis T, Mantzoros CS. Adiponectin and cancer: a systematic review. *Br J Cancer* **2006**; 94:1221–1225.

Khan S, Shukla S, Sinha S, Meeran SM. Role of adipokines and cytokines in obesity-associated breast cancer: therapeutic targets. *Cytokine Growth Factor Rev* **2013**; 24(6):503-13.

Kharroubi I, Rasschaert J, Eizirik DL, Cnop M. Expression of adiponectin receptors in pancreatic cells. *Biochem Biophys Res Commun* **2003**; 312:1118–1122.

Kim AY, Lee YS, Kim KH, Lee JH, Lee HK, Jang SH, Kim SE, Lee GY, Lee JW, Jung SA, Chung HY, Jeong S, Kim JB. Adiponectin represses colon cancer cell proliferation via AdipoR1- and -R2-mediated AMPK activation. *Mol Endocrinol* **2010**; 24:1441–1452.

Kim KY, Baek A, Hwang JE, Choi YA, Jeong J, Lee MS, Cho DH, Lim JS, Kim KI, Yang Y. Adiponectin-activated AMPK stimulates dephosphorylation of AKT through protein phosphatase 2A activation. *Cancer Res* **2009**; 69:4018–4026.

Körner A, Pazaitou-Panayiotou K, Kelesidis T, Kelesidis I, Williams CJ, Kaprara A, Bullen J, Neuwirth A, Tseleni S, Mitsiades N, Kiess W, Mantzoros CS. Total and high- molecular-weight adiponectin in breast cancer: in vitro and in vivo studies. *J Clin Endocrinol Metab* **2007**; 92(3):1041-8.

Korsse SE, Peppelenbosch MP, van Veelen W. Targeting LKB1 signaling in cancer. *Biochim Biophys Acta* **2013**; 1835(2):194-210.

Kubota N, Terauchi Y, Yamauchi T, Kubota T, Moroi M, Matsui J, Eto K, Yamashita T, Kamon J, Satoh H, Yano W, Froguel P, Nagai R, Kimura S, Kadowaki T, Noda T. Disruption of adiponectin causes insulin resistance and neointimal formation. *J Biol Chem* **2002**; 277:25863–6.10.1074/jbc.C200251200.

Kubota N, Yano W, Kubota T, Yamauchi T, Itoh S, Kumagai H, Kozono H, Takamoto I, Okamoto S, Shiuchi T, Suzuki R, Satoh H, Tsuchida A, Moroi M, Sugi K, Noda T, Ebinuma H, Ueta Y, Kondo T, Araki E, Ezaki O, Nagai R, Tobe K, Terauchi Y, Ueki K, Minokoshi Y, Kadowaki T. Adiponectin stimulates AMP-activated protein kinase in the hypothalamus and increases food intake. *Cell Metab* **2007**; 6 55–68.

Kusminski CM, McTernan PG, Schraw T, Kos K, O'Hare JP, Ahima R, Kumar S, Scherer PE. Adiponectin complexes in human cerebrospinal fluid: distinct complex distribution from serum. *Diabetologia* **2007**; 50:634 – 642.

Lam JB, Chow KH, Xu A, Lam KS, Liu J, Wong NS, Moon RT, Shepherd PR, Cooper GJ, Wang Y. Adiponectin haploinsufficiency promotes mammary tumor development in MMTV-PyVT mice by modulation of phosphatase and tensin homolog activities. *PLoS One* **2009**; 4(3):e4968.

Landskroner-Eiger S, Park J, Israel D, Pollard JW, Scherer PE. Morphogenesis of the developing mammary gland: stage-dependent impact of adipocytes. *Dev Biol* **2010**; 344:968–78.

Landskroner-Eiger S, Qian B, Muise ES, Nawrocki AR, Berger JP, Fine EJ, Koba W, Deng Y, Pollard JW, Scherer PE. Proangiogenic contribution of adiponectin toward mammary tumor growth in vivo. *Clin Cancer Res* **2009**; 15(10):3265-76.

Law JH, Habibi G, Hu K, Masoudi H, Wang MY, Stratford AL, Park E, Gee JM, Finlay P, Jones HE, Nicholson RI, Carboni J, Gottardis M, Pollak M, Dunn SE. Phosphorylated insulin-like growth factor-i/insulin receptor is present in all breast cancer subtypes and is related to poor survival. *Cancer Res* **2008**; 68:10238–46.

Lee MH, Klein RL, El-Shewy HM, Luttrell DK, Luttrell LM. The adiponectin receptors AdipoR1 and AdipoR2 activate ERK1/2 through a Src/Ras-dependent pathway and stimulate cell growth. *Biochemistry* **2008**; 47(44):11682-92.

LeRoith D, Roberts CT. The insulin-like growth factor system and cancer. *Cancer Lett* **2003**; 195:127–37.

Li G, Cong L, Gasser J, Zhao J, Chen K, Li F. Mechanisms underlying the anti-proliferative actions of adiponectin in human breast cancer cells, MCF7-dependency on the cAMP/protein kinase-A pathway. *Nutr Cancer* **2011**; 63:80–88.

Liu J, Lam JB, Chow KH, Xu A, Lam KS, Moon RT, Wang Y. Adiponectin stimulates Wnt inhibitory factor-1 expression through epigenetic regulations involving the transcription factor specificity protein 1. *Carcinogenesis* **2008**; 29: 2195-202.

Love MI, Huber W, Anders S. Moderated estimation of fold change and dispersion for 1191 RNA-seq data with DESeq2. *Genome Biol* **2014**; 15:550.

Luo Z, Saha AK, Xiang X, Ruderman NB. AMPK, the metabolic syndrome and cancer. *Trends Pharmacol Sci* **2005**; 26:69-76.

Macciò A, Madeddu C. Obesity, inflammation, and postmenopausal breast cancer: therapeutic implications. *Sci World J* **2011**; 11:2020-36.

Maccio` A, Madeddu C, Mantovani G. Adipose tissue as target organ in the treatment of hormone-dependent breast cancer: new therapeutic perspectives. *Obes Rev* **2009**; 10:660–70.

MacDougald OA, Burant CF. The rapidly expanding family of adipokines. *Cell Metab* **2007**; 6:159–161.

Maeda N, Shimomura I, Kishida K, Nishizawa H, Matsuda M, Nagaretani H, Furuyama N, Kondo H, Takahashi M, Arita Y, Komuro R, Ouchi N, Kihara S, Tochino Y, Okutomi K, Horie M, Takeda S, Aoyama T, Funahashi T, Matsuzawa Y. Diet-induced insulin resistance in mice lacking adiponectin/ACRP30. *Nat Med* **2002**; 8:731–7.10.1038/nm724.

Maeda N, Takahashi M, Funahashi T, Kihara S, Nishizawa H, Kishida K, Nagaretani H, Matsuda M, Komuro R, Ouchi N, Kuriyama H, Hotta K, Nakamura T, Shimomura I, Matsuzawa Y. PPAR-ligands increase expression and plasma concentrations of adiponectin, an adipose-derived protein. *Diabetes* **2001**; 50:2094–2099.

Mantzoros C, Petridou E, Dessypris N, Chavelas C, Dalamaga M, Alexe DM, Papadiamantis Y, Markopoulos C, Spanos E, Chrousos G, Trichopoulos D. Adiponectin and breast cancer risk. *J Clin Endocrinol Metab* **2004**; 89:1102-7.

Mao X, Kikani C K, Riojas RA, Langlais P, Wang L, Ramos FJ, Fang Q, Christ-Roberts CY, Hong JY, Kim RY, Liu F, Dong LQ. APPL1 binds to adiponectin receptors and mediates adiponectin signaling and function. *Nat Cell Biol* **2006**; 8:516–23.

Mauro L, Naimo GD, Ricchio E, Panno ML, Andò S. Cross-Talk between Adiponectin and IGF-IR in Breast Cancer. *Front Oncol* **2015**; 5:157.

Mauro L, Pellegrino M, De Amicis F, Ricchio E, Giordano F, Rizza P, Catalano S, Bonofiglio D, Sisci D, Panno ML, Andò S. Evidences that estrogen receptor α interferes with adiponectin effects on breast cancer cell growth. *Cell Cycle* **2014**; 13(4):553-64.

Mauro L, Pellegrino M, Giordano F, Ricchio E, Rizza P, De Amicis F, et al. Estrogen receptor- α drives adiponectin effects on cyclin D1 expression in breast cancer cells. *FASEB J* **2015**; 29(5):2150-60.

McTiernan A, Rajan KB, Tworoger SS, Irwin M, Bernstein L, Baumgartner R, Gilliland F, Stanczyk FZ, Yasui Y, Ballard-Barbash R. Adiposity and sex hormones in postmenopausal breast cancer survivors. *J Clin Oncol* **2003**; 21:1961–6.

Milburn CC, Boudeau J, Deak M, Alessi DR. van Aalten DMF. Crystal structure of MO25α in complex with the *C* terminus of the pseudo kinase STE20-related adaptor. *Nat Struct Mol Biol* **2004**; *11* 193–200.

Mistry T, Digby JE, Chen J, Desai KM, Randeva HS. The regulation of adiponectin receptors in human prostate cancer cell lines. *Biochem Biophys Res Commun* **2006;** 348:832– 838.

Miyoshi Y, Funahashi T, Kihara S, Taguchi T, Tamaki Y, Matsuzawa Y, Noguchi S. Association of serum adiponectin levels with breast cancer risk. *Clin Cancer Res* **2003**; 9:5699-704.

Munsell MF, Sprague BL, Berry DA, Chisholm G, Trentham-Dietz A. Body mass index and breast cancer risk according to postmenopausal estrogen-progestin use and hormone receptor status. *Epidemiol Rev* **2014**; 36114-136.

Nakano Y, Tajima S, Yoshimi A, Akiyama H, Tsushima M, Tanioka T, Negoro T, Tomita M, Tobe T. A novel enzyme-linked immunosorbent assay specific for high-molecular-weight adiponectin. *J Lipid Res* **2006**; 47 1572–1582.

Nath-Sain S, Marignani PA. LKB1 catalytic activity contributes to estrogen receptor alpha signaling. *Mol Biol Cell* **2009**; 20(11):2785-95.

Nishida M, Funahashi T, Shimomura I. Pathophysiological significance of adiponectin. *Med Mol Morphol;* **2007** 40 55–67.

Obeid S, Hebbard L. Role of adiponectin and its receptors in cancer. *Cancer Biol Med* **2012**; 9:213-220.

Okamoto Y, Kihara S, Funahashi T, Matsuzawa Y, Libby P. Adiponectin: a key adipocytokine in metabolic syndrome. *Clin Sci* **2006**; 110:267–78.10.1042/CS20050182.

Osborn O, Olefsky JM. The cellular and signaling networks linking the immune system and metabolism in disease. *Nat Med* **2012**; 18:363–74.

Otvos L Jr, Haspinger E, La Russa F, Maspero F, Graziano P, Kovalszky I, Lovas S, Nama K, Hoffmann R, Knappe D, Cassone M, Wade J, Surmacz E. Design and development of a peptide-based adiponectin receptor agonist for cancer treatment. *BMC Biotechnol* **2011**; 11:90. 52.

Otvos L Jr, Kovalszky I, Olah J, Coroniti R, Knappe D, Nollmann FI, Hoffmann R, Wade JD, Lovas S, Surmacz E. Optimization of adiponectin-derived peptides for inhibition of cancer cell growth and signaling. *Biopolymers* **2015**; 104:156-166.

Ouchi N, Kihara S, Arita Y, Maeda K, Kuriyama H, Okamoto Y, Hotta K, Nishida M, Takahashi M, Nakamura T, Yamashita S, Funahashi T, Matsuzawa Y. Novel modulator for endothelial adhesion molecules adipocyte-derived plasma protein adiponectin. *Circulation* **1999**; 2473–2476.

Ouchi N, Kihara S, Arita Y, Okamoto Y, Maeda K, Kuriyama H, Hotta K, Nishida M, Takahashi M, Muraguchi M, Ohmoto Y, Nakamura T, Yamashita S, Funahashi T, Matsuzawa Y. Adiponectin, an adipocyte-derived plasma protein, inhibits endothelial NF-B signaling through a cAMP-dependent pathway. *Circulation* **2000**; 102:1296 –1301.

Ouchi N, Kobayashi H, Kihara S, Kumada M, Sato K, Inoue T, Funahashi T, Walsh K. Adiponectin stimulates angiogenesis by promoting cross-talk between AMPactivated protein kinase and Akt signaling in endothelial cells. *J Biol Chem* **2004**; 279:1304 –1309 70.

Pajvani UB, Du X, Combs TP, Berg AH, Rajala MW, Schulthess T, Engel J, Brownlee M, Scherer PE. Structure-function studies of the adipocyte-secreted hormone Acrp30/adiponectin. Implications for metabolic regulation and bioactivity. *J Biol Chem* **2003**; 278:9073–9085.

Pan D, Dong J, Zhang Y, Gao X. Tuberous sclerosis complex: from Drosophila to human disease. *Trends Cell Biol* **2004**; 14(2):78-85.

Panno ML, Naimo GD, Spina E, Andò S, Mauro L. Different molecular signaling sustaining adiponectin action in breast cancer. *Curr Opin Pharmacol* **2016**; 31:1-7.

Park J, Euhus DM, Scherer PE. Paracrine and endocrine effects of adipose tissue on cancer development and progression. *Endocr Rev* **2011**; 32:550–70.

Pearson G, Robinson F, Beers Gibson T, Xu BE, Karandikar M, Berman K, Cobb MH. Mitogenactivated protein (MAP) kinase pathways: regulation and physiological functions. *Endocr Rev* **2001**; 22:153–183.

Petridou E, Mantzoros CS, Dessypris N, Dikalioti SK, Trichopoulos D. Adiponectin in relation to childhood myeloblastic leukaemia. *Br J Cancer* **2006**; 94:156-160.

Petridou ET, Mitsiades N, Gialamas S, Angelopoulos M, Skalkidou A, Dessypris N, Hsi A, Lazaris N, Polyzos A, Syrigos C, Brennan AM, Tseleni-Balafouta S, Mantzoros CS. Circulating adiponectin levels and expression of adiponectin receptors in relation to lung cancer: two casecontrol studies. *Oncology* **2007**; 73:261–269.

Petridou ET, Sergentanis TN, Dessypris N, Vlachantoni IT, Tseleni- Balafouta S, Pourtsidis A, Moschovi M, Polychronopoulou S, Athanasiadou-Piperopoulou F, Kalmanti M, Mantzoros CS. Serum adiponectin as a predictor of childhood non-Hodgkin's lymphoma: a nationwide case-control study. *J Clin Oncol* **2009;** 27:5049-5055.

Pfeiler GH, Buechler C, Neumeier M, Schäffler A, Schmitz G, Ortmann O, Treeck O. Adiponectin effects on human breast cancer cells are dependent on 17-beta estradiol. *Oncol Rep* **2008**; 19(3):787-93.

Pin˜eiro R, Iglesias MJ, Gallego R, Raghay K, Eiras S, Rubio J, Die´guez C, Gualillo O, Gonza´lez-Juanatey JR, Lago F. Adiponectin is synthesized and secreted by human and murine cardiomyocytes. *FEBS Lett* **2005**; 579:5163–5169.

Pischon T, Nothlings U, Boeing H. Obesity and cancer. *Proc Nutr Soc* **2008**; 67:128–145.

Pollak MN, Schernhammer ES, Hankinson SE. Insulin-like growth factors and neoplasia. *Nat Rev Cancer* **2004**; 4:505–18.

Roberts DL, Dive C, Renehan AG. Biological mechanisms linking obesity and cancer risk: new perspectives. *Annu Rev Med* **2010**; 61:301–16.

Rose DP, Vona-Davis L. Interaction between menopausal status and obesity in affecting breast cancer risk. *Maturitas* **2010**; 66(1)33-38.

Sablina AA, Hahn WC. The role of PP2A A subunits in tumor suppression. *Cell Adh Migr* **2007**; 1:140–141.

Saito K, Tobe T, Minoshima S, Aakawa S, Sumiya J, Yoda M, Nakano Y, Shimizu N, Tomita M. Organization of the gene for gelatin-binding protein (GBP28). *Gene* **1999**; 229:67–73.10.1016/S0378-1119 (99)00041-4.

Scherer PE, Williams S, Fogliano M, Baldini G, Lodish HF. A novel serum protein similar to C1q, produced exclusively in adipocytes. *J Biol Chem* **1995**; 26746–26749.

Shapiro L, tsa. The crystal structure of a complement-1q family protein suggests an evolutionary link to tumor necrosis factor. *Curr Biol* **1998**; 8:335–8.10.1016/S0960-9822 (98)70133-2.

Shaw RJ, Cantley LC. Ras, PI(3)K and mTOR signalling controls tumour cell growth. *Nature* **2006**; 441: 424-30.

Siegel R, Naishadham D, Jemal A. Cancer statistics, 2012. *CA Cancer J Clin* **2012**; 62:1029.

Singletary SE. Rating the risk factors for breast cancer. *Ann Surg* **2003**; 237:474–82.

Smith DP, Spicer J, Smith A, Swift S, Ashworth A. The mouse Peutz-Jeghers syndrome gene LKB1 encodes a nuclear protein kinase. *Hum Mol Genet* 1**999**; 8(8):1479-85.

Stefan N, Vozarova B, Funahashi T, Matsuzawa Y, Weyer C, Lindsay RS, Youngren JF, Havel PJ, Pratley RE, Bogardus C, Tataranni PA. Plasma adiponectin concentration is associated with skeletal muscle insulin receptor tyrosine phosphorylation, and low plasma concentration precedes a decrease in whole-body insulin sensitivity in humans. *Diabetes* **2002**; 51:1884–1888.

Surmacz E, Otvos L. Molecular targeting of obesity pathways in cancer. *Horm Mol Biol Clin Investig* **2015**; 22:53-62.

Surmacz E. Leptin and adiponectin: emerging therapeutic targets in breast cancer. *J Mammary Gland Biol Neoplasia* **2013**; 18:321–32.

Suzuki R, Orsini N, Saji S, Key TJ, Wolk A. Body weight and incidence of breast cancer defined by estrogen and progesterone receptor status–a meta-analysis. *Int J Cancer* **2009**; 124(3)698-712.

Swarbrick MM, Havel PJ. Physiological, pharmacological, and nutritional regulation of circulating adiponectin concentrations in humans. *Metab Syndr Relat Disord* **2008**; 6:87–102.

Takahashi M, Arita Y, Yamagata K, Matsukawa Y, Okutomi K, Horie M, et al. Genomic structure and mutations in adipose-specific gene, adiponectin. *Int J Obes Relat Metab Disord* **2000**; 24:861–8.10.1038/sj.ijo.0801244.

Takahata C, Miyoshi Y, Irahara N, Taguchi T, Tamaki Y, Noguchi S. Demonstration of adiponectin receptors 1 and 2 mRNA expression in human breast cancer cells. *Cancer Lett* **2007**; 250:229–236.

Tilg H, Moschen AR. Adipocytokines: mediators linking adipose tissue, inflammation and immunity. *Nat Rev Immunol* **2006**; 6:772–83.

Tishinsky JM, Dyck DJ, Robinson LE. Lifestyle factors increasing adiponectin synthesis and secretion. *Vitam. Horm.* **2012**; 90 1–30.

Torre LA, Bray F, Siegel RL, Ferlay J, Lortet-Tieulent J, Jemal A. Global cancer statistics, 2012. *CA Cancer J Clin* **2015**; 65 (2), 87e108.

Treeck O, Lattrich C, Juhasz-Boess I, Buchholz S, Pfeiler G, Ortmann O. Adiponectin differentially affects gene expression in human mammary epithelial and breast cancer cells. *Br J Cancer* **2008**; 99(8):1246-50.

Trujillo ME, Scherer PE. Adiponectin—journey from an adipocyte secretory protein to biomarker of the metabolic syndrome. *J Intern Med* **2005**; 257:167–175 69.

Tsao TS, Murrey HE, Hug C, Lee DH, Lodish HF. Oligomerization state-dependent activation of NF-B signaling pathway by adipocyte complement-related protein of 30 kDa (Acrp30). *J Biol Chem* **2002**; 277:29359–29362.

Tsao TS, Tomas E, Murrey HE, Hug C, Lee DH, Ruderman NB, Heuser JE, Lodish HF. Role of disulfide bonds in Acrp30/adiponectin structure and signaling specificity. Different oligomers activate different signal transduction pathways. *J. Biol. Chem.* **2003**; 278:50810–50817 54.

Vaupel P. The role of hypoxia-induced factors in tumor progression. *Oncologist* **2004**; 9(Suppl. 5):10–7.

Vona-Davis L, Rose DP. Adipokines as endocrine, paracrine and autocrine factors in breast cancer risk and progression. *Endocr Relat Cancer* **2007**; 14:189–206.

Waki H, Yamauchi T, Kamon J, Ito Y, Uchida S, Kita S, Hara K, Hada Y, Vasseur F, Froguel P, Kimura S, Nagai R, Kadowaki T. Impaired multimerization of human adiponectin mutants associated with diabetes. Molecular structure and multimer formation of adiponectin. *J Biol Chem* **2003**; 278:40352–63.

Waki H, Yamauchi T, Kamon J, Kita S, Ito Y, Hada Y, Uchida S, Tsuchida A, Takekawa S, Kadowaki T. Generation of globular fragment of adiponectin by leukocyte elastase secreted by monocytic cell line THP-1. *Endocrinology* **2005**; 146:790–6.10.1210/en.2004-1096.

Wang C, Mao X, Wang L, Liu M, Wetzel MD, Guan KL, Dong LQ, Liu F. Adiponectin sensitizes insulin signaling by reducing p70 S6 kinase-mediated serine phosphorylation of IRS-1. *J Biol Chem* **2007**; 282:7991–7996.

Wang H, Zhang H, Jia Y, Zhang Z, Craig R, Wang X, Elbein SC. Adiponectin receptor 1 gene (ADIPOR1) as a candidate for type 2 diabetes and insulin resistance. *Diabetes* **2004**; 53:2132–6.

Wang Y, Lam JB, Lam KS, Liu J, Lam MC, Hoo RL, Wu D, Cooper GJ, Xu A. Adiponectin modulates the glycogen synthase kinase-3beta/beta-catenin signaling pathway and attenuates mammary tumorigenesis of MDA-MB-231 cells in nude mice. *Cancer Res* **2006**; 66:11462-70.

Wang Y, Lam KS, Chan L, Chan KW, Lam JB, Lam MC, Hoo RC, Mak WW, Cooper GJ, Xu A. Post-translational modifications of the four conserved lysine residues within the collagenous domain of adiponectin are required for the formation of its high molecular weight oligomeric complex. *J Biol Chem* **2006**; 281:16391–16400.

Wei S, Yang J, Lee SL, Kulp SK, Chen CS. PPARgamma independent antitumor effects of thiazolidinediones. *Cancer Lett* **2009**; 276:119-124.

Wolin KY, Carson K, Colditz GA. Obesity and cancer. *Oncologist* **2010**; 15:556–65.

Woods A, Vertommen D, Neumann D, Turk R, Bayliss J, Schlattner U, Wallimann T, Carling D, Rider MH. Identification of phosphorylation sites in AMP-activated protein kinase (AMPK) for upstream AMPK kinases and study of their roles by site-directed mutagenesis. *J Biol Chem* **2003**; 278, 28434–28442.

Yamauchi T, Kamon J, Ito Y, Tsuchida A, Yokomizo T, Kita S, Sugiyama T, Miyagishi M, Hara K, Tsunoda M, Murakami K, Ohteki T, Uchida S, Takekawa S, Waki H, Tsuno NH, Shibata Y, Terauchi Y, Froguel P, Tobe K, Koyasu S, Taira K, Kitamura T, Shimizu T, Nagai R, Kadowaki T. Cloning of adiponectin receptors tha mediate antidiabetic metabolic effects. *Nature* **2003**; 423:762–9.

Yamauchi T, Kamon J, Waki H, Imai Y, Shimozawa N, Hioki K, Uchida S, Ito Y, Takakuwa K, Matsui J, Takata M, Eto K, Terauchi Y, Komeda K, Tsunoda M, Murakami K, Ohnishi Y, Naitoh T, Yamamura K, Ueyama Y, Froguel P, Kimura S, Nagai R, Kadowaki T. Globular adiponectin protected ob/ob mice from diabetes and ApoE-deficient mice from atherosclerosis. *J BiolChem* **2003**; 278:2461–8.

Yamauchi T, Kamon J, Waki H, Terauchi Y, Kubota N, Hara K, Mori Y, Ide T, Murakami K, Tsuboyama-Kasaoka N, Ezaki O, Akanuma Y, Gavrilova O, Vinson C, Reitman ML, Kagechika H, Shudo K, Yoda M, Nakano Y, Tobe K, Nagai R, Kimura S, Tomita M, Froguel P, Kadowaki T. The fat-derived hormone adiponectin reverses insulin resistance associated with both lipoatrophy and obesity. *Nat Med* **2001**; 7:941–6.

Yamauchi T, Nio Y, Maki T, Kobayashi M, Takazawa T, Iwabu M, Okada-Iwabu M, Kawamoto S, Kubota N, Kubota T, Ito Y, Kamon J, Tsuchida A, Kumagai K, Kozono H, Hada Y, Ogata H, Tokuyama K, Tsunoda M, Ide T, Murakami K, Awazawa M, Takamoto I, Froguel P, Hara K, Tobe K, Nagai R, Ueki K, Kadowaki T. Targeted disruption of AdipoR1 and AdipoR2 causes abrogation of adiponectin binding and metabolic actions. *Nat Med* **2007**; 13:332–339.

Ye J, Gao Z, Yin J, He Q. Hypoxia is a potential risk factor for chronic inflammation and adiponectin reduction in adipose tissue of ob/ob and dietary obese mice. *Am J Physiol Endocrinol Metab* **2007**; 293:E1118–28.

Yokota T, Oritani K, Takahashi I, Ishikawa J, Matsuyama A, Ouchi N, Kihara S, Funahashi T, Tenner AJ, Tomiyama Y, Matsuzawa Y. Adiponectin, a new member of the family of soluble defense collagens, negatively regulates the growth of myelomonocytic progenitors and the functions of macrophages. *Blood* **2000**; 96:1723–32.

Yu JG, Javorschi S, Hevener AL, Kruszynska YT, Norman RA, Sinha M, Olefsky JM. The effect of thiazolidinediones on plasma adiponectin levels in normal, obese, and type 2 diabetic subjects. *Diabetes* **2002**; 51:2968–2974.

Zeqiraj E, Filippi BM, Deak M, Alessi DR, van Aalten DMF. Structure of the LKB1–STRAD–MO25 complex reveals an allosteric mechanism of kinase activation. *Science* **2009**; 326 1707–1711.

Ziemke F, Mantzoros CS. Adiponectin in insulin resistance: lessons from translational research. *Am J Clin Nutr* **2010**; 91:258S–261S.

Appendix A. Table 1: Differentially expressed genes identified by RNA sequencing in MCF-7 and MDA-MB-231 cells upon adiponectin.

	MCF-7			MDA-MB-231				
Ensembl_Name	**C**	**A5**	**A30**	**C**	**A5**	**A30**	**gene_type**	**gene_name**
ENSG00000000971.15	-2,59090003	-2,60378106	-2,516407154	1,975664235	2,914437664	2,820986341	protein_coding	CFH
ENSG00000002587.9	-2,699408667	-2,34269174	-2,628753765	2,658275271	2,588721254	2,423857646	protein_coding	HS3ST1
ENSG00000003436.14	-2,624474758	-2,78604097	-2,37734034	2,166175278	2,734118909	2,887561886	protein_coding	TFPI
ENSG00000005379.15	-2,782704254	-2,79452111	-2,713940665	3,31567895	2,619260603	2,356226479	protein_coding	BZRAP1
ENSG00000006047.12	2,653044109	2,810477091	2,827617007	-2,77846762	-2,74449714	-2,768173443	protein_coding	YBX2
ENSG00000006210.6	-3,155915699	-3,1640355	-3,107726375	1,846246169	3,558766219	4,022665182	protein_coding	CX3CL1
ENSG00000006468.13	-3,072025414	-3,08184517	-3,013771065	3,053902146	3,065466811	3,048272692	protein_coding	ETV1
ENSG00000007264.13	2,82313251	2,562472042	2,305129543	-2,32390215	-2,672508925	-2,694323021	protein_coding	MATK
ENSG00000008517.16	-2,809624774	-2,82342421	-2,728592891	1,612952113	3,263565223	3,485124535	protein_coding	IL32
ENSG00000010438.16	-2,280440436	-2,67679147	-2,592540997	1,911464299	2,70443685	2,933871755	protein_coding	PRSS3
ENSG00000018510.12	-2,930283944	-3,32137964	-3,117241155	3,297500029	3,106578618	2,964826091	protein_coding	AGPS
ENSG00000019549.8	-2,638327503	-2,49416184	-2,549872158	3,034889964	2,416790846	2,230680692	protein_coding	SNAI2
ENSG00000019582.14	-3,116493317	-3,12622258	-3,167206165	2,68505493	3,370330505	3,354536628	protein_coding	CD74
ENSG00000023445.13	-2,97240405	-2,92540672	-2,23653096	1,325682369	3,431448098	3,377211267	protein_coding	BIRC3
ENSG00000026025.13	-3,11735155	-3,24102641	-3,178915455	3,085088414	3,192024487	3,260180512	protein_coding	VIM
ENSG00000028137.16	-3,097379467	-3,10629714	-3,044682161	1,79832695	3,364914452	4,085117365	protein_coding	TNFRSF1B
ENSG00000041982.15	-2,585111391	-2,67440399	-2,487880566	2,025189896	2,719049059	3,003156994	protein_coding	TNC
ENSG00000042980.12	-2,486654082	-2,83605878	-2,758378914	2,860051345	2,708547682	2,512492751	protein_coding	ADAM28
ENSG00000048052.21	-2,917073705	-2,92973692	-2,700407015	2,204400745	3,107917092	3,234899801	protein_coding	HDAC9
ENSG00000048740.17	-2,784200685	-2,79585175	-2,341376187	2,63845719	2,708872245	2,574099184	protein_coding	CELF2
ENSG00000049192.14	-2,655435874	-2,66979344	-2,571779385	2,323132662	2,906872509	2,667003529	protein_coding	ADAMTS6
ENSG00000049249.8	-2,694585099	-2,70712416	-2,621896166	1,332017616	3,478308655	3,213279148	protein_coding	TNFRSF9
ENSG00000050730.15	-2,219905163	-2,23449364	-2,136462033	-0,26587207	3,169044883	3,687688021	protein_coding	TNIP3
ENSG00000059804.15	-3,094166417	-2,95690264	-2,672023012	2,440514726	3,05880434	3,223772999	protein_coding	SLC2A3

ENSG00000060558.3	-3,208489709	-3,21572833	-2,943308627	2,515280544	3,318054356	3,53419177	protein_coding	GNA15
ENSG00000060982.14	-3,224254062	-3,41283392	-3,178627773	3,005559941	3,344364487	3,465791329	protein_coding	BCAT1
ENSG00000064225.12	-2,564691665	-2,89583389	-2,821047433	2,384146746	2,930320378	2,967105861	protein_coding	ST3GAL6
ENSG00000064270.12	2,674852072	3,318495399	3,532368811	-3,18380547	-3,164061789	-3,177849028	protein_coding	ATP2C2
ENSG00000064787.12	3,096009384	2,638728194	2,117184096	-2,095573	-2,866941622	-2,889407055	protein_coding	BCAS1
ENSG00000064886.13	-2,966555694	-2,6819377	-2,582416235	0,560001635	3,553707463	4,11720053	protein_coding	CHI3L2
ENSG00000065320.8	2,545688908	2,548064503	2,685083184	-2,83574242	-2,457697203	-2,485396976	protein_coding	NTN1
ENSG00000066468.20	2,84794099	2,560844574	2,466456151	-2,76045499	-2,730057452	-2,384729274	protein_coding	FGFR2
ENSG00000066735.14	3,120228667	2,568995351	2,357513118	-2,69603065	-2,664310101	-2,686396383	protein_coding	KIF26A
ENSG00000067798.13	-3,132121841	-3,14042993	-2,627778753	2,278650444	3,321175742	3,300504335	protein_coding	NAV3
ENSG00000067840.12	2,602338994	2,520916315	2,628318027	-2,5981631	-2,565250978	-2,588159259	protein_coding	PDZD4
ENSG00000068366.19	-2,539814869	-2,67197314	-2,736545362	2,382492646	2,713079375	2,852761354	protein_coding	ACSL4
ENSG00000069122.18	-3,399107561	-3,40301972	-3,245317133	3,350165102	3,383115764	3,314163547	protein_coding	ADGRF5
ENSG00000070882.12	-3,216502143	-3,28984995	-3,244558268	3,618715227	3,228470558	2,903724572	protein_coding	OSBPL3
ENSG00000071967.11	-3,079756865	-2,82911519	-2,911168408	3,031726239	2,963669495	2,824644728	protein_coding	CYBRD1
ENSG00000072840.12	-3,01206372	-3,02270523	-2,949153122	2,887241584	2,993051903	3,103628588	protein_coding	EVC
ENSG00000072858.10	2,649899794	2,953144983	3,013969774	-2,82005113	-2,887427849	-2,90953557	protein_coding	SIDT1
ENSG00000073756.11	-2,546316826	-2,89369705	-2,814997963	-0,05762249	3,691576321	4,621058003	protein_coding	PTGS2
ENSG00000074370.17	3,319116895	2,785830237	2,732190117	-2,8534671	-2,94645561	-3,037214544	protein_coding	ATP2A3
ENSG00000075461.5	2,719042572	2,507172685	2,535693805	-2,35725851	-2,794170701	-2,61047985	protein_coding	CACNG4
ENSG00000076716.8	2,841204396	2,949857651	3,054649802	-3,0494265	-3,025380793	-2,77090456	protein_coding	GPC4
ENSG00000077420.15	-2,987358703	-2,71485784	-2,928684801	2,844548446	2,850945167	2,935407728	protein_coding	APBB1IP
ENSG00000077984.5	-2,661634703	-2,67413021	-2,589210781	2,681454716	2,52494088	2,718580092	protein_coding	CST7
ENSG00000079215.13	-2,79875009	-2,8118349	-2,722147455	2,615558728	3,079191758	2,637981962	protein_coding	SLC1A3
ENSG00000080007.7	2,499551516	2,609972386	2,535466489	-2,5627862	-2,529528898	-2,552675291	protein_coding	DDX43
ENSG00000080200.9	-2,36530028	-2,38418668	-2,913432472	2,546467843	2,57763666	2,53881493	protein_coding	CRYBG3
ENSG00000081041.8	-3,027132809	-3,23067527	-2,96451088	0,956560105	4,089102297	4,176656554	protein_coding	CXCL2
ENSG00000081665.13	-2,765271357	-2,77716358	-2,696103977	2,908587003	2,692982666	2,63696924	protein_coding	ZNF506
ENSG00000082175.14	3,013012639	3,021446403	2,923826583	-2,82565025	-3,058275612	-3,074359761	protein_coding	PGR
ENSG00000082269.16	-2,526322133	-2,86399204	-2,437034549	2,562438501	2,668318481	2,596591743	protein_coding	FAM135A
ENSG00000083307.10	3,05027238	3,226232025	3,214101888	-2,98840164	-3,245063178	-3,257141477	protein_coding	GRHL2
ENSG00000084207.15	-2,867615961	-3,36627958	-3,193988305	3,138888863	3,074055133	3,214939848	protein_coding	GSTP1

ENSG00000085552.16	2,636399991	2,633786134	2,539038828	-2,37029558	-2,708761269	-2,730168102	protein_coding	IGSF9
ENSG00000085662.13	-3,264200126	-3,49536498	-3,386756192	2,399521951	3,799025239	3,947774105	protein_coding	AKR1B1
ENSG00000086548.8	2,606092947	2,640742992	3,127225133	-2,80434074	-2,774448713	-2,795271621	protein_coding	CEACAM6
ENSG00000089356.16	3,137763353	2,929960803	2,914407672	-3,00598675	-2,978473353	-2,997671723	protein_coding	FXYD3
ENSG00000090530.9	-3,047026596	-3,18068149	-3,122812052	3,013027151	3,265288767	3,072204219	protein_coding	P3H2
ENSG00000091592.15	-2,614960514	-2,58271192	-2,416346509	2,38889805	2,580915533	2,64420536	protein_coding	NLRP1
ENSG00000091656.15	-2,779636151	-2,79143173	-2,710992429	2,974123428	2,69309113	2,614845747	protein_coding	ZFHX4
ENSG00000091831.21	3,415905155	3,335933087	3,014589966	-3,12661339	-3,392553371	-3,247261452	protein_coding	ESR1
ENSG00000091986.15	-2,767525337	-2,9789197	-2,760143212	2,972486804	2,885308194	2,64879325	protein_coding	CCDC80
ENSG00000095627.9	2,867198751	2,897320657	2,8627707	-2,88800442	-2,859823095	-2,879462592	protein_coding	TDRD1
ENSG00000099284.13	2,680928179	2,799606987	3,044233288	-2,8541578	-2,825225988	-2,845384665	protein_coding	H2AFY2
ENSG00000100867.14	2,650804015	2,867124285	2,960243323	-2,82010555	-2,900566676	-2,757499395	protein_coding	DHRS2
ENSG00000101017.13	-3,049224818	-3,05860049	-2,99395355	2,709239592	3,086799256	3,305740013	protein_coding	CD40
ENSG00000101098.12	2,878498208	2,805802227	2,911712499	-2,87767986	-2,849266524	-2,869066546	protein_coding	RIMS4
ENSG00000101115.12	1,877550353	2,954692607	3,284417625	-2,79091286	-2,54502989	-2,780717837	protein_coding	SALL4
ENSG00000101144.12	2,967741257	3,213705068	3,357159425	-3,14156071	-3,357966955	-3,039078081	protein_coding	BMP7
ENSG00000101160.13	-3,124467716	-3,18005885	-3,119080725	3,206984354	3,143231526	3,073391411	protein_coding	CTSZ
ENSG00000101194.17	-3,009758039	-3,15109794	-3,090072091	2,89776418	3,139152978	3,214010909	protein_coding	SLC17A9
ENSG00000101298.13	-2,604025096	-2,61679022	-2,530156356	2,677516351	2,363428206	2,710027114	protein_coding	SNPH
ENSG00000101333.16	2,430367221	2,61427753	2,492750284	-2,21548795	-2,647324105	-2,674582982	protein_coding	PLCB4
ENSG00000101335.9	-3,096756385	-3,27583081	-3,23220356	3,566127455	3,016267041	3,022396257	protein_coding	MYL9
ENSG00000101441.4	-2,997389013	-3,00859802	-3,079108961	2,731503314	3,210969808	3,142622871	protein_coding	CST4
ENSG00000101670.11	-2,670150146	-3,19577757	-2,915561553	2,811835776	2,951620948	3,018032547	protein_coding	LIPG
ENSG00000101955.14	-2,661294149	-2,67693741	-2,321213129	2,519007933	2,586579643	2,553857109	protein_coding	SRPX
ENSG00000102024.17	-3,320531333	-3,32621613	-3,219466552	3,278648801	3,342001511	3,245563701	protein_coding	PLS3
ENSG00000102038.15	-3,00606418	-2,86964706	-2,938190927	2,964101229	2,983893647	2,865907289	protein_coding	SMARCA1
ENSG00000102271.13	-3,177706701	-3,18544954	-3,131659759	3,771478889	3,017172553	2,70616456	protein_coding	KLHL4
ENSG00000102287.16	-3,09268201	-3,10224245	-3,228890938	3,045700813	3,213756126	3,164358456	protein_coding	GABRE
ENSG00000102683.7	3,090385952	3,060591026	2,662634508	-2,9495054	-2,922714739	-2,941391351	protein_coding	SGCG
ENSG00000103485.17	2,941139986	2,898061306	3,022980646	-2,77308949	-3,148551499	-2,940540948	protein_coding	QPRT
ENSG00000103489.11	2,552796434	2,623552795	2,650133584	-2,37704016	-2,714047653	-2,735395003	protein_coding	XYLT1
ENSG00000104368.17	-3,353820268	-3,41311215	-3,323493006	2,83614315	3,617506857	3,636775418	protein_coding	PLAT

ENSG00000104413.15	2,719389517	3,085990809	3,286110689	-2,95056264	-3,19991425	-2,941014128	protein_coding	ESRP1
ENSG00000104518.10	-2,785577178	-2,79733258	-2,717151297	2,555559305	2,755056842	2,989444905	protein_coding	GSDMD
ENSG00000105497.7	-3,09845492	-3,10723344	-3,046539578	3,231011426	3,015551525	3,005664987	protein_coding	ZNF175
ENSG00000105877.17	-2,634213132	-2,64866429	-2,307197933	2,561505774	2,63001533	2,39855425	protein_coding	DNAH11
ENSG00000105928.13	-3,124164318	-3,13322017	-3,070263542	2,795660873	3,125285907	3,406701248	protein_coding	DFNA5
ENSG00000105974.11	-2,630652565	-2,47663899	-2,468033562	3,014069867	2,470944799	2,090310455	protein_coding	CAV1
ENSG00000106366.8	-3,194241925	-3,1024109	-2,749633251	1,629190188	3,460998939	3,956096954	protein_coding	SERPINE1
ENSG00000106538.9	-2,877914385	-2,88897084	-2,813310687	3,140667374	2,896349643	2,543178894	protein_coding	RARRES2
ENSG00000107551.20	-2,394678799	-2,74309315	-2,539920837	2,446530106	2,665280255	2,565882429	protein_coding	RASSF4
ENSG00000107738.19	-2,635712899	-2,64835581	-2,562488553	3,057808896	2,361720771	2,427027599	protein_coding	C10orf54
ENSG00000108342.12	-2,484445894	-2,49863641	-1,916155316	-1,23553486	3,650847104	4,483925378	protein_coding	CSF3
ENSG00000109113.17	-2,911855035	-3,01257208	-2,93453128	2,857495275	2,981050087	3,020413031	protein_coding	RAB34
ENSG00000109738.10	-2,689746737	-2,98940918	-2,92015927	3,05133634	2,940998643	2,606980207	protein_coding	GLRB
ENSG00000109943.8	-2,653382785	-2,66594955	-2,580573806	3,009186856	2,560599755	2,330119534	protein_coding	CRTAM
ENSG00000110975.8	2,859927894	3,013655587	3,17336629	-2,71218934	-3,250219716	-3,084540712	protein_coding	SYT10
ENSG00000111341.9	2,08184695	2,686368497	3,127693599	-2,40351821	-2,735609189	-2,756781644	protein_coding	MGP
ENSG00000111716.12	-2,646844729	-3,32489034	-3,398232013	3,018607431	3,223745119	3,127614536	protein_coding	LDHB
ENSG00000111799.20	-2,560933639	-2,67546687	-2,583680215	2,733573289	2,693546843	2,392960595	protein_coding	COL12A1
ENSG00000111846.15	-3,148051066	-3,15706822	-3,180980187	2,832553427	3,352726164	3,300819884	protein_coding	GCNT2
ENSG00000111981.4	1,380575804	3,070191697	3,360634946	-2,61818991	-2,58508521	-2,608127328	protein_coding	ULBP1
ENSG00000112299.7	-2,392990275	-2,40700343	-2,312462152	0,307767269	3,284640282	3,520048306	protein_coding	VNN1
ENSG00000112902.11	-2,498579263	-2,51423497	-2,767743007	3,261560596	2,535424836	1,983571809	protein_coding	SEMA5A
ENSG00000113083.12	-3,214185036	-3,10417352	-3,242410417	2,300947854	3,528840712	3,730980411	protein_coding	LOX
ENSG00000113396.12	2,82596665	2,568734579	2,352097468	-2,59659214	-2,563632851	-2,58657371	protein_coding	SLC27A6
ENSG00000113739.10	2,624530932	2,808993513	2,656289132	-2,71292878	-2,715808209	-2,661076587	protein_coding	STC2
ENSG00000115008.5	-3,066285141	-3,07766748	-2,999808483	-0,66379354	4,216767615	5,590787033	protein_coding	IL1A
ENSG00000115009.11	-1,933276035	-2,42302605	-1,823540292	-1,39853163	3,530471197	4,047902808	protein_coding	CCL20
ENSG00000115295.19	-2,459308449	-2,73473637	-2,46764139	2,599228551	2,622937393	2,439520264	protein_coding	CLIP4
ENSG00000115355.15	-2,715219867	-2,54602276	-2,625101866	2,71114697	2,617366603	2,557830921	protein_coding	CCDC88A
ENSG00000115363.13	-2,586607742	-2,59948741	-2,512125815	2,075962073	2,778432247	2,843826643	protein_coding	EVA1A
ENSG00000115457.9	3,085918511	2,828269045	2,856583511	-2,85425482	-2,82214189	-3,094374361	protein_coding	IGFBP2
ENSG00000115461.4	3,369716787	3,325645832	3,054248354	-3,13861173	-3,424351653	-3,186647587	protein_coding	IGFBP5

ENSG00000115616.2	2,874890402	2,757108228	2,651902269	-2,64434424	-2,808511418	-2,831045244	protein_coding	SLC9A2
ENSG00000116299.16	3,096349369	3,054789589	2,819027781	-2,7619898	-3,143375649	-3,06480129	protein_coding	KIAA1324
ENSG00000117020.16	-3,00903485	-3,0188377	-2,951374373	3,015383085	3,06710133	2,896762504	protein_coding	AKT3
ENSG00000117114.19	-3,007105807	-3,01693059	-2,949323277	3,103797035	2,897202245	2,972360388	protein_coding	ADGRL2
ENSG00000117152.13	-2,794872094	-2,80656425	-2,726789287	3,059120776	2,723615688	2,545489168	protein_coding	RGS4
ENSG00000117519.15	-3,325413931	-3,36829302	-3,334335789	3,53803373	3,357867309	3,132141699	protein_coding	CNN3
ENSG00000117525.13	-3,022922712	-3,15285731	-2,930740674	2,684530334	3,29033224	3,131658117	protein_coding	F3
ENSG00000117983.17	2,622232327	2,769654477	2,821484945	-2,9393533	-2,556314671	-2,717703784	protein_coding	MUC5B
ENSG00000118257.16	-2,543949474	-2,95665105	-2,769947459	2,377616449	2,87978462	3,01314691	protein_coding	NRP2
ENSG00000118508.4	-2,773096207	-2,67586209	-2,462204639	2,36907061	2,814678036	2,727414288	protein_coding	RAB32
ENSG00000118513.18	2,731817145	2,975673286	2,726445221	-2,82241854	-2,889493313	-2,722023804	protein_coding	MYB
ENSG00000119917.13	-2,904780192	-2,8171468	-2,212476688	2,848241413	2,613971788	2,472190476	protein_coding	IFIT3
ENSG00000120217.13	-2,626991147	-2,64266504	-2,535519781	2,388371176	2,750567184	2,66623761	protein_coding	CD274
ENSG00000120262.9	2,951077319	3,300332948	3,327850339	-3,12866355	-3,329233686	-3,121363373	protein_coding	CCDC170
ENSG00000121068.13	3,22196632	2,985080888	2,873145418	-2,77069205	-3,147723117	-3,161777465	protein_coding	TBX2
ENSG00000121406.8	-2,729203298	-2,74118103	-2,269136926	2,566410319	2,560420451	2,612690487	protein_coding	ZNF549
ENSG00000121797.9	-2,855762801	-2,86834142	-3,049269771	3,633370314	2,730278628	2,409725048	protein_coding	CCRL2
ENSG00000121858.10	-2,98636031	-2,67753818	-2,743941296	2,070627922	3,20645334	3,13075852	protein_coding	TNFSF10
ENSG00000122861.15	-3,293817671	-3,46889916	-3,25557223	3,118372606	3,44716774	3,452748713	protein_coding	PLAU
ENSG00000122862.4	-3,109066373	-3,1183941	-3,053613698	1,988623357	3,424963314	3,867487495	protein_coding	SRGN
ENSG00000122870.11	-3,036033907	-3,04555717	-2,979938494	3,058213368	3,133736526	2,86957968	protein_coding	BICC1
ENSG00000123364.4	2,942077099	2,773138062	2,567549359	-2,77414405	-2,743712303	-2,764908165	protein_coding	HOXC13
ENSG00000123689.5	-3,092353552	-3,27438914	-3,230003936	1,915175966	3,431823737	4,249746922	protein_coding	G0S2
ENSG00000123843.12	-2,861115749	-2,87236851	-2,795432539	3,520059919	2,731889928	2,276966951	protein_coding	C4BPB
ENSG00000124126.13	3,711446945	3,270238292	2,792084672	-3,12357717	-3,406340799	-3,243851942	protein_coding	PREX1
ENSG00000124429.17	2,97172923	3,01674611	2,769756021	-2,91473097	-3,122898097	-2,72060229	protein_coding	POF1B
ENSG00000124493.13	2,640615574	2,777131375	2,379740752	-2,73704541	-2,706253778	-2,354188519	protein_coding	GRM4
ENSG00000125538.11	-2,708757059	-2,7215525	-2,634682182	0,409069932	3,306376304	4,349545501	protein_coding	IL1B
ENSG00000126860.11	-3,045780802	-3,05519312	-2,99030492	3,268568667	2,993235424	2,829474753	protein_coding	EVI2A
ENSG00000127152.17	2,357662859	2,574210298	2,61612453	-2,53060527	-2,497004902	-2,520387516	protein_coding	BCL11B
ENSG00000127920.5	-3,102581879	-3,11127188	-2,784089912	3,270462411	2,947220049	2,780261208	protein_coding	GNG11
ENSG00000127955.15	-2,815779552	-2,82875359	-3,01789564	2,710636687	2,92625269	3,025539409	protein_coding	GNAI1

ENSG00000128340.14	-3,266047741	-3,38530512	-3,225780157	3,011468472	3,32013626	3,545528285	protein_coding	RAC2
ENSG00000128510.10	-2,940017245	-2,95157599	-2,871941348	3,350111932	2,775142651	2,638279999	protein_coding	CPA4
ENSG00000128591.15	-3,147547263	-3,15648996	-3,210347515	3,542340807	2,968697109	3,00334682	protein_coding	FLNC
ENSG00000129514.5	3,281200142	3,262333144	3,14029808	-3,22217761	-3,399593349	-3,062060404	protein_coding	FOXA1
ENSG00000129993.14	2,993103736	2,848017316	2,758468455	-2,7896369	-3,03054994	-2,779402667	protein_coding	CBFA2T3
ENSG00000130054.4	2,714249208	2,625509453	2,515877913	-2,75450745	-2,724020967	-2,377108158	protein_coding	FAM155B
ENSG00000130294.14	3,022716549	2,571981105	2,543044588	-2,72614263	-2,694933089	-2,716666524	protein_coding	KIF1A
ENSG00000130413.15	-2,687859027	-2,3275363	-2,616742012	2,87386871	2,495234014	2,263034617	protein_coding	STK33
ENSG00000130558.18	3,114431858	2,917391935	2,905461941	-2,99028655	-2,964514031	-2,982485156	protein_coding	OLFM1
ENSG00000130830.14	-2,614132934	-2,82622088	-2,737879712	2,934318166	2,628492643	2,615422719	protein_coding	MPP1
ENSG00000131080.14	2,564152004	2,748080019	2,74866279	-2,59493197	-2,882578262	-2,583384585	protein_coding	EDA2R
ENSG00000131435.12	-2,841492922	-2,85285773	-2,775201361	2,462095991	2,906721074	3,100734948	protein_coding	PDLIM4
ENSG00000132698.13	3,059729077	3,067325017	3,079521221	-3,06709519	-3,233286328	-2,906193801	protein_coding	RAB25
ENSG00000132746.14	2,801290006	2,97684336	3,123000122	-3,06559769	-3,042044204	-2,793491589	protein_coding	ALDH3B2
ENSG00000132821.11	-2,766434807	-3,04457751	-2,687691478	3,389049319	2,539193394	2,570461083	protein_coding	VSTM2L
ENSG00000133317.14	-3,023078688	-3,03265302	-2,443677453	3,119112895	2,795883188	2,58441308	protein_coding	LGALS12
ENSG00000133424.20	3,007902428	2,787298316	2,607258003	-2,8781867	-2,846910612	-2,677361439	protein_coding	LARGE
ENSG00000134215.15	2,810061703	3,034762651	3,179464195	-2,90394151	-3,226030457	-2,894316581	protein_coding	VAV3
ENSG00000134258.16	2,905825047	2,520200161	2,590255389	-2,45095838	-2,772304551	-2,793017665	protein_coding	VTCN1
ENSG00000134259.3	-2,665941985	-2,67841411	-2,593643254	2,556091108	2,742872306	2,639035932	protein_coding	NGF
ENSG00000134339.8	-2,979523822	-2,98988475	-2,918750167	0,858592755	3,81235127	4,217214713	protein_coding	SAA2
ENSG00000134516.15	-2,591405656	-2,8071119	-2,71746735	2,831884148	2,740981183	2,54311958	protein_coding	DOCK2
ENSG00000134533.6	2,990354554	3,026001006	2,935254688	-2,82293702	-3,056272956	-3,072400269	protein_coding	RERG
ENSG00000134744.13	-2,948964732	-3,27379324	-3,229919472	3,100212361	3,167816865	3,184648214	protein_coding	ZCCHC11
ENSG00000134802.17	-3,04352329	-2,97072575	-3,083605355	2,227901133	3,323867068	3,546086197	protein_coding	SLC43A3
ENSG00000134871.17	-3,296606155	-3,30268279	-3,259936371	2,994246311	3,330971054	3,534007955	protein_coding	COL4A2
ENSG00000134954.14	-3,333574328	-3,33889093	-3,2108413	3,040196401	3,492520961	3,350589196	protein_coding	ETS1
ENSG00000135046.13	-3,064848018	-3,02900299	-2,839231756	3,110767541	2,927683524	2,894631698	protein_coding	ANXA1
ENSG00000135074.15	-3,102002673	-3,11074485	-3,050291421	2,737083964	3,096776163	3,429178812	protein_coding	ADAM19
ENSG00000135111.14	2,819195326	2,838691418	2,714070498	-2,80363185	-2,773757304	-2,794568086	protein_coding	TBX3
ENSG00000135272.9	-2,893272253	-3,13616704	-3,078303157	3,239843832	3,004972846	2,862925772	protein_coding	MDFIC
ENSG00000135318.11	-3,045170479	-3,2789524	-3,231167123	2,944411909	3,335307745	3,275570346	protein_coding	NT5E

ENSG00000135374.9	2,579188491	2,763726412	2,987009581	-2,89686052	-2,869017494	-2,564046466	protein_coding	ELF5
ENSG00000135457.9	-2,67793269	-2,69217762	-2,909593077	2,738800304	2,736225187	2,804677893	protein_coding	TFCP2
ENSG00000135926.12	-2,743108785	-2,48716221	-2,376844073	2,374400974	2,522599444	2,710114653	protein_coding	TMBIM1
ENSG00000135929.8	-2,620664279	-2,63528528	-2,289755835	1,802976225	2,682248193	3,060480975	protein_coding	CYP27A1
ENSG00000136160.14	-2,548457532	-2,56142891	-2,473493185	2,638626026	2,583056366	2,361697234	protein_coding	EDNRB
ENSG00000136231.13	-2,973278966	-3,19137381	-2,907332143	2,931084569	3,048061535	3,092838814	protein_coding	IGF2BP3
ENSG00000136244.11	-3,323204742	-3,32881978	-3,289244317	0,789801172	4,36939821	4,782069459	protein_coding	IL6
ENSG00000136542.8	-2,675904587	-3,29510787	-3,073781271	3,27846856	2,991012023	2,775313143	protein_coding	GALNT5
ENSG00000136859.9	-2,893440142	-2,90437166	-2,829530845	2,974778342	2,843366034	2,809198275	protein_coding	ANGPTL2
ENSG00000136869.13	-2,827758121	-2,83922095	-2,760932383	2,596388875	3,017028608	2,814493968	protein_coding	TLR4
ENSG00000136944.17	2,943166857	2,583070338	2,573549163	-2,33873104	-2,870892533	-2,890162786	protein_coding	LMX1B
ENSG00000137273.3	-2,535851564	-2,54887266	-2,46062633	2,691914388	2,465205244	2,388230918	protein_coding	FOXF2
ENSG00000137462.6	-2,854656745	-2,61747149	-2,122436547	1,598030387	2,950018573	3,046515826	protein_coding	TLR2
ENSG00000137573.13	2,988573963	3,131669236	3,048810287	-2,99712781	-3,183219838	-2,988705839	protein_coding	SULF1
ENSG00000137747.14	2,747648716	2,82969336	2,969810808	-2,66065437	-2,934054369	-2,952444146	protein_coding	TMPRSS13
ENSG00000137965.10	-2,928404954	-2,93894314	-2,536476343	2,855694593	2,683282444	2,8648474	protein_coding	IFI44
ENSG00000138028.14	2,899348978	2,940246584	3,03032222	-2,88776627	-3,103835558	-2,878315952	protein_coding	CGREF1
ENSG00000138131.3	-3,317160791	-3,41655843	-3,186492276	3,067467797	3,302050991	3,550692713	protein_coding	LOXL4
ENSG00000138395.14	-2,599994396	-2,61306397	-2,524461716	3,753428868	2,445463486	1,538627723	protein_coding	CDK15
ENSG00000138675.16	-2,676047145	-2,68847983	-2,603957495	2,348520095	2,876532944	2,74343143	protein_coding	FGF5
ENSG00000139117.13	-2,789373678	-3,06005468	-2,493139285	2,745943057	2,831744818	2,764879768	protein_coding	CPNE8
ENSG00000139209.15	-2,760385995	-2,77233562	-2,690905152	3,137683818	2,671927618	2,414015335	protein_coding	SLC38A4
ENSG00000139278.9	-2,67796889	-2,92984244	-2,845667893	2,487758532	2,949413734	3,01630696	protein_coding	GLIPR1
ENSG00000139865.16	2,588700165	2,710904037	2,529751364	-2,62395356	-2,591354904	-2,614047107	protein_coding	TTC6
ENSG00000140832.9	3,058742445	2,791173309	2,749850871	-2,6816911	-2,949982239	-2,968093291	protein_coding	MARVELD3
ENSG00000140937.13	-3,243520603	-3,37086185	-3,200920298	3,19104315	3,399072492	3,225187113	protein_coding	CDH11
ENSG00000141756.18	2,831250128	2,880992567	2,92277965	-2,85769606	-3,052862137	-2,724464153	protein_coding	FKBP10
ENSG00000142910.15	-3,074975816	-3,08475545	-3,016948858	3,354795477	2,893877007	2,928007639	protein_coding	TINAGL1
ENSG00000143217.8	2,610614292	2,64375583	2,891272349	-2,70599264	-2,966534158	-2,473115672	protein_coding	PVRL4
ENSG00000143412.9	2,722325237	2,584521926	2,393807439	-2,20151572	-2,636737864	-2,862401022	protein_coding	ANXA9
ENSG00000143552.9	2,687592564	2,964993649	3,052965347	-2,91503271	-2,884672713	-2,905846142	protein_coding	NUP210L
ENSG00000144115.16	2,676981781	2,727660263	2,72969493	-2,58959624	-2,760706909	-2,78403383	protein_coding	THNSL2

ENSG00000144290.16	2,445015282	2,902484043	2,528506109	-2,39625276	-2,729281682	-2,750470996	protein_coding	SLC4A10
ENSG00000144452.14	2,958362166	3,404288092	3,298525533	-3,22097462	-3,34035734	-3,099843835	protein_coding	ABCA12
ENSG00000144642.20	-3,096115544	-3,10488407	-2,774678012	3,112734899	2,98564234	2,877300388	protein_coding	RBMS3
ENSG00000144681.10	-2,908873713	-2,91967322	-2,845689823	3,149137053	2,800512978	2,72458672	protein_coding	STAC
ENSG00000144810.15	-3,417003736	-3,42050779	-3,334753667	2,873024517	3,656379461	3,642861215	protein_coding	COL8A1
ENSG00000145147.19	-2,568313321	-2,5841547	-2,476091489	1,675404549	3,036944679	2,916210282	protein_coding	SLIT2
ENSG00000145246.13	-2,558065918	-2,66608293	-2,456967509	2,542415542	2,63089854	2,507802272	protein_coding	ATP10D
ENSG00000145287.10	-2,704388261	-2,71975833	-3,005468293	2,981695197	2,755849559	2,692070124	protein_coding	PLAC8
ENSG00000145349.16	-2,633006523	-2,649418	-2,63238929	2,852894357	2,571129696	2,490789764	protein_coding	CAMK2D
ENSG00000145431.10	-2,905459321	-3,10627045	-2,928380255	3,201192658	2,937268744	2,801648626	protein_coding	PDGFC
ENSG00000145536.15	-2,783489363	-2,79525032	-2,715034267	2,743537092	2,795570855	2,754665998	protein_coding	ADAMTS16
ENSG00000145808.8	3,201200771	3,109605918	2,727205813	-3,0234594	-2,998611278	-3,015941827	protein_coding	ADAMTS19
ENSG00000146373.16	-2,964270023	-2,80605862	-3,131723763	2,805165565	3,051545522	3,04534132	protein_coding	RNF217
ENSG00000146477.5	-2,752765197	-2,76475685	-2,683057866	3,07263698	2,627023007	2,500919928	protein_coding	SLC22A3
ENSG00000146678.9	-2,998765144	-3,00868108	-2,940475758	2,913069307	2,982913102	3,051939573	protein_coding	IGFBP1
ENSG00000146858.7	-2,77668905	-2,78850004	-2,707962241	2,776515238	2,848701599	2,647934493	protein_coding	ZC3HAV1L
ENSG00000146904.8	2,586465777	2,574517222	2,755746331	-2,93660467	-2,594167926	-2,385956737	protein_coding	EPHA1
ENSG00000147041.11	2,834524748	2,881244155	2,845721909	-2,81180525	-2,777370479	-2,972315084	protein_coding	SYTL5
ENSG00000147065.16	-3,377785107	-3,42526291	-3,374916199	3,216814331	3,46697882	3,494171066	protein_coding	MSN
ENSG00000147180.16	2,334791159	2,913925241	2,876737994	-2,72208001	-2,690794099	-2,712580285	protein_coding	ZNF711
ENSG00000147614.3	-2,754902848	-2,41262828	-2,685943791	2,351608586	2,487926791	3,013939542	protein_coding	ATP6V0D2
ENSG00000148346.11	-2,360079182	-2,59332804	-2,184308025	0,341483474	3,027529679	3,768702089	protein_coding	LCN2
ENSG00000148516.21	-2,978801017	-2,81743232	-3,022905402	2,788574333	2,991074928	3,039489478	protein_coding	ZEB1
ENSG00000148677.6	-2,737403513	-2,79448989	-2,900633569	2,818918916	2,941254906	2,672353148	protein_coding	ANKRD1
ENSG00000149948.13	-3,134633801	-3,01210241	-2,809038977	2,859641314	2,995875248	3,100258624	protein_coding	HMGA2
ENSG00000150893.10	3,200884933	3,212500303	2,794769319	-3,1603079	-3,138464056	-2,909382598	protein_coding	FREM2
ENSG00000151388.10	-3,209512199	-3,21718733	-3,163546286	3,386798443	3,193289837	3,010157537	protein_coding	ADAMTS12
ENSG00000151468.10	-2,711007415	-2,72552816	-2,626115043	2,906075755	2,666229159	2,490345705	protein_coding	CCDC3
ENSG00000151892.14	3,309624267	3,307783635	3,056395994	-3,23295465	-3,213689873	-3,227159376	protein_coding	GFRA1
ENSG00000152784.15	-2,831095922	-2,84253133	-2,764419926	2,751084284	3,02600779	2,660955099	protein_coding	PRDM8
ENSG00000152977.9	2,703103517	2,818677943	2,845571873	-2,80211009	-2,772206028	-2,793037212	protein_coding	ZIC1
ENSG00000153292.15	-2,741148804	-2,5448407	-2,661372871	3,394960523	2,536963074	2,015438776	protein_coding	ADGRF1

ENSG00000153551.13	-2,704294773	-2,71968242	-2,547057159	2,509621658	2,648306221	2,813106475	protein_coding	CMTM7
ENSG00000153885.14	2,860255943	2,986526638	2,928799747	-3,08702037	-3,064261143	-2,62430082	protein_coding	KCTD15
ENSG00000153944.10	2,434651517	2,517420631	2,606441298	-2,40066355	-2,658279965	-2,499569929	protein_coding	MSI2
ENSG00000153956.15	-2,398233771	-2,64175202	-2,542712425	2,336266646	2,636368303	2,610063268	protein_coding	CACNA2D1
ENSG00000154133.14	-2,799715241	-2,81140019	-2,731668774	2,223508139	2,989654361	3,129621707	protein_coding	ROBO4
ENSG00000154175.16	-2,97011022	-2,98033129	-2,910127552	3,083851226	2,906052704	2,870665127	protein_coding	ABI3BP
ENSG00000154556.17	-2,656875412	-2,6719425	-2,776136146	2,971874223	2,598882506	2,534197331	protein_coding	SORBS2
ENSG00000154640.14	-3,117805983	-3,12633619	-3,067289144	2,703354911	3,312076339	3,296000069	protein_coding	BTG3
ENSG00000154734.14	-2,883427296	-2,57767362	-2,81942864	2,304473787	3,098024741	2,878031029	protein_coding	ADAMTS1
ENSG00000154760.13	-3,027139645	-3,03677664	-2,970409116	3,331946223	3,037582027	2,66479715	protein_coding	SLFN13
ENSG00000155961.4	2,332098855	2,991227651	3,134972718	-2,83219137	-2,802823697	-2,823284161	protein_coding	RAB39B
ENSG00000156510.12	-3,059226842	-3,25005107	-2,833869509	2,840378017	3,096667526	3,206101878	protein_coding	HKDC1
ENSG00000156959.8	-2,712051894	-2,72425826	-2,641180185	2,682592974	2,676166694	2,718730667	protein_coding	LHFPL4
ENSG00000157168.18	-2,851836297	-2,86442132	-3,045654759	2,976840117	2,996101361	2,788970892	protein_coding	NRG1
ENSG00000157214.13	-2,74499591	-2,75702428	-2,675091568	2,542134205	2,779197107	2,855780446	protein_coding	STEAP2
ENSG00000157227.12	-3,137504537	-3,12514222	-3,080996447	2,744697877	3,173701129	3,425244198	protein_coding	MMP14
ENSG00000157388.13	2,705973708	3,028303916	2,945583642	-2,81864382	-3,05259539	-2,808622055	protein_coding	CACNA1D
ENSG00000157510.13	-2,31958218	-2,89087566	-2,816429886	2,718362042	2,604852862	2,703672821	protein_coding	AFAP1L1
ENSG00000158258.15	2,772437995	3,303906957	3,087493038	-3,06488822	-3,041218127	-3,057731646	protein_coding	CLSTN2
ENSG00000158315.10	-2,440046776	-2,80101217	-2,72148272	2,187749987	2,871757083	2,903034598	protein_coding	RHBDL2
ENSG00000158321.15	2,780822247	2,897385441	2,970552416	-2,87741796	-3,095706594	-2,675635553	protein_coding	AUTS2
ENSG00000158825.5	-2,885468766	-3,30039393	-3,082958626	3,139545793	3,062130213	3,067145313	protein_coding	CDA
ENSG00000159166.13	2,946248633	2,882802792	3,037700923	-3,0214261	-2,994526233	-2,850800014	protein_coding	LAD1
ENSG00000159212.12	-3,068805041	-2,82459173	-3,015159319	2,997917239	2,9700597	2,940579146	protein_coding	CLIC6
ENSG00000159921.14	-3,052876889	-3,18525223	-3,127915423	2,96263273	3,223825764	3,17958605	protein_coding	GNE
ENSG00000160182.2	3,018847557	2,919154573	3,114970202	-2,97913427	-3,140468826	-2,933369232	protein_coding	TFF1
ENSG00000160200.17	2,406059932	2,894775842	2,870954561	-2,73741023	-2,706388008	-2,727992094	protein_coding	CBS
ENSG00000161671.16	-2,787195003	-2,80043954	-2,995358869	3,060066156	2,721069986	2,80185727	protein_coding	EMC10
ENSG00000161905.12	2,908741493	2,85880015	2,850151897	-2,88483682	-2,856583809	-2,876272908	protein_coding	ALOX15
ENSG00000162069.14	2,938418821	2,973653704	2,906454516	-2,9511196	-2,924384743	-2,943022699	protein_coding	CCDC64B
ENSG00000162366.7	-2,843767629	-2,85546312	-2,775649774	0,621031481	3,673443151	4,180405887	protein_coding	PDZK1IP1
ENSG00000162511.7	-2,692999936	-2,55410205	-2,607237107	2,077123398	2,756371083	3,020844615	protein_coding	LAPTM5

ENSG00000162576.16	-2,754164322	-2,76764011	-2,451034428	2,975872204	2,490740183	2,506226474	protein_coding	MXRA8
ENSG00000162614.18	-2,444631489	-2,46192722	-2,732417451	2,866355439	2,483430965	2,28918976	protein_coding	NEXN
ENSG00000162692.10	-2,739481825	-2,75167754	-2,668647074	1,568256753	3,261281499	3,330268191	protein_coding	VCAM1
ENSG00000162981.13	2,864643498	2,451574622	2,357242482	-2,31751565	-2,667064295	-2,688880652	protein_coding	FAM84A
ENSG00000163131.10	-2,746152307	-3,23506911	-2,80477952	1,737872472	3,378835484	3,669292978	protein_coding	CTSS
ENSG00000163283.6	-2,362398478	-2,74361504	-2,660929508	3,565143392	2,122749759	2,079049876	protein_coding	ALPP
ENSG00000163297.16	-3,169505822	-3,27574545	-3,229393241	2,965827318	3,364245576	3,344571622	protein_coding	ANTXR2
ENSG00000163430.9	-2,930661753	-3,06251543	-2,986786583	2,818973947	3,043460073	3,117529746	protein_coding	FSTL1
ENSG00000163453.11	-3,407806449	-3,41151971	-3,20588233	3,441051368	3,325529767	3,258627356	protein_coding	IGFBP7
ENSG00000163565.18	-3,281072602	-3,39450276	-3,24251549	3,066983232	3,401358741	3,44974888	protein_coding	IFI16
ENSG00000163568.13	-2,654277658	-2,66679888	-2,581706331	2,355138018	2,796385868	2,751258983	protein_coding	AIM2
ENSG00000163661.3	-3,223373117	-3,31682335	-3,089540168	1,783257752	3,913588229	3,932890657	protein_coding	PTX3
ENSG00000163734.4	-2,632197906	-2,64515007	-2,12727759	0,473508539	3,275038341	3,656078686	protein_coding	CXCL3
ENSG00000163739.4	-3,167871907	-2,95824643	-2,877952555	-0,07104157	4,387444576	4,687667888	protein_coding	CXCL1
ENSG00000163814.7	-3,353830513	-3,46266979	-3,40236861	3,025630576	3,551442096	3,641796243	protein_coding	CDCP1
ENSG00000163873.9	2,483200655	2,684681073	2,846712748	-2,68536098	-2,653538479	-2,675695016	protein_coding	GRIK3
ENSG00000164128.6	2,762327017	2,849703084	2,505166511	-2,55595398	-2,768211738	-2,79303089	protein_coding	NPY1R
ENSG00000164176.12	-3,246429131	-3,40971582	-3,258242699	3,32041389	3,382438063	3,211535696	protein_coding	EDIL3
ENSG00000164236.11	-2,910032279	-2,59578378	-2,226934562	2,428571585	2,636348694	2,667830343	protein_coding	ANKRD33B
ENSG00000164400.5	-3,000762998	-3,01082536	-2,94160863	0,111680648	4,311061445	4,530454896	protein_coding	CSF2
ENSG00000164418.19	-2,522631363	-2,86433744	-2,787760517	2,264508133	2,955041367	2,955179823	protein_coding	GRIK2
ENSG00000164509.13	-2,94290013	-2,95337518	-2,881504861	2,66323813	3,018239621	3,096302425	protein_coding	IL31RA
ENSG00000164692.17	-3,078345706	-2,83755301	-3,025336572	3,234067339	2,860263376	2,846904574	protein_coding	COL1A2
ENSG00000164742.14	3,318349631	2,995272682	2,695647528	-2,83322165	-3,185022135	-2,991026052	protein_coding	ADCY1
ENSG00000165025.14	2,867102327	2,659652919	2,472621106	-2,79796145	-2,768155986	-2,433258912	protein_coding	SYK
ENSG00000165029.15	-2,920004712	-3,04241807	-3,27796578	2,917325277	2,964350671	3,358712613	protein_coding	ABCA1
ENSG00000165072.9	-2,597786707	-2,81916269	-2,502321287	3,008788502	2,637748065	2,272734113	protein_coding	MAMDC2
ENSG00000165376.10	-2,174771158	-2,7979956	-2,718123583	3,490989077	2,335481422	1,864419839	protein_coding	CLDN2
ENSG00000165548.10	2,509968283	2,564920892	2,707957956	-2,49497159	-2,805002441	-2,482873098	protein_coding	TMEM63C
ENSG00000165731.17	3,484456133	2,986825558	2,804763588	-2,94398826	-3,249423039	-3,082633979	protein_coding	RET
ENSG00000166147.13	-2,591240594	-2,89837356	-2,719682821	2,670571052	2,820174425	2,718551499	protein_coding	FBN1
ENSG00000166250.11	-2,639695648	-2,65563941	-2,648391154	1,821179295	2,84030589	3,282241028	protein_coding	CLMP

ENSG00000166402.8	-2,719144032	-2,73130852	-2,648497596	2,800133895	2,664529021	2,634287234	protein_coding	TUB
ENSG00000166509.10	3,082772462	2,468974325	2,462197317	-2,68516543	-2,65329422	-2,675484457	protein_coding	CLEC3A
ENSG00000166741.7	-3,363607403	-3,36812178	-3,195425104	2,881561869	3,53492402	3,510668397	protein_coding	NNMT
ENSG00000166920.10	-3,152670651	-3,26295651	-2,907254287	1,462965818	3,611332343	4,248583286	protein_coding	C15orf48
ENSG00000167183.2	3,046381083	2,788295378	2,789491496	-2,88697689	-2,85876532	-2,87842575	protein_coding	PRR15L
ENSG00000167601.11	-3,292118319	-3,29851087	-3,020922318	3,41449943	3,18131214	3,015739936	protein_coding	AXL
ENSG00000167608.11	2,805067895	2,588137358	2,458082584	-2,51542776	-2,833322894	-2,502537182	protein_coding	TMC4
ENSG00000167741.10	2,736974459	2,607756531	2,427980565	-2,60517741	-2,572337968	-2,595196181	protein_coding	GGT6
ENSG00000168143.8	2,523563938	2,669240516	2,576001746	-2,53463434	-2,711969192	-2,522202671	protein_coding	FAM83B
ENSG00000168350.7	2,867386441	2,515915957	2,197284047	-2,38777464	-2,583417798	-2,609394008	protein_coding	DEGS2
ENSG00000168497.4	-3,041611765	-3,05110199	-2,98569913	3,618958932	2,901854485	2,557599468	protein_coding	SDPR
ENSG00000168675.18	2,863957226	3,172060302	3,042319735	-3,11721913	-3,095275821	-2,865842307	protein_coding	LDLRAD4
ENSG00000168685.14	-3,001367893	-2,73295597	-2,943366335	2,386663144	3,322655803	2,96837125	protein_coding	IL7R
ENSG00000168743.12	3,098522144	3,164194818	3,139425956	-3,07926462	-3,251476322	-3,071401977	protein_coding	NPNT
ENSG00000168917.8	-2,893269829	-2,90409656	-2,488538922	2,626469786	2,8513832	2,808052322	protein_coding	SLC35G2
ENSG00000169083.15	3,320483146	3,218497634	3,011923421	-3,16694999	-3,223748597	-3,160205616	protein_coding	AR
ENSG00000169174.10	-3,122534814	-3,29278976	-3,06826298	3,147301049	3,239878208	3,096408294	protein_coding	PCSK9
ENSG00000169252.5	-2,927316688	-2,93794099	-2,865098024	2,685737017	3,005162569	3,039456112	protein_coding	ADRB2
ENSG00000169306.9	-2,829110513	-2,84055558	-2,762382279	2,758924724	2,894369546	2,778754103	protein_coding	IL1RAPL1
ENSG00000169418.9	-2,676760006	-2,68920479	-2,604603303	2,362577729	2,538919101	3,06907127	protein_coding	NPR1
ENSG00000169429.10	-3,130237118	-3,23211395	-3,0959728	0,347791281	4,507181245	4,603351339	protein_coding	CXCL8
ENSG00000169554.16	-2,669049553	-2,97419553	-2,903954262	2,294183602	3,071841138	3,181174604	protein_coding	ZEB2
ENSG00000169715.14	-2,82370487	-3,08681775	-3,024738274	2,591572658	3,02235641	3,321331822	protein_coding	MT1E
ENSG00000169862.18	2,924919846	2,831702472	2,593822904	-2,69940444	-2,962521686	-2,688519093	protein_coding	CTNND2
ENSG00000170369.3	-2,9126299	-2,92340007	-2,849607075	2,546438505	3,073502945	3,065695596	protein_coding	CST2
ENSG00000170373.8	-3,302675482	-3,30875328	-3,343683837	2,726448527	3,598539422	3,630124645	protein_coding	CST1
ENSG00000170430.9	2,819766827	2,516372237	2,487270862	-2,62402523	-2,586688589	-2,612696106	protein_coding	MGMT
ENSG00000170955.9	-2,807090614	-2,81870349	-2,739437715	3,198259476	2,57159993	2,595372415	protein_coding	PRKCDBP
ENSG00000171004.17	2,702346846	2,613699512	2,764718629	-2,47640865	-2,791954364	-2,812401976	protein_coding	HS6ST2
ENSG00000171051.8	-2,624311348	-2,63698153	-2,550946707	2,371879399	2,696025183	2,744335001	protein_coding	FPR1
ENSG00000171208.9	2,829590024	2,640657158	2,569979376	-2,44369029	-2,879932456	-2,716603814	protein_coding	NETO2
ENSG00000171435.13	2,961740079	2,869967911	2,639310947	-2,83640002	-2,807104285	-2,827514632	protein_coding	KSR2

ENSG00000171587.14	2,834604742	3,137801412	3,010806594	-3,09752414	-3,072689726	-2,812998881	protein_coding	DSCAM
ENSG00000172123.12	-2,808725555	-2,82031256	-2,741214777	3,002032201	2,85408673	2,514133957	protein_coding	SLFN12
ENSG00000172461.10	2,745985434	2,633781833	2,619142347	-2,68016006	-2,648274896	-2,670474654	protein_coding	FUT9
ENSG00000172551.10	2,623376116	2,600011623	2,451369463	-2,57266193	-2,539511107	-2,562584168	protein_coding	MUCL1
ENSG00000172818.9	2,556326813	2,470872824	2,500086806	-2,40620221	-2,364995044	-2,756089192	protein_coding	OVOL1
ENSG00000172985.10	-2,744180787	-2,75784703	-2,961906835	2,728887689	2,753335328	2,981711637	protein_coding	SH3RF3
ENSG00000173432.10	-3,31747812	-3,3229969	-3,284243371	1,221810409	4,14600759	4,55690039	protein_coding	SAA1
ENSG00000173482.16	-3,038901421	-3,01756081	-2,937121402	2,926267096	3,048804726	3,018511815	protein_coding	PTPRM
ENSG00000173530.5	-2,763929274	-3,0434094	-2,978078703	2,581687353	3,095727812	3,108002215	protein_coding	TNFRSF10D
ENSG00000173546.7	-2,921146963	-2,4797849	-2,852315483	2,913406369	2,582573088	2,757267887	protein_coding	CSPG4
ENSG00000173638.18	2,778724491	2,402372666	2,418304606	-2,18842478	-2,693350869	-2,717626116	protein_coding	SLC19A1
ENSG00000173918.14	-2,773869888	-2,7860189	-2,703288138	0,977018523	3,47228312	3,813875282	protein_coding	C1QTNF1
ENSG00000174607.10	-2,576071701	-2,90403645	-2,829826388	2,885316774	2,75074229	2,673875475	protein_coding	UGT8
ENSG00000175040.5	-2,642711027	-2,6552798	-2,569887971	2,636002488	2,546874297	2,685002012	protein_coding	CHST2
ENSG00000175287.18	-3,006072787	-3,01585933	-2,645040418	3,175021453	2,744413134	2,747537944	protein_coding	PHYHD1
ENSG00000175707.8	2,631765405	2,514452622	2,490016131	-2,5598819	-2,526591555	-2,549760706	protein_coding	KDF1
ENSG00000176597.11	-2,521795893	-2,69722144	-2,34613879	2,52800521	2,502218105	2,534932808	protein_coding	B3GNT5
ENSG00000176697.18	-3,047494838	-3,24214622	-2,987098224	2,998790212	3,138213543	3,139735525	protein_coding	BDNF
ENSG00000177409.11	-2,729779595	-2,5338029	-2,238764348	2,939259983	2,395838256	2,167248608	protein_coding	SAMD9L
ENSG00000177707.10	-2,998430373	-3,00928257	-3,157893677	3,07716028	3,136770293	2,951676049	protein_coding	PVRL3
ENSG00000177932.6	-2,960941556	-2,68359099	-2,347690648	2,724232978	2,634158585	2,633831629	protein_coding	ZNF354C
ENSG00000178031.15	-3,185374598	-2,98660213	-2,909647891	2,844387175	3,077193265	3,160044182	protein_coding	ADAMTSL1
ENSG00000178163.7	-3,069328674	-3,07844973	-3,01548336	3,13235677	3,072481914	2,958423078	protein_coding	ZNF518B
ENSG00000178538.9	2,680500286	2,86789886	2,666851177	-2,86269245	-2,834108868	-2,518449001	protein_coding	CA8
ENSG00000178568.13	2,625429564	2,617419106	2,351807091	-2,36253287	-2,495092498	-2,737030392	protein_coding	ERBB4
ENSG00000179456.10	-2,584766801	-2,80818631	-2,488605337	2,802960324	2,561629688	2,516968434	protein_coding	ZBTB18
ENSG00000180964.16	-3,034145213	-3,0436889	-2,977935886	2,943531372	3,019213517	3,093025109	protein_coding	TCEAL8
ENSG00000181007.8	-2,831620362	-2,84304498	-2,765003791	2,845628606	2,811635423	2,782405104	protein_coding	ZFP82
ENSG00000181218.5	2,509495765	2,568456677	2,509094855	-2,67315304	-2,641492308	-2,272401945	protein_coding	HIST3H2A
ENSG00000181577.15	-2,739404919	-2,7529703	-2,433827438	2,640232708	2,669589764	2,616380183	protein_coding	C6orf223
ENSG00000182013.17	-2,976777849	-2,98692916	-2,917181835	2,909789189	2,904019466	3,067080185	protein_coding	PNMAL1
ENSG00000182107.6	2,949330468	2,831409973	2,763479126	-2,73668962	-3,082249774	-2,725280169	protein_coding	TMEM30B

ENSG00000182621.16	2,512887617	2,735744847	2,889191518	-2,79728369	-2,55337211	-2,787168183	protein_coding	PLCB1
ENSG00000182986.12	-2,719386968	-3,00978037	-2,638327435	2,699923344	2,84761446	2,819956969	protein_coding	ZNF320
ENSG00000183036.10	2,579375505	2,607581921	2,384433257	-2,53836794	-2,504847619	-2,528175127	protein_coding	PCP4
ENSG00000183287.13	-2,865234041	-3,11511435	-2,792269471	3,066714765	2,934138666	2,771764428	protein_coding	CCBE1
ENSG00000183671.12	-2,84163232	-2,85301793	-2,77522527	3,349739809	2,663648578	2,456487133	protein_coding	GPR1
ENSG00000183853.17	-3,280857624	-3,39435238	-3,242281789	3,358083027	3,315939639	3,243469129	protein_coding	KIRREL
ENSG00000184371.13	-2,914285171	-2,93977074	-2,722714792	1,903513581	3,16133617	3,511920951	protein_coding	CSF1
ENSG00000184564.8	2,681575378	3,195164405	3,229086443	-2,92008097	-3,08433116	-3,101414093	protein_coding	SLITRK6
ENSG00000184937.12	-2,663704324	-2,6762033	-2,59125976	2,699626192	2,876606958	2,354934234	protein_coding	WT1
ENSG00000184985.16	-2,85672206	-2,63812971	-2,270414646	2,48741425	2,655486447	2,622365716	protein_coding	SORCS2
ENSG00000185052.11	2,985921197	2,826151697	2,374846826	-2,85658017	-2,482472767	-2,847866783	protein_coding	SLC24A3
ENSG00000185070.10	-2,748946155	-3,03147793	-2,669374488	3,087768605	2,792091255	2,569938717	protein_coding	FLRT2
ENSG00000185215.8	-2,862430465	-2,80660528	-2,652502324	1,732020134	3,219642608	3,369875331	protein_coding	TNFAIP2
ENSG00000185222.7	-3,186782507	-3,33494096	-3,298589875	3,131439259	3,347645581	3,341228503	protein_coding	WBP5
ENSG00000185483.11	-2,483804181	-2,57898696	-2,555360406	2,92858748	2,451356502	2,238207567	protein_coding	ROR1
ENSG00000185760.15	-3,045418617	-3,05483501	-2,989919973	3,226549529	3,072482654	2,791141419	protein_coding	KCNQ5
ENSG00000185860.13	-2,744108577	-2,39952153	-2,288414164	3,221843911	2,432437435	1,777762928	protein_coding	CCDC190
ENSG00000185862.6	-2,817428215	-2,82894327	-2,750309689	2,963319954	2,834046303	2,599314911	protein_coding	EVI2B
ENSG00000186281.12	-2,721593402	-2,7354477	-2,943839084	2,962479522	2,805450571	2,632950091	protein_coding	GPAT2
ENSG00000187498.14	-3,317757379	-3,17746559	-2,979743083	2,717481677	3,288860959	3,468623411	protein_coding	COL4A1
ENSG00000187867.8	2,461560343	2,494688839	2,602475564	-2,25435441	-2,811397541	-2,492972794	protein_coding	PALM3
ENSG00000187908.15	-2,960455528	-2,67894802	-2,900283868	3,240696939	2,850160602	2,448829876	protein_coding	DMBT1
ENSG00000188015.9	-2,883680659	-2,89456506	-2,220577967	2,257888879	2,899517147	2,841417661	protein_coding	S100A3
ENSG00000188322.4	2,796319472	2,552264056	2,60816956	-2,88464666	-2,522582118	-2,549524312	protein_coding	SBK1
ENSG00000188641.12	-3,300681042	-3,3063925	-3,266322351	3,361614827	3,366981188	3,14479988	protein_coding	DPYD
ENSG00000189334.8	2,838013987	2,94195815	3,250409921	-2,97832761	-3,082962921	-2,969091529	protein_coding	S100A14
ENSG00000189369.8	-2,672984042	-2,68541586	-2,600901425	2,665376888	2,655023554	2,638900889	protein_coding	GSPT2
ENSG00000196154.11	-2,807512612	-2,68166534	-2,687381694	2,914720706	2,728236085	2,533602854	protein_coding	S100A4
ENSG00000196159.11	-2,50415425	-2,52187531	-2,496019991	2,881577179	2,530027215	2,110445159	protein_coding	FAT4
ENSG00000196208.13	2,727072099	2,847985195	2,668087062	-2,6706631	-2,938350571	-2,634130686	protein_coding	GREB1
ENSG00000196427.13	2,641640712	2,573607832	2,458897332	-2,70209637	-2,279462474	-2,692587032	protein_coding	NBPF4
ENSG00000196437.10	-2,467929469	-2,82166807	-2,743318253	2,650187714	2,652267215	2,730460861	protein_coding	ZNF569

ENSG00000196542.8	3,074348946	3,239605767	3,524244773	-3,17563455	-3,434169327	-3,228395614	protein_coding	SPTSSB
ENSG00000196557.10	3,222545991	2,999431646	2,867313708	-2,94308432	-3,064513367	-3,081693664	protein_coding	CACNA1H
ENSG00000196562.14	3,229336178	3,201096819	3,159342015	-3,17748313	-3,277354029	-3,13493785	protein_coding	SULF2
ENSG00000196611.4	-3,056100504	-2,78752251	-2,567285756	1,169171036	3,34581179	3,895925946	protein_coding	MMP1
ENSG00000196620.8	3,010771309	2,75790644	2,403817161	-2,73764674	-2,706620729	-2,728227442	protein_coding	UGT2B15
ENSG00000196639.6	-2,842923118	-3,01644652	-2,94254726	2,88682569	2,987661333	2,927429878	protein_coding	HRH1
ENSG00000196867.7	-2,846436721	-2,85904113	-2,772514077	2,783458261	2,9063344	2,788199263	protein_coding	ZFP28
ENSG00000196876.13	2,529067574	2,553447974	2,619048877	-2,70802286	-2,676793151	-2,316748419	protein_coding	SCN8A
ENSG00000196878.12	-2,882054493	-2,91095077	-2,412933323	2,137989774	2,848010142	3,219938666	protein_coding	LAMB3
ENSG00000197016.11	-2,959128811	-2,96946144	-2,898528425	2,916011735	3,06116556	2,849941383	protein_coding	ZNF470
ENSG00000197142.10	-3,010252462	-3,02159243	-3,014880476	2,978445547	2,903646936	3,164632882	protein_coding	ACSL5
ENSG00000197308.8	2,552645606	2,602067797	2,435353471	-2,54456386	-2,511110968	-2,534392046	lincRNA	GATA3-AS1
ENSG00000197343.10	-2,872270185	-3,04067867	-2,968755685	3,239414266	2,931666839	2,710623432	protein_coding	ZNF655
ENSG00000197467.13	-2,70877857	-2,5544427	-2,569058867	2,593789815	2,605463077	2,633027244	protein_coding	COL13A1
ENSG00000197702.11	-2,69037023	-2,92066013	-2,976692435	3,037960278	2,832863921	2,716898592	protein_coding	PARVA
ENSG00000197937.12	-2,708027425	-3,00289107	-2,934546858	3,148248795	2,942845702	2,554370855	protein_coding	ZNF347
ENSG00000198121.13	-3,106929103	-3,11622976	-2,765759771	2,778294005	3,052917105	3,157707524	protein_coding	LPAR1
ENSG00000198286.9	-2,693829866	-2,70601667	-2,222662215	2,456212917	2,525155288	2,64114055	protein_coding	CARD11
ENSG00000198429.9	-2,540319587	-2,55336543	-2,464955149	2,931701815	2,511983846	2,114954507	protein_coding	ZNF69
ENSG00000198642.6	2,979746395	2,838730302	2,81415245	-2,69490554	-2,959898285	-2,977825324	protein_coding	KLHL9
ENSG00000198768.10	-2,954814953	-3,17948603	-3,125537652	2,634869305	3,271037286	3,353932044	protein_coding	APCDD1L
ENSG00000198771.10	-3,105494851	-3,11414128	-2,788591008	3,091957846	3,034285042	2,881984246	protein_coding	RCSD1
ENSG00000198879.11	2,479654021	3,028617028	3,174107016	-2,71432612	-2,975164508	-2,992887437	protein_coding	SFMBT2
ENSG00000198959.11	-3,006047205	-2,93427114	-2,308224777	2,453146645	2,787259785	3,008136692	protein_coding	TGM2
ENSG00000203805.10	-2,817131101	-2,82873611	-2,749525057	3,477400476	2,53986999	2,378121801	protein_coding	PLPP4
ENSG00000204264.8	-2,795196523	-2,97759106	-2,900225535	2,658615068	2,961825751	3,052572294	protein_coding	PSMB8
ENSG00000204381.11	-3,05984842	-3,25131781	-3,20480986	3,217275079	3,199991612	3,098709398	protein_coding	LAYN
ENSG00000206190.11	-2,538903925	-2,55190787	-2,463769777	2,574846504	2,556262854	2,423472215	protein_coding	ATP10A
ENSG00000206538.7	-2,712134977	-2,72434167	-2,641261389	2,619334266	2,716456157	2,741947613	protein_coding	VGLL3
ENSG00000207422.1	2,972454191	3,075718195	3,101300181	-3,06015798	-3,036354172	-3,052960415	snRNA	RNU6-813P
ENSG00000211445.11	-3,238820222	-3,24560176	-3,198273776	3,518440328	3,106962977	3,057292453	protein_coding	GPX3
ENSG00000213626.11	-2,537970077	-2,76295992	-2,965574758	3,276644861	2,45605263	2,533807259	protein_coding	LBH

ENSG00000213949.8	-2,529683367	-2,66867108	-2,563430801	1,96146218	2,758442769	3,041880298	protein_coding	ITGA1
ENSG00000214189.8	-2,942469435	-2,95294425	-2,881075822	2,997819487	3,021106824	2,757563189	protein_coding	ZNF788
ENSG00000221887.5	-2,536310419	-2,54932311	-2,461130734	2,580127834	2,496935342	2,469701084	protein_coding	HMSD
ENSG00000221923.8	-2,729255075	-2,74135759	-2,658942527	2,593390803	2,700082007	2,83608238	protein_coding	ZNF880
ENSG00000223764.2	2,65917144	2,643566884	2,351464551	-2,41462851	-2,606973568	-2,632600796	lincRNA	RP11-54O7.3
ENSG00000223808.1	2,670055616	3,113785415	3,299751426	-2,96573127	-3,160872675	-2,956988516	lincRNA	RP11-428L9.2
ENSG00000225383.7	-2,690473668	-2,70281197	-2,61889205	2,635647126	2,82186851	2,554662054	lincRNA	SFTA1P
ENSG00000226167.1	2,733254887	2,713463696	2,716198154	-2,73446057	-2,703419593	-2,725036574	antisense	AP4B1-AS1
ENSG00000226278.1	-2,416784997	-2,7824657	-2,702307995	2,522357669	2,642048963	2,737152055	unprocessed pseudogene	PSPHP1
ENSG00000227051.5	2,96697598	3,200403982	3,361730005	-3,0934247	-3,261499131	-3,174186138	lincRNA	C14orf132
ENSG00000227372.10	-2,910345043	-2,92112576	-2,847264932	3,045862258	2,856969624	2,775903847	antisense	TP73-AS1
ENSG00000228630.5	2,423955882	2,85102118	2,8704647	-2,7286884	-2,697526374	-2,719226989	antisense	HOTAIR
ENSG00000231131.6	2,956136916	3,145868526	3,291449964	-3,07937595	-3,24227157	-3,071807885	lincRNA	LINC01468
ENSG00000231205.11	-2,541167083	-2,31632371	-2,799705434	2,549864018	2,591585853	2,515746351	transcribed unprocessed pseudogene	ZNF826P
ENSG00000231298.6	-2,992085104	-3,00208999	-2,93330059	3,302921179	3,047504803	2,577049698	lincRNA	LINC00704
ENSG00000232759.1	-2,831807565	-2,84334402	-2,764571064	1,799234277	3,244389548	3,396098823	antisense	AC002480.3
ENSG00000233117.2	-2,651767988	-2,66429731	-2,579154241	2,804217722	2,663406203	2,42759561	lincRNA	LINC00702
ENSG00000233276.3	-3,049278556	-3,24334086	-2,989025397	3,153773021	2,978413699	3,149458098	protein_coding	GPX1
ENSG00000234685.1	2,42229524	2,691104758	2,478979378	-2,54533457	-2,511881945	-2,535162862	processed pseudogene	NUS1P2
ENSG00000234745.9	-3,030901745	-3,06412655	-2,695720191	2,349765929	3,102945327	3,338037229	protein_coding	HLA-B
ENSG00000235123.5	3,283392821	3,363319375	3,276001505	-3,19746093	-3,472081199	-3,253171576	antisense	DSCAM-AS1
ENSG00000235750.9	2,674144567	2,689556015	2,657240797	-2,57629032	-2,88084732	-2,563803739	protein_coding	KIAA0040
ENSG00000236699.8	2,52904901	3,017769125	3,132919716	-2,90535379	-2,877478191	-2,896905875	protein_coding	ARHGEF38
ENSG00000237289.9	2,658647184	2,499046051	2,448675961	-2,12922124	-2,728019731	-2,749128225	protein_coding	CKMT1B
ENSG00000240216.7	1,845871422	2,606965531	3,149696842	-2,60817316	-2,39813597	-2,596224662	unitary pseudogene	CPHL1P
ENSG00000240476.1	-2,860268587	-2,87138867	-2,442895279	2,394614855	2,902356799	2,877580885	lincRNA	LINC00973

ENSG00000241361.8	2,473219221	2,69695302	2,879396319	-2,69694523	-2,665291707	-2,687331624	transcribed unprocessed pseudogene	SLC25A24P1
ENSG00000241484.9	2,598369354	2,700077982	2,641257469	-2,66052149	-2,628415413	-2,650767901	protein_coding	ARHGAP8
ENSG00000242779.6	-2,480337184	-2,49605906	-2,75212046	2,881327782	2,573920434	2,273268492	transcribed processed pseudogene	ZNF702P
ENSG00000244468.1	2,687637621	2,949857225	3,472169963	-2,88688659	-3,103821726	-3,118956492	antisense	RP11-206M11.7
ENSG00000246082.2	-2,639613293	-2,65220971	-2,566640992	2,359787384	2,709029831	2,78964678	unitary pseudogene	NUDT16P1
ENSG00000247516.4	-2,706309403	-2,71855405	-2,635231197	2,5402739	2,740671999	2,779148756	lincRNA	MIR4458HG
ENSG00000248663.6	2,535506822	2,791365857	2,451620099	-2,35821273	-2,699380357	-2,720899694	lincRNA	LINC00992
ENSG00000249242.7	2,488531315	2,606991828	2,492983715	-2,38401633	-2,658364605	-2,546125924	protein_coding	TMEM150C
ENSG00000249364.5	2,375623131	2,589987257	2,827036351	-2,61179345	-2,579020407	-2,601832886	lincRNA	RP11-434D9.1
ENSG00000250786.1	-2,442239316	-2,80204105	-2,72275747	2,542151107	2,681708466	2,743178265	lincRNA	SNHG18
ENSG00000253125.1	2,272392213	2,834475251	3,049953759	-2,50606945	-2,815293163	-2,835458611	processed transcript	RP11-459E5.1
ENSG00000253522.3	-2,9295309	-2,94040413	-2,865930168	0,89567571	3,899867503	3,940321986	lincRNA	MIR3142HG
ENSG00000255248.6	-3,18328238	-3,33251841	-3,13457815	2,880262217	3,423889014	3,346227709	sense_overlapping	RP11-166D19.1
ENSG00000257732.1	-2,938198883	-2,9487197	-2,876550991	2,680006999	3,117072093	2,966390479	antisense	RP11-818F20.5
ENSG00000259129.5	2,281859332	2,590219396	2,684360117	-2,53341312	-2,499826137	-2,523199587	lincRNA	LINC00648
ENSG00000259207.7	-2,824537515	-2,83589342	-2,395592205	2,661743764	2,647242462	2,747036911	protein_coding	ITGB3
ENSG00000261116.1	2,526977178	2,618045851	2,652843246	-2,73709786	-2,706323532	-2,354444884	sense overlapping	RP3-523K23.2
ENSG00000261786.1	-2,99705392	-3,20860345	-2,932609091	3,66333675	2,916909576	2,558020137	lincRNA	RP4-555D20.2
ENSG00000262943.7	2,502357463	2,830263488	2,861956454	-2,7449442	-2,714063413	-2,735569793	transcribed unprocessed pseudogene	ALOX12P2
ENSG00000263753.6	-2,788709607	-2,45599155	-2,720960535	2,803407255	2,615870325	2,546384112	lincRNA	LINC00667
ENSG00000265190.6	-2,98703074	-2,71432464	-2,928316437	2,702431773	3,043234419	2,884005628	protein_coding	ANXA8
ENSG00000267131.1	2,342208359	2,746743124	2,584092733	-2,31745859	-2,666889356	-2,688696272	antisense	RP11-332H18.5
ENSG00000267280.5	2,791356438	2,912332407	2,853481473	-2,66467569	-2,937079692	-2,955414936	antisense	TBX2-AS1

ENSG00000269416.5	-2,668992025	-2,97423094	-2,903966377	3,31860046	2,907454908	2,321133969	lincRNA	LINC01224
ENSG00000270069.1	-2,783185527	-2,79721617	-2,580605583	2,704520684	2,714778672	2,741707925	lincRNA	MIR222HG
ENSG00000271605.5	-2,798312356	-2,80996892	-2,730424007	2,928721614	2,700673477	2,709310196	protein_coding	MILR1
ENSG00000272620.1	-2,662447514	-3,10912661	-3,049095171	2,671254249	3,025151903	3,124263143	antisense	AFAP1-AS1
ENSG00000273802.2	2,764706214	2,999553442	2,861024081	-2,88734402	-2,85914345	-2,878796268	protein_coding	HIST1H2BG
ENSG00000273983.1	2,599649342	2,68044176	2,653605374	-2,65853072	-2,626397158	-2,648768602	protein_coding	HIST1H3G
ENSG00000274750.2	2,742249314	2,799412189	2,753273991	-2,77816369	-2,747817558	-2,768954244	protein_coding	HIST1H3E
ENSG00000275216.1	-3,287703747	-3,36479569	-3,24914582	3,294740803	3,443995814	3,162908637	lincRNA	RP11-54H7.4
ENSG00000275713.2	2,249399956	2,776665316	2,660055989	-2,57644685	-2,543303035	-2,566371376	protein_coding	HIST1H2BH
ENSG00000275832.4	-2,770437335	-3,04584862	-2,470121275	3,033743322	2,744176896	2,508487012	protein_coding	ARHGAP23
ENSG00000275896.4	-2,715133682	-2,72733889	-2,644266001	2,982083958	2,68163129	2,42302332	protein_coding	PRSS2